UNIVERSITÀ DEGLI STUDI DI MILANO

FACOLTÀ DI AGRARIA

Philosophy Doctorate School In
Scienze Molecolari e Biotecnologie Agrarie, Alimentari ed
Ambientali

Philosophy Doctorate Course In
Chimica, Biochimica ed Ecologia degli Antiparassitari, XXIII ciclo

THE CONTROL OF DELETERIOUS BIOFILM ON ABIOTIC SURFACES: FROM A MORE SUSTAINABLE USE OF BIOCIDES TO A NEW ENVIRONMENTALLY-FRIENDLY APPROACH

ANDREA POLO
No. Matr. R07423

SUPERVISOR: Dr. Francesca Cappitelli
COORDINATOR: Prof. Claudia Sorlini

Academic Year 2009/2010

COVER
Labirinto dorato from "Titani preziosi" collection by Pietro Pedeferri (1985), size 35x35 cm.
Picture helpfully supplied by prof. Maria Pia Pedeferri.

It is well established that bacteria are the first organisms to adhere and colonize both abiotic and biotic surfaces. Their subsequent multiplication and production of exopolymeric substances (EPS) bring to biofilm formation which is believed to influence the settlement of following colonisers starting biofouling process on surfaces. Biofilm and fouling often have a deleterious effect on colonized surfaces and materials. They explicate a complex and various range of processes on abitic surfaces that cause physical damages, chemical alterations, loss of functionality and discolouration of surfaces, generating tremendous environmental and economical harm for human society. The control of the deleterious biofilm and the following fouling is today a great challenge. Currently, we have two choices: to remove biofilm by traditional methods or to research new effective antifouling approaches.

Traditional techniques consist mainly in the application of biocides, however this practice has several disadvantages. In fact, traditional biocides are not generally specifically target against detrimental microorganisms and they are often potentially toxic both for humans and the environment. In addition, biological matter released by their use can offer a favourable substratum for subsequent colonisations. Others problems concern the development of resistance in target pest populations and the low biodegradability of these chemicals. Moreover, biocides are not always effective at low concentrations because life inside the biofilm leads to increased resistance to antimicrobial products up to 1000-fold compared to planktonic cells. Finally, current legislation in UE and USA regulates the use of biocides and lately several products have been withdrawn from the market. New antifouling strategies need to be effective, economic, safe for the public and to pose negligible risk to human health and the environment. In the last years new strategies able to control biofilm growth have been proposed as alternative to traditional active substances. However, several years will be required to set up and test satisfactory methods, so, these novel strategies can be only a long term solution. In the meantime, as short term solution, it is vital to study methods for a more sustainable use of traditional antimicrobial agents. Therefore, the aims of the PhD project here presented were:

1) to use biocides for the removal of deleterious biofilm from relevant abiotic surfaces in the most sustainable way;
2) to exploit the ability of a new promising inorganic compound, the photocatalytic titanium dioxide, as an innovative non-toxic antifouling system to control biofilm formation on abiotic surfaces.

The study reported in the chapter 3 addresses the first aim. Generally, broad-range biocides are used to remove alterative biofilms from historical and artistic surfaces. In order to obtain a use as sustainable as possible of antimicrobial agents, the strategy has been to identify alterative microorganisms so as to use a suitable biocidal product which targets specifically the biodeteriogen agents.

In this work, for the first time, an integrated biotechnological system that enables the cleaning of cultural heritage stone affected by both biological and chemical alteration process was used.

The study was conducted on alterations found on two stone sculptures decorating the courtyard of the Buonconsiglio Castle in Trento (Italy). Stone, especially if exposed to the weather, is subject to chemical, physical and aesthetical deterioration. In this regard, pollution and environmental parameters play an important role since they are most responsible of deterioration process. Samples from altered and unaltered areas were characterized using stereomicroscope, cross-section observations and Fourier transform infrared (FTIR) analyses.

Results reveled that stone was an oolitic limestone and changes were both discolorations ascribed to biological agents and chemical alteration represented by black crusts composed mainly by gypsum with a small amount of calcite, nitrate and silicates.

Cultural and biomolecular methods were adopted to study microbial biofilm from powders samples. The cultural analyses proved that heterotrophic bacteria, fungi and prokaryotic and eukaryotic algae were present on surfaces and that in some samples the counts were quite high (up to 7 logCFU/g for bacteria and up to 6 logCFU/g for fungi). Denaturing gradient gel electrophoresis (DGGE) and sequencing from total DNA extracted allowed to identify taxa of microorganisms causing discolorations: they were *Cyanobacteria*, *Chlorophyta* green algae (*Myrmecia* and *Friedmannia*), *Streptophyta* green algae (*Klebsormidium*), microcolonial black fungi (*Alternaria* and *Cladosporium*) and other species of fungi able to deposit melanin in the cell wall (*Verticillium*). Fluorescent in situ hybridisation (FISH) highlighted that the *Cyanobacteria* generally were dominant (more than 60%) among the other prokaryotics belonging to the Bacteria domain. In this case, in order to remove the discolourations, despite the initial purpose to use a product that targeted only the small population of harmful microorganisms, we were forced to choose the biocide BIOTIN N (constituted by a mixture of tributyltin naphthenate (20% w/v) and didecyl dimethyl ammonium chloride (35% w/v)) with a broad spectrum of activity due to the taxonomical variety of the biodeteriogens.

The same traditional and biomolecular methods were carried out on the samples collected after the cleaning to verify the removal of alterative microorganisms. Treatment with the biocide resulted in a decrease of the bacterial load (up to five orders of magnitude), and neither culturable fungi nor culturable prokaryotic and eukaryotic algae grew. Indeed the DGGE profiles showed far fewer bands than before treatment and proved that *Cyanobacteria* and most of the green algae and dematiaceous fungi had been efficiently removed.

Chemical alterations were removed by a biocleaning treatment, an innovative, efficient and highly selective bioremediation technology, alternative to the use of chemicals, that uses viable cells of sulphate-reducing bacteria able to remove sulphates from stone ornamental surfaces. In this work for the first time this approach was applied on limestone. Sulphate-reducing bacteria have been *Desulfovibrio vulgaris* subsp. *vulgaris* (ATCC 29579). The treatment consisted in three 12-h applications for a total duration of 36 h. Comparison of the results of the chemical analyses performed before and after the biocleaning proved that gypsum, nitrates and silicates were almost completely removed. In addition, both optical evidence and FTIR analysis showed that the limestone substratum was preserved.

In general, the cases of biofilms with large taxonomical variety (as the biofilms on the sculptures from Buonconsiglio Castle in Trento) are very frequent. Therefore, due to the side-effects of biocides, the development of alternative strategies for the prevention and control of deleterious biofilm becomes imperative. They must allow to protect materials from biodeterioration, and thus preserve their usefulness for as long as possible. In addition, new approaches must be safe for human beings and the environment. The study reported in the chapter 4 refers to this second aim of the project. The ability of photoactivated titanium dioxide (TiO_2), a promising alternative to biocide for the biofilm control and prevention, was investigated. The biocidal activity of TiO_2 against planktonic cells thanks to its strong photocatalytic properties has been reported since 1985. TiO_2 per se is non-toxic, as the tests in rats prove, and has been approved by the American Food and Drug Administration (FDA) for use in human food, drugs, cosmetics and food contact materials. Moreover, it is considered an environmentally friendly photocatalyst, it is relatively inexpensive, chemically stable and effective under weak solar irradiation in ambient atmospheric environment.

Few attention was dedicated to study the potential of photocatalytic TiO$_2$ against the bacterial biofilm so far. The aim was to investigate the ability of photocatalytic TiO$_2$ as a new non-toxic antifouling nanotechnology to deter and prevent the attachment and biofilm formation of selected bacteria on TiO$_2$-coated surfaces.

Aeroxide P25 (Degussa) was employed as source of TiO$_2$. The effects of both photocatalyst nanopowder suspensions (3g/l concentration) and thin TiO$_2$-film applied on glass coverslides by sol-gel method were valued. During the experiments TiO$_2$ was photoactivated by a lamp emitting radiation over a UV-A wavelength range with light intensity similar to outdoor solar irradiation (between 3000 and 500 μW/cm^2). An efficient protocol for the photoactivation of TiO$_2$ was set up degrading the dye rhodamine B. Thus activity was investigated on *Bacillus cereus*-group sp. (Gram-positive) and *P. stutzeri* and *P. aeruginosa* (Gram-negative) planktonic cells. The results proved that photoactivated TiO$_2$ provoked a significant decrease of CFU/ml. Biocidal activities of nanopowder suspension in demineralised water in *Bacillus* sp., *P. stutzeri* and *P. aeruginosa* were respectively 1-log reduction after 24 h, 2-log reduction after 30 min and 1-log reduction after 2 h compared to non-photoactivated TiO$_2$. TiO$_2$ thin film also produced a complete disinfection of *P. aeruginosa* planktonic cells in 24 h. Finally, the activity of photoactivated TiO$_2$ was investigated on *P. aeruginosa* biofilm at various formation steps both at the solid-liquid and at the solid-air interface. It was proved that neither TiO$_2$ nanopowder nor photocatalytic film showed any biocidal activity on *P. aeruginosa* biofilm at all the interfaces investigated. The experiments have demonstrated that the lack of cell inactivation by photocatalytic action on biofilm was not due to 1) the presence of phosphates that could block active sites on the catalyst surface, 2) scavenge oxidative radicals produced at the surface, nor to insufficient presence of O$_2$ at the TiO$_2$ surface, which maintains charge transfer in photocatalytic reactions, 3) biofilm growth that screens UV-A light, deactivating TiO$_2$, 4) insufficient build-up of photocatalytically-generated reactive species necessary for cell inactivation. In addition, confocal laser scanning microscope analysis demonstrated that not even exopolysaccharides produced by biofilm cells were the cause of fail inhibition since almost absent in the very young tested biofilms. The only possible explanation for these findings was that the cells, when live in sessile form, invoke a genetic response that imparts them an increased resistance to oxidative stress generated by photoactivated TiO$_2$.

In conclusion, the studies reported here have demonstrated that:
   a) Biotechnologies could facilitate a more sustainable use of biocides addressing the choice toward a suitable product that targets only the biodeteriogen microorganisms.
   b) The biocleaning treatment is an effective technology, alternative to use of chemicals, to remove selectively sulphates from stone.
   c) The photocatalytic TiO$_2$ is not a good candidate to develop an effective technology that is alternative to traditional biocides for the control of deleterious biofilm.

Further studies with other promising environmentally-friendly compounds may provide new ways to move forward in the search and to pursue the goal of an efficient surface coating methods able to prevent biofilm formation or, at least, to interfere with their inconvenient increased resistance to biocides, respecting the human health and environment.

The research for new non-toxic antifouling strategies continues.

Introduction

It is known that bacteria are the first microorganisms to colonize every surface that offer minimal condition for the life. They are present on a broad variety of systems as rhizospheres of plants and bodies of animals and humans, and of substrata as minerals, metals, stones, medical implants, paper, plastic, engineered and industrial systems, food processing equipments and artworks. Bacterial cells occur on surfaces mainly as biofilm. They promote microbial growth and support the following biofouling process, the undesirable accumulation of microorganisms, plants and animals on a surface (Flemming 2002, Whelan et al. 2006). Therefore, the biofilm formation is a fundamental step of the fouling accumulation. Biofilm and biofouling often have deleterious effect on colonized surfaces causing infections, physical damages, chemical alterations, loss of functionality and aesthetic changes. As a consequence, biofilms have dramatic practical and economical implications for human beings.

When freefloating (planktonic) cells adhere to a surface, they come together to form a community surrounded by a self-produced extracellular polymer matrix (EPS) consisting of polysaccharides, proteins, DNA and other substances. This structured consortium of cells is called biofilm (Stewart et al. 2008). In the last 40 years researchers realized that biofilms are universally present: most microorganisms can form biofilms and it is thought that more than 99% of all microorganisms on Earth are living in such aggregates (Costerton et al. 1987).

Biofilm formation is a complex dynamic process. Many studies have examined biofilm formation at the liquid-solid interface in various ecosystems and concluded that bacteria form biofilms in essentially the same manner regardless of which environment they inhabit. Bacteria adhere to the surfaces initially in a reversible association generally mediated by non-specific interactions such as electrostatic, hydrophobic, or van der Waals forces, whereas adhesion to biotic surface such as tissue is through specific molecular (lectin or adhesin) docking mechanisms (Dunne 2002). By binding to the surface through exopolymeric matrix, bacterial cells start the process of irreversible adhesion, proliferation, and accumulation as multilayered cell clusters. The extracellular matrices are considered to be essential in cementing bacterial cells together in the biofilm structure, in helping to trap and retain nutrients for biofilm growth, and in protecting cells from dehydration, environmental stress and the effects of antimicrobial agents. Once having irreversibly attached to a surface, bacterial cells undergo phenotypic changes, and the process of biofilm maturation begins. Bacteria start to form microcolonies either by aggregation of already attached cells or cell division, or cell recruitment of planktonic cells or cell flocs from the bulk liquid. Mature biofilms typically consist of differentiated three-dimensional mushroom- and pillar-like structures of cells embedded in copious amounts of EPS which are separated by water-filled channels and voids to allow convective flows that transport nutrients and oxygen from the interface to the interior parts of the biofilm, and remove metabolic wastes (Hall-Stoodley et al. 2004). Within a biofilm there are many heterogenic microenvironments and both structural and metabolic heterogeneity. Cells with diverse genotypes and phenotypes that express distinct metabolic pathways, stress responses and other specific biological activities are juxtaposed. The factors that contribute to this genetic and physiological heterogeneity include microscale chemical and metabolites gradients, differences in local conditions such as nutrient availability, pH, oxidizing potential, stochastic gene expression and the genotypic variation that occurs through mutation and selection (Stewart et al. 2008). It is now well-established that in a biofilm bacterial cells communicate through the secretion and uptake of small diffusible signal molecules (Rasmussen et al. 2006b). Recent evidence indicates that biofilm formation might be regulated at the level of population density-dependent gene expression

controlled by the cell-to-cell signaling quorum sensing (QS). QS is a regulatory mechanism which enables bacteria to make collective decisions with respect to the expression of a specific set of genes. A large number of bacterial species are known to possess this communication mechanism, through which bacteria can sense changes in their environment and coordinate gene expression in favor of the survival for the entire community. These cell–cell communication systems regulate various functions as motility, virulence, sporulation, antibiotic production, DNA exchange, and development of multicellular structures such as biofilm and fruiting body formation (Daniels et al. 2004). Finally bacterial cells detached from the biofilm reenter the planktonic state, and may reattach to virgin areas and initiate a new round of biofilm formation. Therefore, biofilm formation may be cyclical in nature.

Life in biofilm supplies several advantages compared to the planktonic form. Researchers are united in considering biofilm mode of growth as a strategy of environmental bacteria to survive in hostile environments (Simões et al. 2010). The accumulated knowledge proves that the biofilm mode of growth is extremely resistant to any hostile chemicals in the environment, including antimicrobial molecules. Resistance of biofilm cells is up to three or more orders in magnitude greater than that displayed by planktonic bacteria of the same strain (Høiby et al. 2001, Simões et al. 2010). Antimicrobial resistance in biofilms is due to multiple and complex mechanisms, some of these are still not fully understood (Mah et al. 2001, Vilain et al. 2004). The production of an exopolysaccharide matrix is one of the distinguishing characteristics of biofilms. It has been observed that this matrix, among other functions, represents an initial barrier either by physically slowing diffusion or chemically reacting with these compounds, preventing the access of the antimicrobial agent to the bacterial cells embedded in the community. The slow growth of the bacteria observed in mature biofilms due to nutrient limitation also contributes since it is generally accompanied by an increase in resistance to antimicrobial molecules. Living in biofilm starts also a stress responses that results in physiological changes which act to protect the cell from various environmental stresses. Thus, the cells are protected from the detrimental effects of heat shock, cold shock, changes in pH and many chemical agents. The high resistance of biofilms may be explained in part also by the hypermutation phenomenon as observed in stressed bacterial cells. Both environmental and physiological stress conditions, such as starvation and antimicrobial treatment, can transiently increase the mutation rates in sub-populations of bacteria allowing the bacteria to evolve faster (Blazquez 2003). The heterogeneity of biofilm is another relevant factor that provides increased tolerance. In fact, besides to the environmental conditions to which biofilms are exposed, the metabolic activities of bacteria within biofilms result in microscale heterogeneities in the chemical and physical parameters of the biofilm interstitial fluid. Chemical gradients of nutrients, waste products and signalling compounds develop, and can overlap or intersect, resulting in unique environmental niches. Microorganisms within the biofilms can respond to these local environmental conditions in various ways, including: i) altering gene-expression patterns or physiological activities to adapt to a particular location within the biofilm, ii) enriching for populations of a particular species that are best adapted to a particular condition and iii) selecting for mutant strains that can better survive under a given condition. Natural variants within biofilm subpopulations can increase fitness by providing tolerance to antimicrobial challenges and resilience to changing environmental conditions (Stewart et al. 2008). Recent advances have highlighted the relevance of modifications at the gene-expression level in sessile bacteria compared to suspended cultures (Vilain et al. 2004). Petrova et al. (2009) reported that, in vitro, biofilm formation proceeds through an ordered, temporal series of events, which is thought to rely on the controlled expression of a collection of biofilm-specific genes. Some products of these biofilm-specific phenotypes reduce the susceptibility of cells to oxidative antimicrobial agents (Mah et al. 2003). QS systems are

involved in the control of this gene expression and, thus, in the elevated antimicrobial tolerance of biofilms to conventional antimicrobials (Rasmussen et al. 2006a and 2006b). It is also likely that gene transfer by conjugation plays an important role for spreading antimicrobial resistance among different bacterial species. In fact, biofilms are ideally suited to the exchange of genetic material of various origins due to the close contact and relative spatial stability of bacteria within biofilms. This multicellular behavior permits biofilm cells to efficiently utilize resources for cell growth and provide collective defense.

Stewart (2001) proposed that one possible explanation might be that bacteria in the surface layer of biofilms degrade or modify antimicrobial compounds, long after they have lost their viability, shielding their more deeply embedded neighbor cells from harmful antimicrobial agents.

Resistance of bacterial biofilm make their control a hard problem. Conventional anti-fouling approaches usually rely on the efficacy of mechanical action and disinfection, aiming respectively for biofilm removal and inhibition of their growth. However, these practices do not assure the attainment of goal due to increased resistance. Mechanical action can remove up to 90% of microorganisms associated with the surface, but cannot be relied upon to kill them. Bacteria can redeposit at other locations and given time, water and nutrients can form a biofilm. Therefore, disinfection must be implemented (Gram et al. 2007). In addition, cleaning process are often impractical due to aggressiveness against the material surface and can be very expensive.

Disinfection consists in the use of antimicrobial products to kill microorganisms. Interfering organic substances, pH, temperature, water hardness, chemical inhibitors, concentration and contact time generally control the disinfectants efficacy (Cloete et al. 1998, Bremer et al. 2002, Kuda et al. 2008). However, antimicrobial products often are not fully effective, safe, easy to use, and easily rinsed off from surfaces. A lot of products are toxic, and, generally, not specifically target against detrimental microorganisms. Their use can scatter residues that could potentially affect human health and the environment (Simões et al. 2010). The European Federation of Agricultural Workers' Unions (EAF) made known that the use of pesticides can cause acute headaches, vomiting, stomach-aches, and diarrhea on workers and operators through exposure during the application, preparation or mixing of pesticides, and the handling of containers (about 20% of 2160 workers in all Member States reported adverse incidents, EFA 1997). Long run, low but constant exposure levels may lead to chronic health impairment (e.g. cancer, birth defects, reproductive problems, sensitisation). Through misuse of antimicrobials, chemical substances may end up contaminating water, air and soil, with adverse effects on plants and wildlife, and a loss of biodiversity in general. In particular, products released into the environment in an uncontrolled way by spray drift, leaching or run-off may pollute soil, surface water and ground water. Environmental contamination can also occur during and after application, when cleaning equipment, or through the uncontrolled illegal disposal of products or of their containers. According to the European water suppliers' organisation (EUREAU 2001), chemicals contamination of raw water is very severe in lowland rivers. Indeed, a high proportion of contamination exceeds the 0.1 µg/l threshold value, in which case the water must be treated to remove the pesticides in excess before it can be distributed as drinking water.

Above all that, it is important to know that most of the biocides that are used are based upon the results of planktonic tests (European Standard – EN 1276, 1997). Since tests did not mimic the behavior of biofilm cells, biocide can be highly ineffective when applied to control biofilms. In addition, if a microbial population faces high concentrations of an antimicrobial product, susceptible cells will be inactivated, but some cells may possess a degree of natural resistance or they may acquire it later through mutation or genetic exchange. These processes

allow the microorganism to survive and grow (Mah et al. 2001, McBain et al. 2002, Davies 2003, Gilbert et al. 2003). Moreover, the killing of biofilm organisms usually does not solve biofouling problems as mostly the biomass can supply a favorable substrate of following colonizations and must be removed. Finally, because of their adverse effects, legislation in force in UE and USA strictly regulates and discourages the use of biocides (European Commission Environment Directorate-General 2009). The UE stated that active substances cannot be released in the environment unless they are included in a positive EU list (Council Directive 91/414/EEC and Council Directive 98/8/EC). Consequently, since 1991 several products have been withdrawn from the market.

These disadvantages impose to move forward towards the following strategies: i) as longer-term perspective, to develop new safer alternatives control strategies that are efficient and pose negligible risks for humans and the environment and ii) as short-term strategy, since several years will be required in order to set up alternative practices and in meantime the use of biocides remain the only way to remove microbial biofilms from surfaces, to optimize and improve conventional treatments in order to make them more sustainable.

A more sustainable use of biocides is today one of the thematic strategies adopted by European Commission on 12 July 2006 for environment policy (COM 2006 372 final) and it was considered a key mechanism delivering the objectives set out in the Sixth Environmental Action Programme (6th EAP, 2002) adopted by the Council and Parliament for the period 2002-2012. However, existing legislation on products focuses on the placing on the market and on the end of the life-cycle of such products (Council Directive 91/414/EEC, Regulation EC No 396/2005), but scarcely solves the problems of the actual use-phase. The research is a fundamental key into reducing and rendering more sustainable the way of antimicrobials and, focusing the attention on the use-phase of products, can provide for this deficiency. The objective is to minimize the hazards and risks to health and the environment.

Young et al. (2008) proposed a polyphasic approach: a new practice to remove deleterious biofilm in which conventional biocides are combined with other chemical treatments, as permeabilisers, pigment and exopolysaccharide inhibitors and photodynamic agents, which increase the vulnerability of organisms, leading to success at minimal biocide concentrations thus reducing the health hazard for operators and the general public. However the method is complex and, although treatments proved successful in the laboratory, until now field trials were inconclusive.

An alternative and more viable solution is to evolve a practice of treatment with biocide paired up with studies of microbial communities inside the biofilm by cultural and biomolecular analyses. The accurate characterization of microbial communities of biofilm allows both to select a suitable biocidal product that targets uniquely biodeteriogen agents, and to achieve the following effective and representative monitoring of unwanted biofilm development. To know the variety of adhered microorganisms and the choice of a suitable product are a fundamental step in order to set up a removal treatment that is satisfactory, more sustainable and respectful for surfaces, as suggested by Flemming 2002.

At the same time, the current research is exploiting new non-toxic strategies to control or prevent biofilm formation on abiotic surfaces. Simões et al. (2010) reported the use of enzyme-based detergents, bacteriophages and microbial interactions/metabolite molecules as possible non-toxic antifouling practices alternative to biocides. However these solutions are complex, not always easily practicable in environmental application and, often, not very efficient. Other works concerned new promising antifouling compounds tested at non-toxic concentrations to prevent biofilm formation. Hentzer et al. (2003) reported that furanones produced by the alga *Delisea pulchra* perturbed biofilm processes interfering with bacterial cell-to-cell communication without affecting the growth rate. Ren et al. (2005) reported that

ursolic acid from the tree *Diospyros dendo* inhibited *Escherichia coli* biofilm formation 6 to 10-fold. More recently, Villa et al. (2009 and 2010) tested the properties of N-vanillylnonanamide, an analogue of hot pepper capsaicin, and zosteric acid, a secondary metabolite produced by the eelgrass *Zoostera marina*. Zosteric acid was reported to supply the best antifouling performance. It counteracted the effects of some colonization-promoting factors producing a significant decrease of biomass and thickness in *Escherichia coli* biofilm. Among inorganic compounds, the photocatalytic titanium dioxide (TiO_2) is considered a good candidate as a new antifouling-biocide agent, and it is reckoned safe for humans and the environment. The test in rats proved that TiO_2 per se is not toxic for human beings (Oka et al. 2008) and the American Food and Drug Administration (FDA) approved the use of TiO_2 in human food, drugs, cosmetics and food contact materials (Gurr et al. 2005, Chawengkijwanich et al. 2008). When TiO_2 is exposed to nearultraviolet light, it exhibits bactericidal activity due to its strong photocatalytic properties. Matsunaga and coworkers (1985) first highlighted the effect of titanium dioxide (TiO_2) on planktonic bacterial cells. In the last years it has become the most important photocatalyst in environmental bio-decontamination for a large variety of organics, bacteria, viruses, fungi and cancer cells, which can be totally degenerated and converted to CO_2, H_2O and harmless inorganic anions (Blake et al. 1999, Banerjee et al. 2006, Choi et al. 2007, van Grieken et al. 2009). A part of the current literature sustains that photocatalytic TiO_2 has potential to provide a robust solution to the persistent problem of biofilm growth and fouling. A lot of companies already market various products, as glass, tiles, coverings, etc., with declared anti-microbial properties because composed or coated with TiO_2 based-materials. The properties of TiO_2 to inhibit bacterial colonization were also tested for medical application on percutaneous implants and osteointegrative dental implants (Del Curto et al. 2005, Oka et al. 2008). It was reported that TiO_2 is a chemically stable and effective under weak solar irradiation in ambient atmospheric environment (Hamal et al. 2010, Chen et al. 2009). Finally, it is relatively inexpensive. The opportunity of achieving self-protected surfaces by a non toxic practice thanks to photocatalytic properties of TiO_2 coatings able to deter and prevent attachment of bacterial cells and biofilm formation is extremely attractive. However, the action of photocatalyst on bacterial biofilm is not well proved so far and must be investigated in order to develop an effective biocide and antifouling technique.

The improvement of well-known methods toward a more sustainable use and the development of an innovative and alternative safer approach are today the big challenges and the research to obtain these aims a fascinating task.

References

6th EAP (2002). Sixth Community Environment Action Programme. Decision 1600/2002/EC, OJ L 242, 10.9.2002, p. 8.

Banerjee S., Gopal J., Muraleedharan P., Tyagi A. K., Raj B. (2006). Physics and chemistry of photocatalytic titanium dioxide: visualization of bactericidal activity using atomic force microscopy. *Curr Sci India*, 90, 1378–1383.

Blake D. M., Maness P.-C., Huang Z., Wolfrum E. J., Huang J. (1999). Application of the photocatalytic chemistry of titanium dioxide to disinfection and the killing of cancer cells. *Separ Purif Method*, 28, 1–50.

Blazquez J. (2003). Hypermutation as a factor contributing to the acquisition of antimicrobial resistance. *Clin Infect Dis*, 37, 1201–1209.

Bremer P. J., Monk I., Butler R. (2002). Inactivation of Listeria monocytogenes/Flavobacterium spp. biofilms using chlorine: impact of substrate, pH, time and concentration. *Lett Appl Microbiol*, 35, 321–325.

Chawengkijwanich C., Hayata Y. (2008). Development of TiO$_2$ powder-coated food packaging film and its ability to inactivate Escherichia coli in vitro and in actual tests. *Int J Food Microbiol*, 123, 288–292.

Chen J., Poon C.-S. (2009). Photocatalytic construction and building materials: from fundamentals to applications. *Build Environ*, 44, 1899–1906.

Cloete T. E., Jacobs L., Brozel V. S. (1998). The chemical control of biofouling in industrial water systems. *Biodegradation*, 9, 23–37.

Choi H., Stathatos E., Dionysiou D. D. (2007). Photocatalytic TiO$_2$ films and membranes for the development of efficient wastewater treatment and reuse systems. *Desalination*, 202, 199–206.

COM (2006) 372 final. Communication from the commission to the council, the european parliament, the european economic and social committee and the committee of the regions.

Council Directive 91/414/EEC of 15 July 1991 on the placing of plant protection products on the market, OJ L 230, 19.8.1991, p. 1.

Council Directive 98/8/EC of 16 February 1998 concerning the placing of biocidal products on the market, L 123/1, 24.4.98, p. 1.

Costerton J. W., Cheng K.-J., Geesey G. G., Ladd T. I., Nickel J. C., Dasgupta M., Marrie T. J. (1987). Bacterial biofilms in nature and disease. *Annu Rev Microbiol*, 41, 435–464.

Daniels R., Vanderleyden J., Michiels J. (2004). Quorum sensing and swarming migration in bacteria. *FEMS Microbiol Rev*, 28, 261–289.

Davies D. (2003). Understanding biofilm resistance to antibacterial agents. *Nat Rev Drug Discov*, 2, 114–122.

Del Curto B., Brunella M. F., Giordano C., Pedeferri M. P., Valtulina V., Visai L., Cigada A. (2005). Decreased bacterial adhesion to surface-treated titanium. *Int J Artif Organs*, 28 (7), 718–730.

Dunne W. M. Jr. (2002). Bacterial adhesion: seen any good biofilms lately? *Clin Microbiol Rev*, 15, 155–166.

EUREAU (2001). Position paper 'keeping raw drinking water resources safe from pesticides'.

European Commission Environment Directorate-General (2009). Assessment of different options to address risks from the use phase of biocides. Final report, 5 March 2009.

European Standard – EN 1276. (1997). Chemical disinfectants and antiseptics – quantitative suspension test for the evaluation of bactericidal activity of chemical disinfectants and antiseptics used in food, industrial, domestic, and institutional areas – test method and requirements (phase 2, step 1).

Flemming H.-C. (2002). Biofouling in water systems – cases, causes and countermeasures. *Appl Microbiol Biot*, 59, 629–640.

Gilbert P., McBain A. J. (2003). Potential impact of increased use of biocides in consumer products on prevalence of antibiotic resistance. *Clin Microbiol Rev*, 16, 189–208.

Gram L., Bagge-Ravn D., Ng Y. Y., Gymoese P., Vogel B. F. (2007). Influence of food soiling matrix on cleaning and disinfection efficiency on surface attached Listeria monocytogenes. *Food Control*, 18, 1165–1171.

Gurr J.-R., Wang A. S. S., Chen C.-H., Jan K.-Y. (2005). Ultrafine titanium dioxide particles in the absence of photoactivation can induce oxidative damage to human bronchial epithelial cells. *Toxicology*, 213, 66–73.

Hall-Stoodley L., Costerton J. W., Stoodley P. (2004). Bacterial biofilms: from the natural environment to infectious diseases. *Nat Rev Microbiol*, 2, 95–108.

Hamal D. B., Haggstrom J. A., Marchin G. L., Ikenberry M. A., Hohn K., Klabunde K. J. (2010). A multifunctional biocide/sporocide and photocatalyst based on titanium dioxide (TiO$_2$) codoped with silver, carbon, and sulfur. *Langmuir*, 26, 2805–2810.

Hentzer M., Wu H., Andersen J. B., Riedel K., Rasmussen T. B., Bagge N., Kumar N., Schembri M. A., Song Z., Kristoffersen P., Manefield M., Costerton J. W., Molin S., Eberl L., Steinberg P., Kjelleberg S., Høiby N., Givskov M. (2003). Attenuation of Pseudomonas aeruginosa virulence by quorum sensing inhibitors. *EMBO J*, 22, 3803–3815.

Høiby N., Krogh Johansen H., Moser C., Song Z., Ciofu O., Kharazmi A. (2001). Pseudomonas aeruginosa and the in vitro and in vivo biofilm mode of growth. *Microbes Infect*, 3, 23−35.

Kuda T., Yano T., Kuda M. T. (2008). Resistances to benzalkonium chloride of bacteria dried with food elements on stainless steel surface. *LWT-Food Sci Technol*, 41, 988–993.

Mah T.-F. C., O'Toole G. A. (2001). Mechanisms of biofilm resistance to antimicrobial agents. *Trends Microbiol*, 9, 34–39.

Mah T.-F., Pitts B., Pellock B., Walker G. C., Stewart P. S., O'Toole G. A. (2003). A genetic basis for Pseudomonas aeruginosa biofilm antibiotic resistance. *Nature*, 426, 306–310.

Matsunaga T., Tomoda R., Nakajima T., Wake H. (1985). Photoelectrochemical sterilization of microbial cells by semiconductor powders. *FEMS Microbiol Let*, 29, 211–214.

McBain A. J., Rickard A. H., Gilbert P. (2002). Possible implications of biocide accumulation in the environment on the prevalence of bacterial antibiotic resistance. *J Ind Microbiol Biot*, 29, 326–330.

Oka Y., Kim W.-C., Yoshida T., Hirashima T., Mouri H., Urade H., Itoh Y., Kubo T. (2008). Efficacy of titanium dioxide photocatalyst for inhibition of bacterial colonization on percutaneous implants. *J Biomed Mater Res* B, 86B, 530–540.

Petrova O. E., Sauer K. (2009). Novel signaling network essential for regulating Pseudomonas aeruginosa biofilm development. *PLoS Pathog*, 5 (11), e1000668.

Rasmussen T. B., Givskov M. (2006a). Quorum sensing inhibitors: a bargain of effects. *Microbiology*, 152, 895–904.

Rasmussen T. B., Givskov M. (2006b). Quorum-sensing inhibitors as anti-pathogenic drugs. *Int J Med Microbiol*, 296, 149–161.

Regulation (EC) No 396/2005 of the European Parliament and of the Council of 23 February 2005 on maximum residue levels of pesticides in or on food and feed of plant and animal origin, OJ L 70, 16.3.2005, p. 1.

Ren D., Zuo R., González Barrios A. F., Bedzyk L. A., Eldridge G. R., Pasmore M. E., Wood T. K. (2005). Differential gene expression for investigation of Escherichia coli biofilm inhibition by plant extract ursolic acid. *Appl Environ Microbiol*, 71, 4022–4034.

Simões M., Simões L. C., Vieira M. J. (2010). A review of current and emergent biofilm control strategies. *Lebensm-Wiss Technol*, 43, 573–583.

Stewart P. S. (2001). Multicellular resistance: biofilms. *Trends Microbiol*, 9 (5), 204.

Stewart P. S., Franklin M. J. (2008). Physiological heterogeneity in biofilms. *Nat Rev Microbiol*, 6, 199–210.

EFA (1997). Summary of the EFA questionnaire on the health and safety linked to pesticides presented in the second EFA colloquium on pesticides, 6-8/3/1997.

Van Grieken R., Marugàn J., Sordo C., Pablos C. (2009). Comparison of the photocatalytic disinfection of E. coli suspensions in slurry, wall and fixed-bed reactors. *Catal Today*, 144, 48–54.

Vilain S., Cosette P., Hubert M., Lange C., Junter G.-A., Jouennea T. (2004). Comparative proteomic analysis of planktonic and immobilized Pseudomonas aeruginosa cells: a multivariate statistical approach. *Anal Biochem*, 329, 120–130.

Villa F., Albanese D., Giussani B., Stewart P., Daffonchio D., Cappitelli F. (2010). Hindering biofilm formation with zosteric acid. *Biofouling*, 26, 739–752.

Villa F., Giacomucci L., Polo A., Principi P., Toniolo L., Levi M., Turri S., Cappitelli F. (2009). N-vanillylnonanamide tested as a non-toxic antifoulant, applied to surfaces in a polyurethane coating. *Biotechnol Lett*, 31, 1407–1413.

Whelan A., Regan F. (2006). Antifouling strategies for marine and riverine sensors. *J Environ Monitor*, 8, 880–886.

Young M. E., Alakomi H.-L., Fortune I., Gorbushina A. A., Krumbein W. E., Maxwell I., McCullagh C., Robertson P., Saarela M., Valero J., Vendrell M. (2008). Development of a biocidal treatment regime to inhibit biological growths on cultural heritage: BIODAM. *Environ Geol*, 56, 631–641.

Aim of the work

Deleterious biofilms often cause damage or deterioration of engineered structures, industrial settings, health therapies and artworks. Their recalcitrance to traditional control practices, the rise of resistance compared to cells in planktonic form and the harmful effect of many biocides towards the environment and human beings make the battle against unwanted biofilm a hard challenge.

This problem has two possible solutions: as short-term strategy to optimize and improve conventional treatments with traditional biocides to make their use more sustainable, and as longer-term perspective to develop new safer alternative control strategies that are efficient and pose negligible risks for humans and the environment.

The present PhD thesis has a twofold goal:

1) **to set up a more sustainable practice to use conventional biocides** in order to remove alterative biofilms on abiotic surfaces;

2) **to test the ability of photocatalytic titanium dioxide as a new promising compound to hinder deleterious biofilm growth on abiotic surfaces**. Our scope is to create an effective safer antifouling technology as non-toxic alternative to traditional biocides.

Feasibility of removing surface deposits on stone using biological and chemical remediation methods[1]

Abstract

The study was conducted on alterations found on stone artwork and integrates microbial control and a biotechnological method for the removal of undesirable chemical substances. The Demetra and Cronos sculptures are two of 12 stone statues decorating the courtyard of the Buonconsiglio Castle in Trento (Italy). An initial inspection of the statues revealed putative black crusts and highlighted the microbial contamination causing discoloration. In 2006, the Cultural Heritage Superintendence of Trento commissioned the Dipartimento di Scienze e Tecnologie Alimentari e Microbiologiche (DiSTAM) to study and remove these chemical and biological stains. Our aim was to remove both alterations by a efficient and more sustainable way compared to the conventional chemical products that are often toxic and harmful for the environment. Stereomicroscopy characterised the stone of the sculptures as oolitic limestone, and infrared analyses confirmed the presence of black crusts. To remove the black crusts, we applied a remediation treatment of sulphate-reducing bacteria, which removes the chemical alteration but preserves the original stone and the patina noble. Using traditional and biomolecular methods, we studied the putative microbial contamination and confirmed the presence of biodeteriogens. Denaturing gradient gel electrophoresis fluorescent in situ hybridisation established that Cyanobacteria and green algae genera were responsible for the green staining whereas the black microbial contamination was due to dematiaceous fungi. We chose biocide Biotin N for the removal of the agents causing the discolouration. After the biocide Biotin N treatment, we applied molecular methods and demonstrated that the Cyanobacteria, and most of the green algae and dematiaceous fungi, had been efficiently removed. The reported case study reveals that conservators can benefit from an integrated biotechnological approach aimed at the biocleaning of chemical alterations and the abatement of biodeteriogens. Despite that, the large variety of bioteteriogens into biological discolorations imposed us to use a broad-range biocidal product.

Introduction

Many historic, cultural and artistic objects and buildings are made of stone. Like all materials, stone is subject to inexorable deterioration, especially if exposed to the weather. In this regard, a particularly important role is played by pollution, which is the factor most responsible for depositing various chemical substances and biological agents on outdoor stone surfaces. Generally, in the conservation treatment, chemical alterations are removed by chemical solvents and biological alterations by biocides. The problem concerning these chemicals is that both are often dangerous for human and environment health. The study reported here combines two more sustainable approaches to remove these alterations from art

---

[1] Published as: **Polo A**., Cappitelli F., Brusetti L., Principi P., Villa F., Giacomucci L., Ranalli G., Sorlini C. (2010). Feasibility of removing surface deposits on stone using biological and chemical remediation methods. *Microbial Ecology*, 60(1), 1-14.

objects: chemical alterations were removed by a bioremediation treatment and biological alterations were eliminated by a more sustainable use of a traditional biocide.

This work concerns two outdoor stone sculptures housed at the Buonconsiglio Castle, Trento, Italy. Before the conservation intervention, visual inspection revealed that most of the sculptures in the castle courtyard showed signs of deterioration. On first inspection, the two investigated sculptures presented alterations putatively attributed to chemical agents (possible black crusts) and to microorganisms (putative microbial contamination of different colors).

In the presence of atmospheric pollution and a humid environment calcareous stone is transformed into hydrated calcium sulfate, namely gypsum ($CaSO_4 \cdot 2H_2O$), which should be removed from surfaces as, because of hygrometric fluctuations, it undergoes dissolving and crystallizing processes that lead to mechanical stress. In areas sheltered from the rain gypsum embeds mineral and smog particles, leading to the formation of the so-called black crusts that represent chemical alteration and aesthetic disfigurement.

In addition, in the same conditions, many biodeteriogens, organisms capable of causing deterioration, can be found on stone: bacteria, algae, fungi and lichens (Warscheid et al. 2000, McNamara et al. 2005, Cappitelli et al. 2009, Scott James et al. 2007). Biodeterioration can cause chemical, physical, and aesthetic damage (Krumbein 1992, Gorbushina et al. 2000). The colour of the microbial contamination depends on the pigments produced by the microorganisms, and an understanding of the complex microbial ecosystem of cultural heritage surfaces is a prerequisite for controlling the growth of microbial species that cause biodeterioration (Leznicka et al. 1988, Warscheid et al. 2000).

The importance of an efficient and careful cleaning of stone artwork for the removal of chemical and biological alterations cannot be overstressed. Indeed, before cleaning, it is fundamental to have knowledge of the type of stone and the characterization of the chemical and biological alterations in order to choose the optimal cleaning intervention. The use of solvents and physical methods (like abrasion) for the removal of chemical alterations can affect the sound stone material, and result in low selectivity (Gauri et al. 1999). In the past few years much progress has been made using viable cells able to remove sulfates from stone ornamental surfaces (Webster et al. 2006, Cappitelli et al. 2006). In removing of black crusts, Cappitelli and co-workers (2007b) demonstrated the advantages of using microbial technologies over traditional chemical technologies: the biological procedure resulted in a more homogeneous removal of the surface deposits without chemically compromising the substrata, and preserved the patina noble under the black crust itself. In addition, biocleaning is a environmentally-friendly practice and it has proved to allow a more selective removal than chemicals.

With regard to biodeterioration, microbial abatement is commonly achieved using biocides. As the biocide is a toxic compound, it is very important to identify the biodeteriogens to choose a suitable product that targets only specific biodeteriogen taxa.

In our study we successfully used, for the first time, an integrated biotechnological system that enables the cleaning of stone cultural heritage affected by chemical and biological agents. It is our belief that this system provides a useful, safer, and reliable model for conservation intervention in similar case-studies.

Methods

Sculpture description

The Buonconsiglio Castle, built in the 13th century for defence purposes, is the most important secular monument in Trento (Italy). In the second half of the 18th century the courtyard was embellished with 12 statues probably made by Jacob Eberle in 1764. Two of these sculptures were studied in this work: Demetra and Cronos (see supporting information in Appendix 1, Figure SI 1). Visual inspection revealed that the two sculptures presented the following forms of alteration: i) putative black crusts and ii) green, green-black and black staining putatively attributed to the presence of microorganisms.

Sampling

All the samples were taken by scalpel (sterile for biological analysis) according to the Italian Cultural Heritage Ministry Recommendation (Commissione Normal 1980).

Table 1 reports all the samples, indicating the sculpture from which they were taken, sampling location and description of the alteration (for the images of Demetra and Cronos sculptures with the location of sampling points see supporting information in Appendix 1, Figure SI 1). For the chemical analyses, six samples were taken from the Cronos sculpture (1b to 6b) and two from the Demetra (7b and 8b). Samples 4b and 8b were taken from apparently non-altered areas whereas specimens 1b and 2b were putative black microbial contaminations, and samples 3b, 5b, 6b, 7b showed a putative black crust alteration. After the biocleaning, two samples were taken. The sample 3p was collected close to the sampling area of the specimen 3b, and the sample 5p was collected close to the sampling area of the specimen 5b.

In addition, eleven samples affected by putative biological discolouration (green, black and green-black) and black crust were selected to study the microbial community (see supporting information in Appendix 1, Table SI 1). Four of them were collected from the Demetra sculpture (9b to 13b) and six specimens were taken from the Cronos sculpture (14b to 19b). Three specimens were representative of green microbial contamination (9b, 16b and 17b), three specimens were representative of black microbial contamination (13b, 18b and 19b), samples 11b and 14b were representative of green-black microbial contamination and sample 12b most likely presented a black crust. In addition, samples 10b and 15b were taken from apparently non-altered areas. After the treatment, three samples were taken. Samples 14p, 17p, 19p were collected close to the sampling area of the specimen 14b, 17b, and 19b respectively.

Chemical analyses

Stereomicroscope and cross section observations

Samples were observed by Wild Makroskop M420 stereomicroscope (Heerbrugg, Switzerland), equipped with an Olympus OM1 camera (Chicago, USA). The cross sections were prepared for the 5b and 6b samples and observed using the optical Leitz Ortholux microscope (Wetzlar, Germany).

Fourier transform infrared (FTIR) spectroscopy

Fourier transform infrared (FTIR) analyses, used to detect both inorganic minerals and organic compounds in the samples, were carried out by a Nicolet Nexus spectrophotometer (Washington, USA) coupled with a Nicolet Continuum Fourier transform infrared spectroscopy microscope equipped with a HgCdTe detector cooled with liquid N_2. Spectra were recorded by a Graseby-Specac diamond cell accessory in transmission mode between

4000 and 700 cm^{-1}. The FTIR analyses were performed on samples collected both before and after the treatments.

Biocleaning

The remediation treatment using sulfate-reducing bacteria (SRB) was applied for the removal of the chemical alterations due mainly to gypsum. The biomass entrapped in the delivery system was prepared as described by Cappitelli and co-workers (2006): the SRB employed was *Desulfovibrio vulgaris* subsp. *vulgaris* ATCC 29579 maintained in DSMZ 63 medium, and the delivery system was Carbogel (CTS, Vicenza, Italy). Before use in the treatment, the cells were grown in DSMZ 63 medium modified by eliminating any iron source. After centrifugation and prior to mixing with the Carbogel powder, the cell pellet was suspended in deaerated phosphate buffer supplemented with 0.599 g l^{-1} sodium lactate at pH 7.0 at a concentration of 10^8 cells/ml. All the manipulations described above were done under anaerobic conditions in a glove box. The surfaces to be treated were moistened and covered with tissue paper before any applications began. The biologically treated areas underwent three 12-h applications for a total duration of 36 h. The biological cleaning system was covered with a polyvinylchloride film (Silplast, Italy) to reduce undesirable evaporation. After the treatment, removal of the bioformulate was accomplished by removing the tissue paper and subsequently washing the area with distilled water (Cappitelli et al. 2007b).

Biological analyses
Culturable community analyses

Sample powders were inoculated in two cultural media to determine the microbial counts on the Demetra and Cronos surfaces: Plate Count Agar medium (PCA, Merck) for aerobic heterotrophic bacteria with incubation at 30°C for 3-5 days and Potato Dextrose Agar medium (PDA, Merck) for fungi with incubation at 30°C for 3-5 days. The samples collected after the cleaning treatment were also inoculated in PCA and PDA, under the same conditions adopted before the treatment. Quantification of microorganisms grown on PCA and PDA was expressed as colony forming unit (CFU)/g.

Sample powders were also inoculated in Chu and Detmer media (Cappitelli et al. 2007a) to study the *Cyanobacteria* and *Chlorophyta* communities respectively. The samples were incubated for 30 days under natural light at room temperature. The samples collected after the cleaning treatment were also inoculated in Chu and Detmer media under the same conditions adopted before the treatment. Presence or absence of *Cyanobacteria* and eukaryotic algal growths was recorded.

DNA extraction

Total DNA was extracted directly from the stone samples as described by Ausubel et al. (1994) but with the following modifications: no lysozyme was added and 3 cycles - 80°C/70°C were performed before the addition of the proteinase K. The *Cyanobacteria* and eukaryotic algal DNA were also extracted from communities grown, respectively, in Chu and Detmer media, using the same protocol.

Both the microbial communities present on the sculptures before and after the treatment were studied.

Analysis of Bacteria community

The 16S rRNA gene fragments extracted from altered stone samples were amplified with primers GC-357 F and 907 R with the following chemical conditions: 1X of PCR Rxn Buffer, 1.5 mM of MgCl$_2$, 0.12 mM of dNTP mix, 0.3 μM of each primer and 1 U of Taq DNA

polymerase in 50 µl PCR reaction. The thermal cycling program included an initial denaturation at 94°C for 4 min followed by 10 cycles consisting of denaturation at 94°C for 30 s, annealing at 61°C for 1 min and extension at 72°C for 1 min, 20 cycles consisting of denaturation at 94°C for 30 s, annealing at 56°C for 1 min and extension at 72°C for 1 min and a final extension step at 72°C for 10 min.

Analysis of fungal community
The 18S rRNA gene fragments extracted from altered stone samples were amplified by two-step PCRs performed as follows: a first amplification step using the combination of primers NS1 and EF3 (Oros-Sichler et al. 2006) with 1X of PCR Rxn Buffer, 1.5 mM of $MgCl_2$, 0.2 mM of dNTP mix, 0.2 µM of each primer and 1 U of Taq DNA polymerase in 25 µl PCR reaction, and the cycling program as reported in Oros-Sichler and co-workers (2006) except for the 56°C annealing temperature. The first PCR product was used as template for a second amplification step performed with the primers NS2 and GC clamped NS1. The reaction mixture was identical to first-step PCR except for 0.12 mM of dNTP mix and 0.3 µM of each primer. The cycling program consisted in an initial denaturation at 94°C for 4 min followed by 35 cycles of denaturation at 94°C for 45 s, annealing at 50°C for 45 s and extension at 72°C for 2 min, and a final extension at 72°C for 10 min.
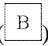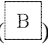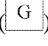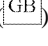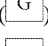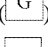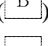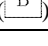
Analysis of culturable cyanobacterial community
The 16S rRNA gene fragments extracted from Chu medium cultures were amplified by two-step PCRs performed as follows: a first amplification step using the primers 27 F and 1495 R with 1X of PCR Rxn Buffer, 1.5 mM of $MgCl_2$, 0.2 mM of dNTP mix, 0.25 µM of each primer and 2.5 U of Taq DNA polymerase in 50 µl PCR reaction and with a touchdown thermal protocol consisting in an initial denaturation at 95°C for 1 min and 30 s followed by 5 cycles of denaturation at 95°C for 30 s, annealing at 60°C for 30 s and extension at 72°C for 4 min, 5 cycles of denaturation at 95°C for 30 s, annealing at 55°C for 30 s and extension at 72°C for 4 min and 25 cycles of denaturation at 95°C for 30 s, annealing at 50°C for 30 s and extension at 72°C for 4 min and a final extension at 72°C for 10 min. The first PCR product was used as template for a second amplification step performed with the primers GC-357 F and 907 R and with 1X of PCR Rxn Buffer, 1.5 mM of $MgCl_2$, 0.2 mM of dNTP mix, 0.3 µM of each primer and 1 U of Taq DNA polymerase in 50 µl PCR reaction. The PCR included an initial denaturation at 94°C for 4 min followed by 10 cycles consisting of denaturation at 94°C for 30 sec, annealing at 61°C for 1 min and extension at 72°C for 1 min, by 20 cycles consisting of denaturation at 94°C for 30 s, annealing at 56°C for 1 min and extension at 72°C for 1 min and a final extension step at 72°C for 10 min.

Analysis of culturable eukaryotic algal community
The 18S rRNA gene fragments extracted from Detmer medium cultures were amplified by PCR with the primers NS2 and GC clamped NS1 with 1X of PCR Rxn Buffer, 1.2 mM of $MgCl_2$, 0.2 mM of dNTP mix, 0.2 µM of each primer and 0.8 U of Taq DNA polymerase in 50 µl PCR reaction and the cycling program as reported in Oros-Sichler and co-workers (2006) except for the 63°C annealing temperature.

Table 1 - *Samples collected: sculpture, location, description and chemical and microbiological analyses carried out. Samples marked with b were collected before the treatment and specimens marked with p after the treatment.*

Samples	Sculpture	Location	Putative alteration (symbol)	Type of analysis carried out
1b	Cronos	child collar	Black microbial contamination (B)	Chemical
2b	Cronos	Arm	Black microbial contamination (B)	
3b	Cronos	Cloak	Black crust (⬢)	
4b	Cronos	Knee	Non altered sample (○)	
5b	Cronos	Cloak	Black crust (⬢)	
6b	Cronos	Cloak	Black crust (⬢)	
7b	Demetra	Shoulder	Black crust (⬢)	
8b	Demetra	Dress	Non altered sample (○)	
9b	Demetra	right-hand	Green microbial contamination (G)	Biological
10b	Demetra	Dress	Non altered sample (○)	
11b	Demetra	left-arm	Green-black microbial contamination (GB)	
12b	Demetra	left-hand	Black crust (⬢)	
13b	Demetra	right-shoulder	Black microbial contamination (B)	
14b	Cronos	left-elbow	Green-black microbial contamination (GB)	
15b	Cronos	left-knee	Non altered sample (○)	
16b	Cronos	Breasts	Green microbial contamination (G)	
17b	Cronos	child abdomen	Green microbial contamination (G)	
18b	Cronos	left-arm	Black microbial contamination (B)	
19b	Cronos	left-elbow	Black microbial contamination (B)	
3p	Cronos	cloak (area of the specimen 3)	-	Chemical
5p	Cronos	cloak (area of the specimens 5)	-	
19p	Cronos	left-elbow (area of the specimen 19)	-	Biological
14p	Cronos	left-elbow (area of the specimen 14)	-	
17p	Cronos	child abdomen (area of the specimen 17)	-	

Denaturing Gradient Gel Electrophoresis (DGGE) and sequencing
The amplicons obtained by amplifying bacterial and eukaryotic DNA were analysed by DGGE. The DGGE was performed as follows: 8% polyacrylamide (Sigma) gels were prepared according to the method of Muyzer and co-workers (1993) using a gradient maker (Amersham Biosciences) according to the manufacturer's guidelines. The DNA fragments were separated by electrophoresis run for 15 h at 90 V performed by D-Code Universal Mutation Detection system (Bio-Rad). The gels were stained by SYBR-Green (Armerscham Pharmacia Biotech) and the results observed by GelDoc (Bio-Rad) apparatus. The excised bands were eluted in 50 µl milli-Q water by incubation at 37°C for 3 h and successively overnight at 4°C. In order to compare the results both samples, collected before and after the treatment, were loaded on the same gel.
The DGGE was performed with the following denaturant gradients: 40%-60% for the Bacteria community, 25%-40% for the fungal community, 30%-60% for the culturable cyanobacterial community and two types of denaturing gradients, namely 35-45% and 25-35%, for the eukaryotic algal community.
All the excised bands were identified by sequencing (Primm, Milan). The sequences were analyzed using the BLASTN software (www.ncbi.nlm.nih.gov/BLAST).

Fluorescent In Situ Hybridization (FISH)
The abundance of *Cyanobacteria* within the Bacteria community before the treatment was investigated by Fluorescent In Situ Hybridization (FISH). Powder samples collected before the treatment were fixed with paraformaldehyde solution (4% in phosphate buffered solution, PBS, 0.01 M phosphate buffer, 0.0027 M potassium chloride pH 7.4 at 25 °C) and incubated for 2 h on ice. After two PBS washings, the powdered samples were resuspended in an aliquot of 1/1 ethanol/PBS solution, and stored at −20 °C. A small amount of sample (25 µl) was pipetted onto silane coated slides (Sigma-Aldrich), allowed to air dry and then dehydrated with an alcohol series (ethanol solutions 50%, 80% and 96% V/V). The spots with the samples were treated with 30 µl of hybridization buffer made with 2 µl (100 ng) of the labelled probes in 28 µl hybridization buffer. The probes chosen for the hybridization protocol were as follows: EUB338 fluorescein labelled, targeting *Bacteria*; CIV/V 1342, CYA762, CYA361 and CYA664 Texas red labelled, targeting *Cyanobacteria* (Loy et al. 2003). Details of the probes (sequences, coverage percentage, annealing temperature and references) are reported at www.probebase.net. The slides were observed by epifluorescence microscope Leica DM 4000 B (Leica Microsystems, Milano, Italy). Images of samples were acquired by CoolSNAP CF (Photometrics Roper Scientific, Rochester, USA), and cells positive after hybridization were counted.

Statistical analyses
Quantitative data of FISH images were analyzed by one-way factorial analysis of variance (ANOVA). The positive cells were counted from 10 digital images for each sample considered, and the means were compared separately for Bacteria and *Cyanobacteria* by post hoc comparison according to Tukey-Kramer.

Biocidal treatment
A chemical cleaning was applied to remove the biodeteriogens. The selected chemical was Biotin N (CTS, Italy), a broad range biocide, soluble in water and constituted by a mixture of tributyltin naphthenate (20 % w/v) and didecyl dimethyl ammonium chloride (35 % w/v). It was applied as a 1.5% aqueous solution, as per manufacturer instructions.

Results

Microscopy observations and chemical analyses

Using the stereomicroscope, the stone of the samples 4b and 8b was characterized as an oolitic limestone with oval or semi-circular grain structure. Despite the specimens being collected from areas that were apparently non-altered by visual inspection, FTIR spectra showed a slight degree of surface sulfatation. The samples 3b, 5b, 6b, 7b were all characterized by the presence of gypsum (3,540, 3,406, 1,685, 1,621, 1,132, and 670 cm^{-1}) and calcite (1,798, 1,429, 875, and 712 cm^{-1}) with a small amount of silicate (1,034, 1,001, 797 and 779 cm^{-1}) (figure 1). The speculation of the presence of black crusts was therefore confirmed. The sample 3b also contained calcium nitrate (1,384 cm^{-1}). Optical and chemical analyses of the specimens 5b and 6b showed the presence of a thin yellow-ochre inner layer composed of a mixture of calcium oxalate (1,646 and 1,324 cm^{-1}) and gypsum. In addition to calcite, silicates and a small amount of gypsum, FTIR analyses of samples 1b and 2b revealed the presence of a peptidic bond (see the peaks at 1,647 and 1,540 cm^{-1}).

Biocleaning treatment

The biocleaning procedure was applied to three areas of the Cronos sculpture strongly altered by thick black crust. One area was where samples 5b and 6b were taken, the other areas had very similar features and corresponded to the abdomen region. Cronos' abdomen before, during and after the biocleaning is presented in figure 2 (1, 2, 3): complete removal of the black crust was observed after three applications of 12 h each. FTIR analyses performed on the samples after the treatment confirmed that the gypsum was removed almost completely. After the biocleaning process, in the area corresponding to samples 5b and 6b, the presence of a yellow-ochre layer definitively different from the limestone colour was observed, and the presence of calcium oxalate was proved by FTIR spectra.

Figure 1 - *(1): top view of sample 6b under the stereomicroscope. (2): cross-section of sample 6b under optical microscopy in reflected light with the presence of the three layers: oolitic limestone (a), noble patina (b) and black crust (c). (3) top view of sample 2b under the stereomicroscope. (a): FTIR spectrum of the layer a showing the characteristic peaks of calcite (Ca). (b): FTIR spectrum of layer b showing the presence of calcium oxalate (Ox) and gypsum (Gy). (c): FTIR spectrum of layer c. The black crust is composed mainly of gypsum with a small amount of silicate (Si). (d) FTIR spectrum of the black patina on sample 2b. The spectrum shows mainly the presence of organic material of proteinaceus nature (amide I and amide II) (Am).*

Figure 2 - *Bioremediation treatment of Cronos statue: (1) untreated surfaces showing a black crust; (2) result after the first 12-h application; (3) result after tree 12-h applications, before the final washing with water and a soft brush.*

Biological analyses
To obtain preliminary information on the microbial community present on the samples before and after the treatments we performed a study on the culturable community. More detailed information on the total microbial community was obtained by a molecular approach (DGGE, sequencing, and FISH).

Culturable community analyses
The bacterial and fungal counts evaluated by cultural methods in the samples collected before any treatments were between 5 and 7 log(CFU/g) and between 4 and 6 log(CFU/g) respectively, with the only exception of sample 13b in which neither heterotrophic bacteria nor fungi were found.
In the samples collected after the biocidal treatment no fungi were found and the bacterial counts were 2-5 orders of magnitude lower than those found in the samples collected before the treatment.
Cyanobacteria and eukaryotic algae grew in all the samples except specimens 12b, 13b, 15b and 17b. The cultural results demonstrated that the microbial communities in the samples were complex and included heterotrophic bacteria, microfungi and algae. Neither *Cyanobacteria* nor eukaryotic algae grew from the samples collected after treatment.

DGGE and sequencing
To better characterize the microflora, DGGE analyses coupled with partial sequencing of 16S and 18S rRNA gene fragments were performed. Even though the amplification efficacy differed among the samples, the 16S gene amplification clearly showed a total of 28 bands separated in the DGGE gel, while for the 18S gene amplification 9 bands were evidenced. The corresponding sequences were determined. Tables 2 and 3 show the band number with the identification to the closest relative strain and similarity percentage.

FISH
FISH was performed to evaluate the importance of the *Cyanobacteria* within the total community of *Bacteria*. Figure 3 shows the mean values of the *Bacteria* and *Cyanobacteria* cells positive after hybridization in several samples. With the sole exception of samples 16b and 17b, most of the cells belonging to the domain Bacteria were also positive to the *Cyanobacteria* probes. Sample 13b was found to have no Bacteria cells positive to the EUB338 probe (according to cultural analysis results). The ANOVA analysis revealed statistically significant differences in the number of cells positive after hybridization with probes specific to *Bacteria* and *Cyanobacteria* among the samples.

Biocidal treatment
Figure 4 (1, 2, 3) shows green, green-black and black microbial contamination before the treatment, and its complete removal after treatment (4, 5). To confirm the visual observations, DGGE analyses were repeated after the biocidal treatment. Figure 5 shows the taxa identified by DGGE analyses before and after the biocidal treatment, and it is to be noted how the biodiversity of the microbial community was reduced: before the biocidal treatment fifteen taxa were recovered from the DGGE bands, while after treatment only six taxa were retrieved. The biocidal treatment was effective against *Cyanobacteria*, *Betaproteobacteria*, *Alfaproteobacteria*, *Actinobacteria*, *Bacteroidetes*, *Acidobacteria*, *Deinococcus-thermus*, *Cholophyta*, *Cladosporium*, *Alternaria*, *Geosmithia*. In fact, these taxa were found before the treatment, but were not identified after it.

Table 2 - *Identification of partial 16S rRNA gene sequences from DGGE profiles. A cross indicates the presence of the taxon in the sample.*

Bands	Samples											BlastN reference strains				RDP tassonomic Classifier	
	9b	10b	11b	12b	13b	14b	15b	16b	17b	18b	19b	Closest relative strain	Strain	Accession number	Similarity (%)	Most probable taxon	Similarity (%)
1, 4	x	x	x	x	x	x		x	x	x	x	*Halospirulina tapeticola*	CCC Baja-95 Cl.2	NR_026510	90	*Cyanobacteria*	100
2		x	x									*Hymenobacter aerophilus*	I/26Cor1; DSM 13606	NR_025398	90	*Adhaeribacter*	96
3		x		x	x	x	x	x	x	x	x	*Pseudomonas geniculata*	ATCC 19374	NR_024708	98	*Stenotrophomonas*	100
5						x						*Meiothermus chliarophilus*	ALT-8	NR_026244	83	*Truepera*	100
6		x	x			x						*Loktanella salsilacus*	R-8904	NR_025539	92	*Rhodobacteraceae*	100
7						x		x	x		x	*Arthrobacter agilis*	DSM 20550	NR_026198	99	*Arthrobacter*	100
8				x								*Arthrobacter nitroguajacolicus*	G2-1	NR_027199	98	*Arthrobacter*	100
9		x	x	x	x	x		x	x		x	*Cryptosporangium minutisporangium*	IFO 15962	NR_024746	90	*Actinomycetales*	99
11		x				x						*Sphingomonas wittichii*	RW1	NR_027525	86	*Sphingomonadaceae*	84
14			x		x	x	x	x	x	x		*Methylocystis echinoides*	IMET 10491	NR_025544	91	*Rhizobiales*	94
15			x			x			x			*Mesorhizobium plurifarium*	LMG 11892	NR_026426	94	*Rhizobiales*	94
20								x		x		*Sphingomonas aquatilis*	JSS-7	NR_024997	98	*Sphingomonas*	100
21, 22						x				x		*Sporocytophaga myxococcoides*	DSM 11118	NR_025463	89	*Flexibacteraceae*	99.5±0.5
23								x				*Ralstonia mannitolilytica*	LMG6866	NR_025385	92	*Burkholderiales*	94
24						x		x	x			*Herbaspirillum frisingense*	GSF30	NR_025353	93	*Burkholderiales*	97
25								x				*Herbaspirillum chlorophenolicum*	CPW301	NR_024804	93	*Oxalobacteraceae*	90
26						x		x		x		*Herbaspirillum chlorophenolicum*	CPW301	NR_024804	91	*Oxalobacteraceae*	98
27, 32						x						*Methylobacterium extorquens*	TK 0001	NR_025856	93.5±0.5	*Rhizobiales*	99.5±0.5
28						x		x		x		*Methylobacterium fujisawaense*	DSM 5686	NR_025374	96	*Methylobacterium*	100
29						x		x		x		*Sphingomonas aquatilis*	JSS-7	NR_024997	94	*Sphingomonadaceae*	99

Bands						Closest relative	Strain	Accession number		Taxon	
30		x		x		*Sphingomonas aquatilis*	JSS-7	NR_024997	91	*Alphaproteobacteria*	100
31		x	x	x		*Methylobacterium extorquens*	TK 0001	NR_025856	95	*Microvirga*	89
33		x				*Pseudomonas geniculata*	ATCC 19374	NR_024708	88	*Xanthomonadaceae*	84
35, 37, 38		x	x	x		*Rubritepida flocculans*	H-8	NR_025221	93	*Belnapia*	91±5.5
36		x				*Rubritepida flocculans*	H-8	NR_025221	92	*Acetobacteraceae*	100
39					x	*Bacteroides capillosus*	ATCC 29799	NR_025670	82	*Acidobacteriaceae*	100
41		x				*Ruminococcus flavefaciens*	C94	NR_025931	77	*Acidobacteriaceae*	97
42	x					*Pseudomonas umsongensis*	Ps 3-10	NR_025227	97	*Pseudomonadaceae*	100

Table 3 - *Identification of partial 18S rRNA gene sequences from DGGE profiles. A cross indicates the presence of the taxon in the sample.*

Bands	Samples											BlastN reference strains			
	9b	10b	11b	12b	13b	14b	15b	16b	17b	18b	19b	Closest relative	Strain	Accession number	Similarity (%)
1, 7	x	x	x	x		x	x	x	x	x		*Geosmithia* sp.	MKA1-b	AM947666	98
11, 13, 14	x	x	x	x		x	x	x	x	x		*Isaria fumosorosea*	IFO 7072	AB086629	99
2, 3, 4, 5, 6, 12, 15, 17, 19, 21	x	x	x	x		x	x	x	x	x		*Verticillium leptobactrum*	IAM 14729	AB214657	99±0.5
16		x		x					x			*Verticillium leptobactrum*	CBS 414.70	EF641846	99
28	x	x			x	x	x	x	x			*Cladosporium* sp.	CPC11224	DQ780937	99
30, 31		x					x		x	x		*Alternaria* sp.	CPCC 480375	EU826479	99
20, 24, 25, 26, 27	x	x	x	x	x	x	x	x	x	x		*Klebsormidium fluitans*	SAG 9.96	AM490839	99.5±0.5
18		x		x					x	x		*Myrmecia astigmatica*	IB T76	Z47208	99
22, 32		x							x	x		*Myrmecia* sp.	H1VF1	AF513369	99
23									x	x		*Friedmannia israeliensis*		M62995	99
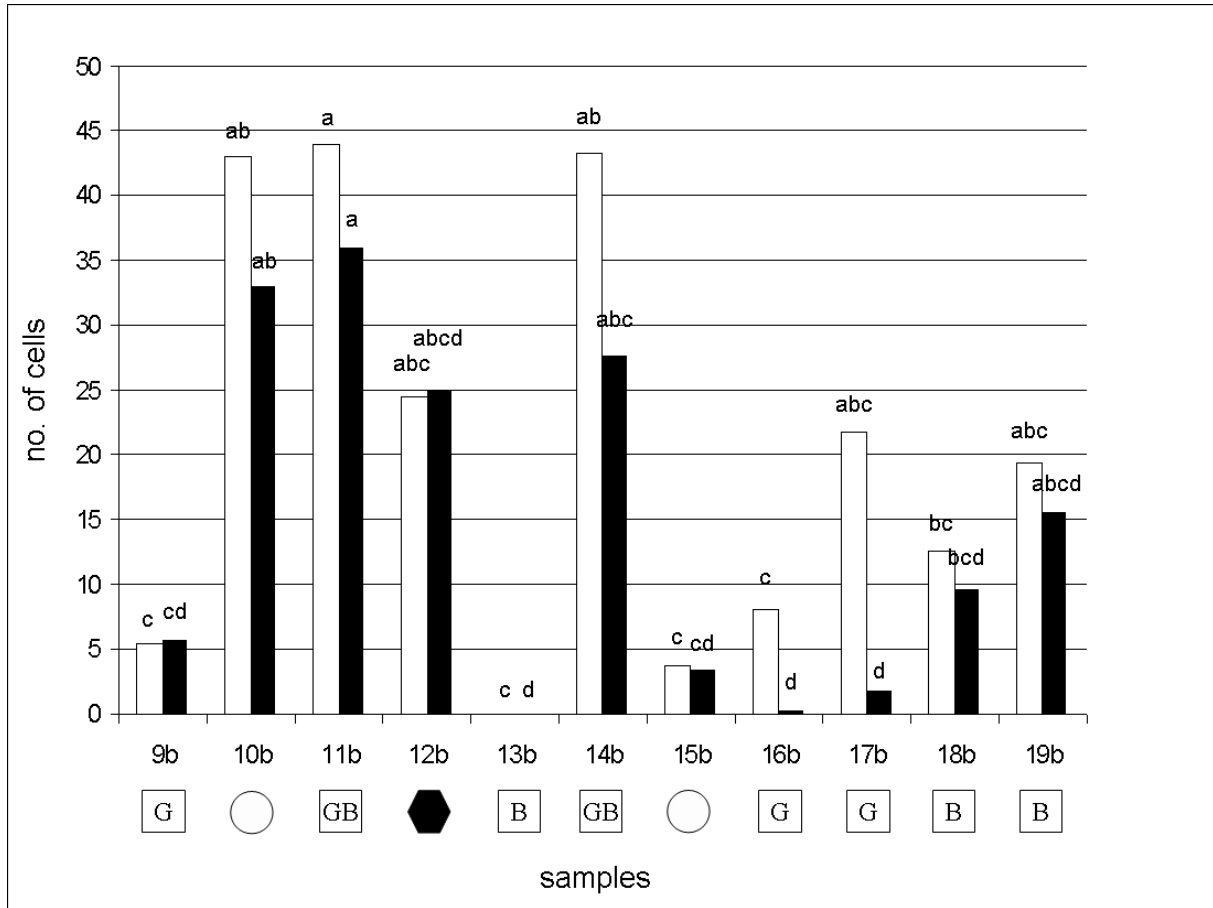
Figure 3 - *Mean values of cells positive after hybridization with the Bacteria domain (white bars) probe and specific Cyanobacteria (black bars) probes in several samples. The values with different letters are considered significantly different according to Tukey-Kramer (p<0.05).*
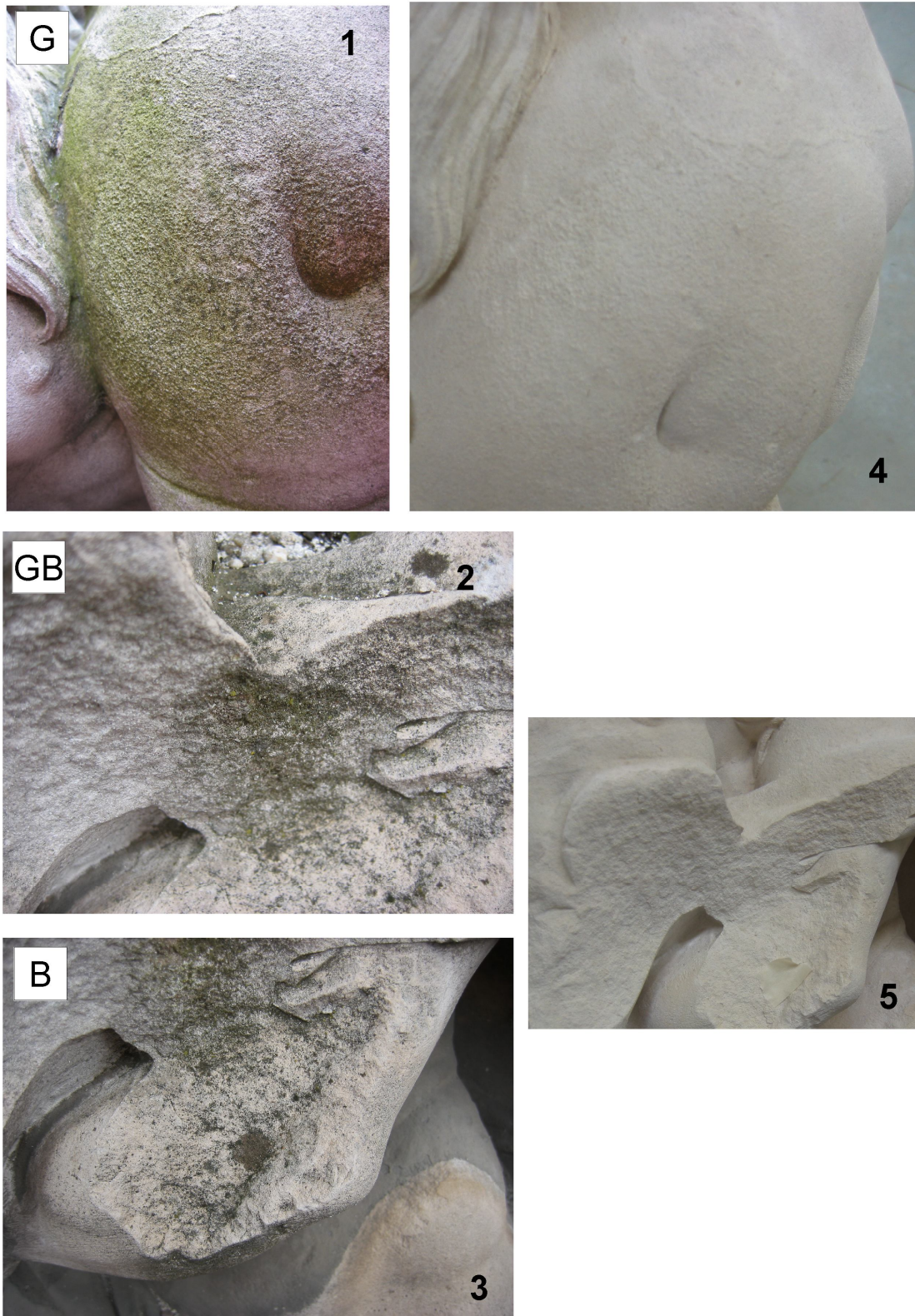
Figure 4 - *Effects of the biocide on the microbial community: before the treatment (1, 2 and 3, green, black and green-black patina respectively) and after the treatment (4 and 5). Chronos child abdomen (1 and 4); Cronos left-elbow upper part (2, 5) and lower part (3, 5)*
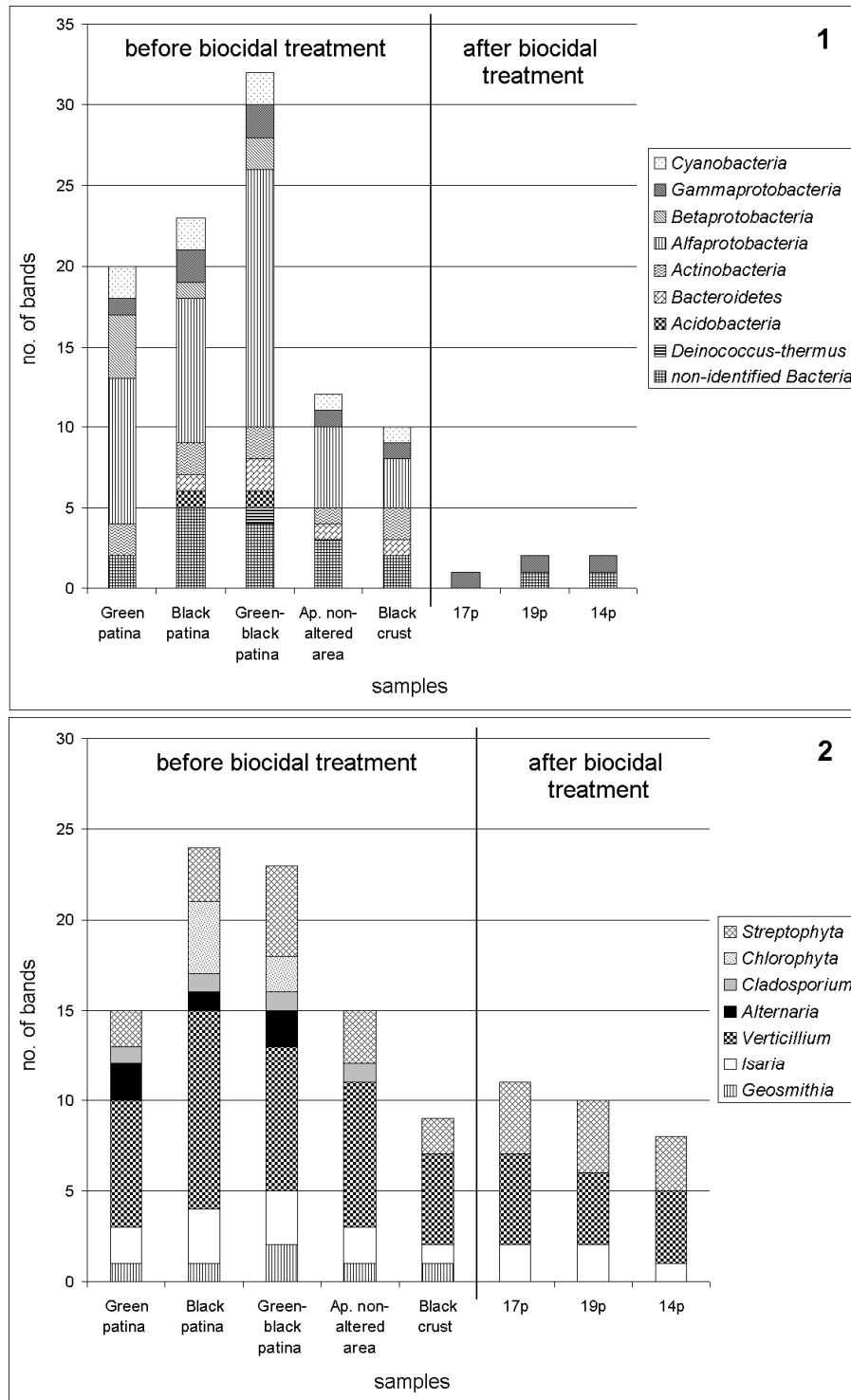
Figure 5 - *Bacterial taxa (1) and fungal and algal taxa (2), identified by DGGE before treatment, in the green microbial contamination (samples 9b, 16b and 17b), black microbial contamination (samples 13b, 18b and 19b), green-black microbial contamination (samples 11b and 14b), black crust (sample 12b) and apparently non-altered area (samples 10b and 15b) in comparison to the taxa identified in the samples collected after the treatment: samples 17p, 19p and 14p collected close to the sampling areas of specimens 17b, 19b, and 14b respectively.*

Discussion

An initial visual inspection of the Demetra and Cronos sculptures allowed the detection of two putative alterations: some black crust and some biological discolouration (green, black and green-black). The chemical analyses demonstrated that the putative chemical alterations were indeed black crusts as they were composed mainly by gypsum. Calcium nitrate was also present: in addition to the transformation of calcite to calcium sulfate it is also possible that calcium nitrate forms due to the interaction of calcite with airborne NO_x in the presence of humidity (Ricci et al. 2006). Also the silicate particles are of atmospheric origin, and are due to pollution (Chapoulie et al. 2008). In addition, peptidic bonds, observed in the FTIR spectra of samples 1b and 2b, were ascribed to the presence of microorganisms, as previously reported (Cappitelli et al. 2007a). Microscopic observations and chemical analyses demonstrated that the stone is an oolitic limestone. Finally, the cross section observations and the FTIR spectra showed that some areas affected by black crust were characterized by the presence of three different layers: the substratum (limestone), a thin yellow-ochre inner layer characterized by the presence of calcium oxalate, characteristic of a patina noble (Rossi Manaresi 1996), and the superficial black crust. In contrast to black crusts, the patina noble is a superficial layer acquired by stone in the course of time and protects the substratum. It is associated with the best-preserved surfaces and should remain intact during cleaning (Maravelaki-Kalaitzaki 2005).

In this work the chemical alterations were removed by a biocleaning treatment before the biocidal treatment intervention on the biological contamination that had caused the discolourations; this was to avoid that the biocide acted also on the SRB cells. In the past a biocleaning treatment by *Desulfovibrio vulgaris* was applied successfully to remove sulfates from marble (Cappitelli et al. 2007b); in the present study we applied it, for the first time, on limestone that is more porous than marble. On comparing the results of the chemical analyses performed before and after the biocleaning it was proved that bioremediation with *D. vulgaris* successfully removes gypsum black crust from the Demetra and Cronos sculptures. After three applications the black crusts were no longer detectable by visual inspection, and the FTIR analyses proved that the gypsum was almost completely removed. Neither nitrate nor silicate were found in the FTIR spectra after the treatment, implying that these compounds were removed together with the gypsum. In addition, as previously demonstrated for marble (Cappitelli et al. 2007b), both optical evidence and FTIR analysis showed that the noble patina was preserved on the limestone substratum of the sculptures.

The cultural analyses proved that all the four groups investigated (heterotrophic bacteria, fungi, prokaryotic and eukaryotic algae) were present and that in some samples the counts were quite high, up to 7 log(CFU/g) for bacteria and up to 6 log(CFU/g) for fungi. However, the microbial abundance in the samples did not seem to be related to the type of alteration. The negative cultural results for samples 13b could be attributed to the small quantity (0.3 mg) of available sample, the other samples ranged from 0.4 to 15 mg. The microbial count on the black crust was comparable to the other samples. It was demonstrated that these alterations host an active microflora able to use accumulated organic pollutants as a carbon and energy source (Saiz-Jimenez 1995). On the apparently non-altered samples, the counts were up to 3 orders of magnitude lower for both bacteria and fungi, partly explaining why visual inspection revealed no discolouration.

The sequences were phylogenetically most closely related to the *Cyanobacteria, Actinobacteria, Bacteroidetes, Alfa-, Beta-* and *Gamma-proteobacteria, Deinococcus-thermus,* and *Acidobacteria*. One of the most common bacterial groups associated with

carbonate stone biodeterioration is *Actinobacteria* (Urzì et al. 2001). In fact, *Actinobacteria*, *Bacteroidetes*, and *Alphaproteobacteria* were identified on a gothic monument made of oolitic and dolomitic limestone (Miller et al. 2008), while *Actinobacteria, Alfa-, Beta-, Gamma-proteobacteria* and *Acidobacteria* were found in limestone from a Maya archaeological site in southern Mexico (McNamara et al. 2006). *Proteobacteria*, *Acidobacteria* and *Actinobacteria* were the major components of microbial communities in coloured colonisations on cave walls with palaeolithic paintings (Portillo et al. 2008, Stomeo et al. 2008). The bacterial group *Deinococcus-thermus* is not commonly associated with limestone, however it was identified in a cave with palaeolithic paintings by Stomeo and co-workers (2007). Despite many of these taxa being found on stone surfaces and producing discolouration (Warscheid et al. 2000), the FISH results demonstrated that the *Cyanobacteria* generally were dominant in among the other prokaryotics belonging to the Bacteria domain: on average, more than 60% of the cells belonging to the Bacteria domain were also positive to the *Cyanobacteria* probes. Several studies conducted on monuments have proved that *Cyanobacteria* are among the most deteriorating biological agents dwelling on stone material (Tomaselli et al. 2000) and are able to form colourful microbial contaminations. *Cyanobacteria* were identified in all the samples, which were stained by green and green-black microbial discolourations, collected before the treatment, thus they can be thought to be among the biological agents responsible for the colour of these alterations. However, in samples 16b and 17b, characterized by green microbial contamination, most of the cells belonging to the bacterial domain were not positive to the *Cyanobacteria* probes. This evidence suggests that the green putative microbial contamination might also be caused by other green pigmented microorganisms such as green algae. Indeed the sequencing of 18S rRNA gene fragments showed that the eukaryotic community included the algal genera *Myrmecia*, *Klebsormidium* and *Friedmannia*. Note that *Myrmecia* and *Friedmannia* are *Chlorophyta* green algae and *Klebsormidium* is a *Streptophyta* green alga characterized by an enhanced freezing tolerance (Nagao et al. 2008), so it probably adapted to the rigorous climate of Trento. Tomaselli and co-workers (2000) claimed that *Chorophyta* algae are very frequently isolated on monuments, and Gaylarde and colleagues (2000) reported that green algae are the first colonisers of outdoor buildings in Latin America. As these were the green algae genera isolated from the green microbial contamination, they, in conjunction with *Cyanobacteria*, can be considered responsible for the alterations on the Demetra and Cronos surfaces. Photosynthetic microorganisms can directly participate in decay processes, causing aesthetic damage and, subsequently, structural and chemical damage and, indirectly, by supporting the growth of other microorganisms (Ariño et al. 1997, Hernandez-Marine et al. 1999).

The sequencing of 18S rRNA gene fragments showed that the eukaryotic community included the fungal genera *Isaria*, *Geosmithia*, *Verticillium*, *Alternaria* and *Cladosporium*. The first, *Isaria*, is an entomogenous genus of fungi. In Spanish caves, the cadavers of arthropods were found covered by *Isaria*, which extended from the insect body to the adjacent soil. Arthropods are vectors of entomogenous fungi and play an important role in fungal dispersion in caves, catacombs and mural paintings (Jurado et al. 2008). *Geosmithia* spp. were recently found to be regular associates of many insect species that invade the phloem or sapwood of various plant genera (Kolarik et al. 2008). Dematiaceous fungi that are characterized by the production of the black pigment melanin and manifest meristematic growth are considered by several authors the most harmful microorganisms of outdoor stone material (Krumbein et al. 1996), causing mechanical damage and aesthetic alterations (black coating) (Wollenzien et al. 1995, Burford et al. 2003, McNamara et al. 2003). *Alternaria* and *Cladosporium* are very well-known microcolonial black fungi (Wollenzien et al. 1995). Many authors have isolated

them on marble and limestone in several environments, including monuments and archaeological sites (Gorbushina et al. 1993, Wollenzien et al. 1995, Sterflinger 1998). The *Verticillium* species are common colonisers of rock substrata (Burford et al. 2003), and many of them are able to deposit melanin in the cell wall (Heale et al. 1964). These mycetes have also been isolated from monuments (Gorbushina et al. 2002). For these reasons *Alternaria*, *Cladosporium* and *Verticillium*, found in black and green-black microbial contamination, can be thought to be the biological agents responsible for black staining. From the above results we concluded that prokaryotic and eukaryotic algae were responsible for the green microbial contamination, and dematiaceous fungi for the black discolouration. Since the biodeteriogen agents were present in all the differently coloured microbial contaminated sites, it is most likely that the colour of the contamination varied from green to black depending on the abundance of the individual biodeteriogen agent.

The variety of biodeteriogens forced us to choose a broad range biocide to remove the discolouration. Treatment with the biocide resulted in a decrease of the bacterial load (up to 5 orders of magnitude), and neither culturable fungi, nor culturable prokaryotic and eukaryotic algae grew on the samples collected after the treatment. Indeed, after the treatment, the DGGE results showed that the samples from surfaces that had, prior to treatment, shown green, black and green-black microbial contamination, now showed far fewer bands than before treatment. The sequencing of these bands testified to the significant decrease, brought about by the biocide, in the biological diversity of the Bacteria, fungal and algal taxa, a result in accordance with the cultural results.

Importantly, the DGGE results proved that *Cyanobacteria* (among those responsible for the green microbial contamination) and most of the green algae and dematiaceous (the latter responsible for the black microbial contamination) were not identified in samples collected after the treatment. Among the taxa present on the surface after the treatment (*Gammaprotobacteria*, *Verticillium*, *Isaria* and *Streptophyta*), only *Streptophyta* and *Verticillium* were potential biodeteriogen agents that remained.

Conclusions

The Demetra and Cronos statues presented two concomitant deterioration phenomena found very frequently on outdoor stone artwork: the sulfatation of limestone caused by air pollution and surface biodeterioration. The first phenomenon caused the thick black crusts in the areas sheltered from rainfall and the second generated colourful microbial contamination on surfaces. This work shows that an integrated biotechnological approach can provide an important solution to both these problems. In fact the bioremediation treatment with *Desulfovibrio vulgaris* successfully removed black crust from limestone in a fully environmentally-friendly way, and the identification of biodeteriogen agents (*Cyanobacteria*, green algae and black pigmented fungi) by DGGE allowed the selection of a suitable cleaning treatment for the colourful microbial contamination. However, the large taxonomical variety of alterative biofilms forced us to use a biocide with a large range of activity, despite the perspective of a more sustainable use of conventional biocides. Given the presence of some green algae and melanin-containing fungi after the treatment, and the constant exposure of the sculptures to atmospheric pollution, we recommended an ongoing maintenance routine to ensure longer lasting conservation.

Supporting information available

Additional Figures and Tables are provided in Appendix 1.

References

Ariño X., Hernandez-Marine M., Saiz-Jimenez C. (1997). Colonization of Roman tombs by calcifying Cyanobacteria. *Phycologia*, 36, 366–373.

Ausubel F. M., Brent R., Kingston R. E., Moore D. D., Seidman J. G., Smith J. A., Struhk K. (1994). Current Protocols in Molecular Biology. John Wiley and Sons, New York.

Burford E. P., Kierans M., Gadd G. M. (2003) Geomycology: fungi in mineral substrata. *Mycologist*, 17, 98–107.

Cappitelli F., Abbruscato P., Foladori P., Zanardini E., Ranalli G., Principi P., Villa F., Polo A., Sorlini C. (2009). Detection and elimination of Cyanobacteria from frescoes: The case of the St. Brizio Chapel (Orvieto Cathedral, Italy). *Microb Ecol*, 57 (4), 633–639.

Cappitelli F., Principi P., Pedrazzani R., Toniolo L., Sorlini C. (2007a). Bacterial and fungal deterioration of the Milan Cathedral marble treated with protective synthetic resins. *Sci Total Environ*, 385, 172–181.

Cappitelli F., Toniolo L., Sansonetti A., Gulotta D., Ranalli G., Zanardini E., Sorlini C. (2007b). Advantages of using microbial technology over traditional chemical technology in removal of black crusts from stone surfaces of historical monuments. *Appl Environ Microbiol*, 73 (17), 5671–5675.

Cappitelli F., Zanardini E., Ranalli G., Mello E., Daffonchio D., Sorlini C. (2006). Improved methodology for bioremoval of black crusts on historical stone artworks by use of sulfate-reducing bacteria. *Appl Environ Microbiol*, 72 (5), 3733–3737.

Chapoulie R., Cazenave S., Duttine M. (2008). Laser cleaning of historical limestone buildings in bordeaux appraisal using cathodoluminescence and electron paramagnetic resonance. *Environ Sci Pollut R*, 15 (3), 237–243.

Commissione Normal (1980). Raccomandazioni Normal B 3/80 Materiali lapidei: campionamento. Roma: C.N.R. - I.C.R..

Gauri K. L., Bandyopadhyay J. K. (1999). Carbonate stone chemical behaviour, durability, and conservation. John Wiley & Sons, New York.

Gaylarde P. M., Gaylarde C. C. (2000). Algae and Cyanobacteria on painted buildings in Latin America. *Int Biodeter Biodegr*, 46 (2), 93–97.

Gorbushina A. A., Lyalikova N. N., Vlasov D. Y., Khizhnyak T. V. (2002). Microbial communities on the monuments of Moscow and St. Petersburg: biodiversity and trophic relations. *Microbiology*, 71 (3), 350–356.

Gorbushina A., Krumbein W. E. (2000). Patina (physical and chemical interaction of sub-aerial biofilms with object of art). In: Ciferri O., Tiano P., Mastromei G., (eds) Of Microbes and Art. The role of Microbial Communities in the Degradation and Protection of Cultural Heritage, vol. 15, Kluwer Academic/Plenum Publishers, New York, 105–120.

Gorbushina A., Krumbein W. E., Panina L., Soukharjevski S., Wollenzien U. (1993). On the role of black fungi in colour change and biodeterioration of antique marbles. *Geomicrobiol J,* 11, 205–222.

Heale J. B., Isaac I. (1964). Dark pigment formation in Verticillium albo-atru. *Nature*, 202, 412–413.

Hernandez-Marine M., Asencio A. D., Canals A., Ariño X., Aboal M., Hoffmann L. (1999). Discovery of population of the lime-incrusting genus Loriella (Stigomenatales) in Spanish caves. *Arch. For Hydrobiologie, Algological Studies*, 94, 121–138.

Jurado V., Sanchez-Moral S., Saiz-Jimenez C. (2008). Entomogenous fungi and the conservation of the cultural heritage: a review. *Int Biodeter Biodegr*, 62, 325–330.

Kolarik M., Kubatova A., Hulcr J., Pazoutova S. (2008). Geosmithia fungi are highly diverse and consistent bark beetle associates: evidence from their community structure in temperate europe. *Microb Ecol*, 55, 65–80.

Krumbein W. E. (1992). Colour change of building stone and their direct and indirect biological causes. In: Delgado Rodriguez J., Henriques F., Telmo Jeremias F. (eds) Proceedings of 7th International Congress on Detection and Conservation of Stone, LNEC, Portugal, 443–452.

Krumbein W. E., Diakumaku E. (1996). The role of fungi in the deterioration of stone. In: Interactive physical weathering and bioreceptivity study on building stones, monitored by Computerized X-Ray Tomography (CT) as a potential non-destructive research tool. Protection and Conservation of the European cultural heritage, Research Report 2, 140–170.

Leznicka S., Strzelczyk A., Wandtychowska D. (1988). Removing of fungal stains from stone-works. In: IV International Congress on Deterioration and Conservation of Stone, Vol. 2, Nicolaus Copernicus University, 12-14 September 1988, Torun, 102–110.

Loy A., Horn M., Wagner M. (2003). ProbeBase: an online resource for rRNAtargeted oligonucleotide probes. *Nucleic Acids Res*, 31, 514–516.

Maravelaki-Kalaitzaki P. (2005). Black crusts and patinas on Pentelic marble from the Parthenon and Erechtheum (Acropolis, Athens): characterization and origin. *Anal Chim Acta*, 532, 187–198.

McNamara C. J., Mitchell R. (2005). Microbial deterioration of historic stone. *Front Ecol Environ*, 3, 445–451.

McNamara C., Perry T. D., Bearce K. A. (2006). Epilithic and endolithic bacterial communities in limestone from a Maya archaeological site. *Microb Ecol*, 51, 51–64.

McNamara C., Perry T. D., Zinn M., Breuker M., Müller R., Hernandez-Duque G., Mitchell R. (2003). Microbial processes in the deterioration of Maya archaeological buildings in southern Mexico. In: Koestler R. J., Koestler V. H., Charola A. E., Nieto-Fernandez F. E. (eds). Art, Biology and Conservation: biodeterioration of works of art. The Metropolitan Museum of Art, New York, 248–265.

Miller A. Z., Laiz L., Gonzalez J. M., Dionísio A., Macedo M. F., Saiz-Jimenez C. (2008). Reproducing stone monument photosynthetic-based colonization under laboratory conditions. *Sci Total Environ*, 405, 278–285.

Muyzer G., De Waal E. C., Uitierlinden A. G. (1993). Profiling of complex microbial populations by denaturing gradient gel electrophoresis analysis of polymerase chain reaction-amplified genes coding for 16S rRNA. *Appl Environ Microb*, 59 (3), 695–700.

Nagao M., Matsui K., Uemura M. (2008). Klebsormidium flaccidum, a charophycean green alga, exhibits cold acclimation that is closely associated with compatible solute accumulation and ultrastructural changes. *Plant Cell Environ*, 31, 872–885.

Oros-Sichler M., Gomes N. C. M., Neuber G., Smalla K. (2006). A new semi-nested PCR protocol to amplify large 18S rRNA gene fragments for PCR-DGGE analysis of soil fungal communities. *J Microbiol Meth*, 65, 63–75.

Portillo M. C., Gonzalez J. M., Saiz-Jimenez C. (2008). Metabolically active microbial communities of yellow and grey colonizations on the walls of Altamira Cave, Spain. *J Appl Microbiol*, 104, 681–691.

Ricci C., Miliani C., Brunetti B. G., Sgamellotti A. (2006). Non-invasive identification of surface materials on marble artifacts with fiber optic mid-FTIR reflectance spectroscopy. *Talanta*, 69 (5), 1221–1226.

Rossi Manaresi R. (1996). Oxalate patinas and conservation treatments. In: Realini M., Toniolo L. (eds). The oxalate films in the conservation of works of art. Proceedings of the 2nd International Symposium, Milan, 25 to 27 March 1996. EDITEAM, Bologna, 113–127.

Saiz-Jimenez C. (1995). Deposition of anthropogenic compounds on monuments and their effect on airborne microorganisms. *Aerobiologia*, 11 (3), 161–175.

Scott James A., Untereiner W. A., Ewaze J. O., Wong B., Doyle D. (2007). Baudoinia, a new genus to accommodate Torula compniacensis. *Mycologia*, 99, 592–601.

Sterflinger K. (1998). Temperature and NaCl tolerance of rock-inhabiting meristematic fungi. *Anton Leeuw Int J G*, 74, 271–281.

Stomeo F., Gonzalez J. M., Saiz-Jimenez C. (2007). Analysis of the bacterial communities on paintings and engravings in Doña Trinidad cave (Ardales, Malaga, Spain). *Coalition*, 14, 24–27.

Stomeo F., Portillo M. C., Gonzalez J. M., Laiz L., Saiz-Jimenez C. (2008). Pseudonocardia in white colonizations in two caves with Paleolithic paintings. *Int Biodeter Biodegr*, 62, 483–486.

Tomaselli L., Lamenti G., Bosco M., Tiano P. (2000). Biodiversity of photosynthetic micro-organisms dwelling on stone monuments. *Int Biodeter Biodegr*, 46 (3), 251–258.

Urzì C., Brusetti L., Salamone P., Sorlini C., Stackebrandt E., Daffonchio D. (2001). Biodiversity of Geodermatophilaceae isolated from altered stones and monuments in the Mediterranean basin. *Environ Microbiol*, 3 (7), 471–479.

Warscheid T., Braams J. (2000). Biodeterioration of stone: a review. *Int Biodeter Biodegr*, 46, 343–368.

Webster A., May E. (2006). Bioremediation of weathered-building stone surfaces. *Trends Biotechnol*, 24 (6), 255–260.

Wollenzien U., de Hoogb G. S., Krumbeina W. E., Urzi C. (1995). On the isolation of microcolonial fungi occurring on and in marble and other calcareous rocks. *Sci Total Environ*, 167, 287–294.

Effects of photoactivated titanium dioxide nanopowders and coating on planktonic and biofilm growth of *Pseudomonas aeruginosa*[2]

Abstract

Here we exploit the ability of photocatalytic titanium dioxide (TiO$_2$) as an agent for the biofilm control. Two photocatalytic systems were investigated: a 3g/l suspension of TiO$_2$ nanopowder (Aeroxide P25) in demineralised water and glass cover slides coated with a thin film of TiO$_2$, achieved by sol-gel deposition. A running protocol for the photoactivation of TiO$_2$ was set up using the dye rhodamine B. The microorganisms studied were *Pseudomonas stutzeri*, *Pseudomonas aeruginosa* and a *Bacillus cereus*-group as planktonic cells. *P. aeruginosa* biofilms were also studied at both the solid-liquid and the solid-air interface. The TiO$_2$ nanopowder produced 1-log reduction of *Bacillus* sp. planktonic cells in 24 h, 2-log reduction of *P. stutzeri* planktonic cells in 30 min and 1-log reduction of *P. aeruginosa* planktonic cells in 2 h compared to non-photoactivated TiO$_2$. TiO$_2$ thin film produced a complete eradication of *P. aeruginosa* planktonic cells in 24 h compared to 3-log reduction caused by UV-A light alone. In contrast, neither the photocatalytic treatment with TiO$_2$ film nor that with TiO$_2$ nanopowder had any effect on *P. aeruginosa* biofilms at all the interfaces investigated. Possible explanations for these findings, and for the discrepancy between this work and literature data, are discussed.

Introduction

In nature, bacteria mostly live in dense communities attached to solid surfaces and embedded in extracellular polymeric substances matrix (EPS) consisting of exopolysaccharides, proteins and DNA. This form of growth is commonly known as biofilm (Stewart et al. 2008, Høiby et al. 2010). Biofilm growth can cause several problems on both biotic and abiotic surfaces. It has been recognized that the ability of bacteria to attach to each other and to biological surfaces, to form biofilm, is a prerequisite to invasion, and a vital step in the infection process (Walker et al. 2004, Bjarnsholt et al. 2010). In addition, bacterial biofilms have a detrimental effect on various materials, and on equipment like medical devices and implants, engineered systems, food-processing equipment, buildings and cultural heritages objects, causing enormous economic damages (Flemming 2002, Hazan et al. 2006, Cappitelli et al. 2009, Simões et al. 2010). For decades, the application of bactericides has been the most common means of achieving bacterial abatement and the control of deleterious biofilms. However, cells in biofilm are remarkably more tolerant to antimicrobial agents than the same cells in planktonic form (Mah et al. 2001). In addition, bactericides are generally not specifically targeted against deteriorating microorganisms, so they often represent a serious risk to both human health and the environment (Padovani et al. 2004). Furthermore, the development of resistance to biocides in target pest populations, and the knowledge of the biomagnification potential of these chemicals, have also discouraged their use (Walsh et al. 2003, Vermeire et

---

[2] Submitted for publication to *Nanotechnology*: **Polo A**., Diamanti M. V., Bjarnsholt T., Høiby N., Villa F., Pedeferri M. P., Cappitelli F. Effects of photoactivated titanium dioxide nanopowders and coating on planktonic and biofilm growth of *Pseudomonas aeruginosa*.

al. 2005). Consequently, current legislation in the European Union and the USA limits the use of biocides, and several products have been withdrawn from the market. By experimenting new targets and new mechanisms of action it might be possible to create an alternative generation of control strategies with the desired safety profile.

In the last 25 years, photocatalytic TiO_2 has been extensively studied for the removal of organic and inorganic compounds from contaminated water and air and for other environmental applications (Hoffmann et al. 1995, Nonami et al. 2004, Malato et al. 2009, Giraldo et al. 2010). It has been well documented that when TiO_2 surfaces are photo-excited by near-ultraviolet light (UV-A, wavelengths 320-400 nm) electrons from the valence band migrate to the conduction band, forming an e^-/h^+ couple that generates, with water and oxygen, strongly reactive species such as hydroxyl radical, hydrogen peroxide (H_2O_2), and superoxide anion (Wang et al. 2010) (see supporting information in Appendix 2, Figure SI 1 and SI 2). These radical species are prevalently responsible for biocidal activity (Banerjee et al. 2006). TiO_2 per se is not toxic for human beings, as its testing on rats and utilization in the human foodstuffs, drugs, and the cosmetic and pharmaceutical industries have proven (Lomer et al. 2002, Oka et al. 2008, Chawengkijwanich et al. 2008). This relatively inexpensive, environmentally friendly, photocatalyst is considered chemically stable and effective under weak solar irradiation in atmospheric environment (Chen et al. 2009, Hamal et al. 2010). Given this background, it would seem appropriate to determine whether the deployment of surface immobilized TiO_2 could become an alternative control technology to counteract sessile microorganisms in the form of biofilm. Indeed, several studies demonstrated the biocidal properties of photoactivated powdered TiO_2 on planktonic cells (Maness et al. 1999, Rincon et al. 2003, Kim et al. 2003, Rizzo 2009) and only a few publications have investigated photocatalytic killing on bacterial biofilm using TiO_2 suspended as powder in solution, or immobilized on a surface (Gage et al. 2005, Li et al. 2005, Ciston et al. 2009).

Sol-gel is one of the most exploited methods for the preparation of TiO_2-based films. This technology has found applications in the development of new materials for fibers, membranes, and chemical sensor and electrochemical devices (Akpan et al. 2010). Sol-gel technology is ideal for the fabrication of bioactive materials as it provides excellent matrices for entrapping inorganic compounds, combining biocompatibility with environmental friendliness (Gupta et al. 2008). However, the literature has only limited information available on the antimicrobial action of a sol-gel TiO_2 surface on biofilms. The only data relates the bactericidal activity against the primary paper industry biofilm former *Deinococcus geothermalis* and the membrane colonizer *Pseudomonas putida* (Raulio et al. 2006, Ciston et al. 2008). To date, no one has explored the performance of sol-gel TiO_2 surface in reducing biofilm formed by a human opportunistic pathogen and plant pathogen organism as *Pseudomonas aeruginosa*, considered a model for studying bacterial biofilms (Wozniak et al. 2003, Walker et al. 2004, Bjarnsholt et al. 2005). In addition, the contrasting results found in scientific literature still leave the question concerning the effectiveness of immobilized TiO_2 against bacterial biofilms open.

The main goal of this work has been to fill these gaps, by investigating the photocatalytic activity of sol-gel TiO_2 surface against *P. aeruginosa* biofilm.

Methods

The tests performed involved the setting up of several experimental techniques. In the early stages of the research work, TiO_2 photoactivity was evaluated on the degradation of an organic dye by irradiating TiO_2 nanopowder suspensions: this allowed us to identify a protocol for subsequent experimental phases, involving the analysis of TiO_2 effect on different microorganisms, in both planktonic form and as structured biofilm. Tests were also performed on immobilized films of nanostructured TiO_2, deposited from an aqueous sol on glass cover slides.

Photocatalyst characterisation and slide preparation
Aeroxide P25 (Degussa) was employed as the commercial source of TiO_2 nanopowder. It is a mixture anatase-rutile 80-20% (Coleman et al. 2005) of 30 nm primary particle size and aggregates up to 200 nm. Aqueous suspensions of the nanopowders were used, in the form of 3 g/l TiO_2 dispersed in demineralised water.
Glass cover slides (2.4x5 cm and 2.4x2.5 cm) were also used to analyze the activity of TiO_2 immobilized as a film on a glass substrate. The film was deposited by dip-coating: glass cover slides were dipped in an acidic sol of TiO_2 nanoparticles, then the coated substrate was calcined for 12 h at 120°C as consolidation treatment. Finally, the coverslides were sterilized before use in photoactivity tests.

Microorganisms tested
Pseudomonas stutzeri ATCC 23856, *Pseudomonas aeruginosa* PA01 tagged with green fluorescent protein (GFP) (Bjarnsholt et al. 2005) and *Bacillus cereus*-group sp. (Villa et al. 2009) were used to test the effect of Aeroxide P25 powder on planktonic cells. *P. aeruginosa* was also used to test the effect of photoactivated TiO_2 thin film and nanopowder on biofilm. *P. stutzeri* and *Bacillus* sp. were grown in plate count broth (PCB, Merck) overnight at 30°C. *P. aeruginosa* was grown in Luria-Bertani broth (LB, Sigma) overnight at 37°C.

Photoactivation-chamber
Samples to be lit were placed in a non-commercial chamber equipped with an 18W BLB lamp (Philips), emitting radiation over a wavelength range of 350-410 nm (maximum emission at 370 nm). With dye rhodamine B (rhoB), *Bacillus* sp. and *P. stutzeri* the distance between the lamp and the samples was set up to obtain 3000 $\mu W/cm^2$ of UV-A light incident on the samples. Since *P. aeruginosa* was more susceptible to UV light, the illumination was 1200 $\mu W/cm^2$ for the tests on planktonic cultures and 500 $\mu W/cm^2$ for the tests on biofilms. The chamber also accommodated a platform shaker in order to maintain the TiO_2 powder in suspension during the tests with dye solutions and planktonic cultures.
In all experiments, four conditions were tested: i) presence of TiO_2 and UV-A light (TiO_2+ UV+), ii) no TiO_2 and presence of UV-A light (TiO_2- UV+), iii) presence of TiO_2 under dark condition (TiO_2+ UV-), iv) no TiO_2 under dark condition (TiO_2- UV-). As described in the photocatalyst preparation section, TiO_2 was added to the system in the form of either a nanopowder suspension or a thin film on glass cover slides.
In the tests with dye solutions and planktonic cultures, the pH was determined by 3210 pH meter (Jenway) before the treatment, and at several tested times.
Whenever vials or plates were used, they were closed by glass seal covers to prevent water evaporation.
All the tests were performed in triplicate.

Degradation tests on organic dye

RhoB 10^{-5} mol/l solutions were prepared in sterile glass vials by dissolving an adequate quantity of rhoB in 25 ml of the following media: demineralised water (DW), ultrapure water (UW), salt solution (0.9% NaCl) (SS), phosphate buffered saline at pH 7 (PBS, Sigma), PCB and PCB dissolved in PBS at pH 7 (PCB-PBS). As rhoB is an organic dye, its discoloration can be considered representative of the molecule degradation: therefore, rhoB concentration variations were calculated using the Beer Lambert equation applied to the dye absorbance peak:

$$abs = \varepsilon \lambda C$$

abs being the rhoB absorbance at 550 nm, *C* its concentration, ε and λ the extinction coefficient of the solution and the optical length of the system (Ingle al. 1988).
RhoB absorbance at 550 nm was measured by a 6705 UV/Visible spectrophotometer (Jenway) before the treatment, and after 10, 30, 60 and 120 min, for the solutions in DW, UW, SS and PBS, and after 10, 30, 60, 120 min and 24 h, for the solutions in PCB and PCB-PBS. The TiO_2 particles were removed from the rhoB solution before the absorbance measurements by centrifuging at 15000 rpm for 5 min.

Susceptibility tests of planktonic bacteria cultures with TiO_2 nanopowder

The spent medium was removed from overnight cultures by centrifugation at 7000 rpm for 15 min at room temperature, and the cells were suspended in the same volume of DW and PCB-PBS for *P. stutzeri* and *Bacillus* sp. and DW and LB dissolved in PBS at pH 7 (LB-PBS) for *P. aeruginosa*. For the tests in DW, the pellet was first rinsed twice with 10 ml DW. Tests were carried out as reported for rhoB degradation tests. Ten ml of bacterial culture were put into glass vials. Both the cellular viability and the colony forming units per ml (CFU/ml) were assessed on a culture (200 µl) of each test condition, before the treatment and after 30, 60, 120 min and 24 h exposure to test conditions for the cultures in DW, and after 24 h, for the cultures in PCB-PBS and LB-PBS. Bacterial viability was assessed by measuring the relative light units per second (RLU/s), using the biomass detection kit (Promicol) according to the manufacturer's protocol and the FB 14 Vega bioluminometer (Berthold Detection Systems). RLU/s values were converted to ATP concentrations (nmol/ml) using ATP Standard Kit (Promicol) as standard and, thus, in nmol/CFU, dividing by CFU/ml values. Before the ATP assay, the supernatant was removed by centrifugation at 7000 rpm for 15 min and the pellet diluted 1:4 in TRIS buffer 100 mM, final pH 7.75. To determine the CFU/ml, the cells were then diluted serially with SS in microtitre plates, and enumerated using the drop-plate method in which 20 µl drops of each dilution were placed onto plate count agar medium (PCA, Merck) for *P. stutzeri* and *Bacillus* sp. or LB plates for *P. aeruginosa*.

Susceptibility test of planktonic culture on TiO_2 thin film

The planktonic culture of *P. aeruginosa* was prepared as reported for the test performed in presence of TiO_2 nanopowder. Cells were suspended in DW to achieve a cell concentration of approximately 10^8 CFU/ml, then 1.5 ml of culture were placed on TiO_2-coated cover slides (2.4x5 cm) and on cover slides without any film, which were used as the control. The cover slides were positioned on a plastic support in glass plates. Three sheets of paper, towel sponged by ultrapure water, were also positioned at the plates bottom to prevent the slides drying out and the dehydration of the cells. The papers were dampened every 12 h. After 30 min, 1, 2, 3, 4, 5 and 24 h of illumination, 50 µl of culture were collected, serially diluted and enumerated using the drop-plate method (10 µl drops), as reported in the previous section.

Biofilm preparation

For the tests with photocatalytic thin film, *P. aeruginosa* biofilm was cultivated on 2.4x2.5 cm glass cover slides, both coated with TiO_2 film and uncoated as the control. The cover slides were incubated in falcon tubes containing ABT minimal medium supplemented with 0.5% (w/v) glucose as carbon source (Alhede et al. 2009). The tubes were inoculated with an aliquot of a *P. aeruginosa* overnight culture grown in LB to obtain an optical density of 0.1 at 450 nm. The samples were incubated at 37°C under dark conditions to allow biofilm formation. Experiments were performed on 4-h old biofilm, to test TiO_2 effect on initial cells adhesions, and on 24-h old biofilm, to test its effect on young biofilm.

For the test with TiO_2 nanopowder, the biofilm was cultivated on sterile polycarbonate membrane filters (side, 2x2 cm; pore size, 0.2 µm; Whatman International Ltd. Maidstone) using the colony biofilm protocol by Anderl et al. (2000). Briefly, an overnight culture of *P. aeruginosa* was diluted in LB up to an optical density of 0.05 at 600 nm. Twenty-five µl of culture were used to inoculate all the membrane surface placed on LB plates. The plates were inverted and incubated at 37°C for 48 h, with the membrane-supported biofilms being transferred to fresh LB plates every 12 h.

Susceptibility tests of biofilm on TiO_2-coated glass cover slides

The biofilm on the cover slides were rinsed by SS to remove planktonic and loosely attached cells before the treatment. Both a solid-liquid and a solid-air system were tested.

In the solid-liquid system the uncovered and covered cover slides were transferred to new glass plates immersed in 15 ml of i) SS, ii) ABT minimal medium supplemented with 0.5% (w/v) glucose, and iii) ABT minimal medium without glucose. The oxygen amount dissolved in the media was measured by YSI DO200 dissolved oxygen meter (YSI Environmental) as reported by manufacturer's instructions.

In the solid-air system, glass cover slides were arranged on a plastic support in glass plates at 37°C. Placed at the bottom of the plates were 3 sheets of paper towel, first sponged by ultrapure water put and dampened every 12 h. In all the tests, the effect of the photocatalytic film was measured after 1, 4, 7 and 24 h for the solid-liquid system. In the tests with the solid-air system, the effect was measured after 1, 4, 5, 7, 9, 11, 13 and 24 h for the 24-h old biofilms and after 1, 4, 7 and 24 h for the 4-h old biofilms. At each time interval, a cover slide for each condition was removed from the plates, rinsed gently with SS to remove unattached cells, and transferred into a falcon tube with 15 ml NaCl 0.9% solution. The samples were then sonicated by the ultrasonic cleaner Branson 2510 (Bransonic, USA) to detach the cells from the surfaces. Each cell suspension was diluted serially and enumerated on LB agar plates using the drop plate method, as reported in previous experimental details.

As exopolysaccharides are the main component of *P. aeruginosa* EPS (Dunne 2002), the biofilm grown on the glass cover slides was washed with SS, then the polysaccharide fraction of EPS was labeled with Texas red-labeled Concanavalin A (ConA, Invitrogen) as per the manufacturer's instructions. After two washings with SS, the biofilm samples were visualized using a Leica TCSNT confocal laser scanning microscope with excitation filters at 488 nm and 568 nm, and emission filters at 530 nm and 590 nm (green and red channels). Images were captured with a 63x and a 40x oil immersion objective, and analyzed with the software Imaris (Bitplane Scientific Software, Switzerland).

Susceptibility test of biofilm with TiO_2 nanopowder

Membranes with 48-h old *P. aeruginosa* biofilms were transferred in fresh LB plates for testing. Three sheets of 2x2 cm tissue paper were placed on top of each *P. aeruginosa* biofilm. In the samples TiO_2+ UV+ and TiO_2+ UV- the tissue paper was moistened with 300

μl of 3g/l TiO_2 suspension in DW, in the samples TiO_2- UV+ and TiO_2- UV- the tissue paper was moistened with DW only. The effect of photoactivated TiO_2 nanopowder was measured after 1, 4, 7 and 24 h. At each predetermined time, a membrane-supported biofilm for each condition was placed in a falcon with 9.0 ml of SS and the mixture was vortexed at high speed for 2 min. The cell suspensions were then serially diluted and enumerated.

Statistical analyses

The mean values, standard errors of the means and variance analysis with ANOVA of all replicates were calculated using GraphPad Prism 4 and MATLAB 7.0 software to assess the significance of differences in the results collected at several time intervals. The bacterial counts were converted to a logarithmic scale before statistic treatment. In all experiments ANOVA was carried out separately for each test condition. Differences were considered significant with P-values < 0.05. Individual comparisons were made post-hoc with the Tukey-Kramer test. In the tests with only two times of measurement the significant variance was evaluated by T test (Student).

Results

Degradation tests on organic dye

Complete discoloration of rhoB solutions containing photoactivated TiO_2 in DW, UW, SS and PBS was already observed after 30 min. The spectrophotometric results confirmed the visual observation. In the presence of photoactivated TiO_2 we detected, just after 10 min, a significant decrease in rhoB concentration, between 71.7 and 86.7%, and after 30 min the degradation was almost complete in all the above media (P-values respectively $2.65343 \cdot 10^{-14}$, $2.78666 \cdot 10^{-14}$, $5.29798 \cdot 10^{-13}$ and 0). Degradation of rhoB in the presence of non-photoactivated TiO_2 was only between 3.4 and 13.8% after 10 min, and no discoloration was observed by the naked eye. Instead, no absorbance variations, or rhoB discoloration, were observed in the solutions without TiO_2, both irradiated with UV-A light and stored in dark. The degradation of rhoB/DW solutions are shown in figure 1 and 2.

In the case of the rhoB/PCB and rhoB/PCB-PBS solutions, we observed significant rhoB degradation in the presence of photoactivated TiO_2 only after 24 h (P-values respectively $1.08598 \cdot 10^{-9}$ and 0.0293). However, in this case, there was no discoloration observed and rhoB concentration decrease was about 35.4% in PCB and 17.4% in PCB-PBS, percentages much lower than those observed in the same conditions in the DW, UW, SS and PBS solutions, which showed approximately 100% decrease. In the presence of non-photoactivated TiO_2 and in the absence of the photocatalyst (both with and without UV-A light) no rhoB degradation was detected after 24 h of treatment.

The pH of the rhoB solutions in PBS, in PCB and in PCB-PBS was about 7 during the test, while in the rhoB solutions in DW, in UW and in SS the pH decreased respectively from 5.9 to 4.1, from 5.1 to 3.9 and from 6.3 to 5.6 in the presence of TiO_2.
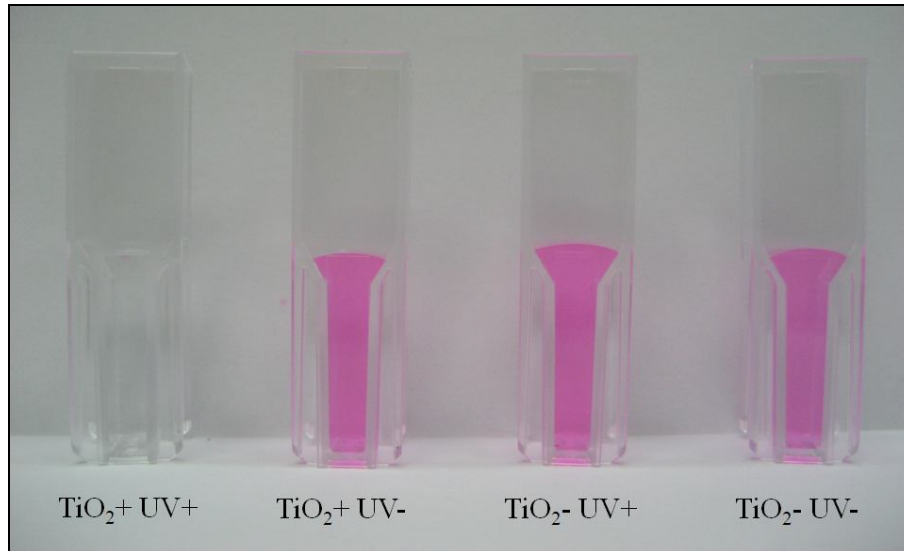
Figure 1 - *Discoloration of rhoB in DW solution caused by 3g/l photoactivated TiO$_2$ after 30 min of treatment compared to the control tests.*
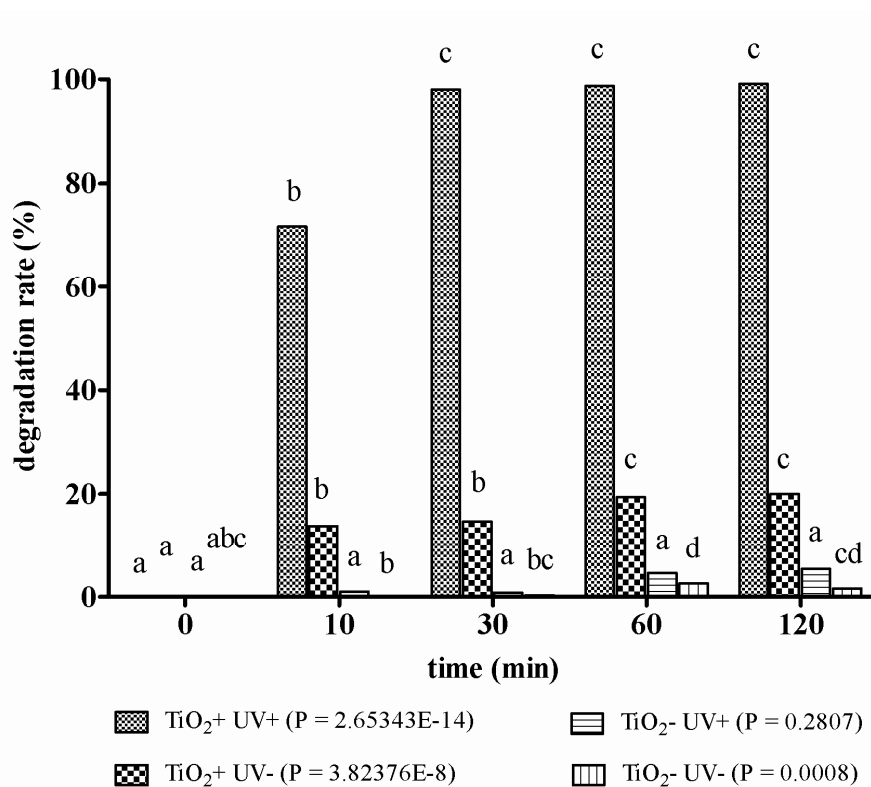

Figure 2 - *Degradation of rhoB in DW solution caused by 3g/l photoactivated TiO$_2$ and in the control tests. The graph provides the P-values obtained by ANOVA analysis. According to post-hoc analysis (Tukey-Kramer, P<0.05), means sharing the same letter do not differ significantly. The statistical analysis was performed separately for each experimental condition.*

Effect of photocatalytic TiO$_2$ nanopowder on planktonic cultures

The cellular activity of bacterial cultures in DW showed no significant changes during the tests under all conditions (P-values between 0.0711 and 0.8709), the exception being the sample TiO$_2$+ UV+ for *Bacillus* sp. culture where the P-values was 0.0003. However, in this case, the mean values of ATP per CFU did not differ form those detected in the controls. The ATP values of *Bacillus* sp., *P. stutzeri* and *P. aeruginosa* planktonic cells in DW were altogether between $2.5 \cdot 10^{-12}$ and $3.3 \cdot 10^{-5}$ nmol/CFU. Likewise, no significant variations were observed in the cultures in the PCB-PBS and LB-PBS media (P-values between 0.0665 and 0.3731), the exception being the samples TiO$_2$+ UV- for *Bacillus* sp. (P-value 0.0315) and TiO$_2$+ UV+ for *P. stutzeri* (P-value 0.0248) but, also in these cases, the values were not different from the controls. In cultural media, the ATP values of plankonic cells were altogether between $1.6 \cdot 10^{-11}$ and $3.5 \cdot 10^{-8}$ nmol/CFU.

Figure 3 shows the CFU/ml values from the tests with *Bacillus* sp., *P. stutzeri* and *P. aeruginosa* in DW. In the case of *Bacillus* sp., 1 log reduction of CFU/ml values was observed after 24 h only in presence of photoactivated TiO$_2$ compared to cultures with non-photoactivated TiO$_2$ and without photocatalyst (figure 3a).

When the *P. stutzeri* cultures were analyzed, photoactivated TiO$_2$ induced in 30 min a 6 log reduction of CFU/ml values, compared to those found in samples without TiO$_2$; the CFU/ml values were null after 2 h irradiation. Significant but less pronounced decreases of CFU/ml values were detected also in presence of non-photoactivated TiO$_2$ (4 log reduction after 30 min; P-value 0.0044). A 4-log decrease of CFU/ml was also verified in samples exposed to UV-A light without TiO$_2$ after 24 h (figure 3b).

The *P. aeruginosa* results exhibited the same trend as those of *P. stutzeri*. Significant CFU/ml decreases (1 log) were observed after 30 min in both TiO$_2$-containing systems (both lit and unlit, P-values respectively $5.72875 \cdot 10^{-14}$ and $3.44893 \cdot 10^{-6}$). Likewise, a stronger biocidal effect was observed after 2 h only in the sample with photoactivated TiO$_2$, with a significant reduction of 2 log units. After 24 h the CFU/ml values were null in the samples exposed to UV-A light, both in the presence and absence of the photocatalyst (figure 3c).

In cultures with PCB-PBS and LB-PBS no decrease of CFU/ml was observed. On the contrary, after 24 h there was a significant increase in CFU/ml (about 1 order of magnitude) for *Bacillus* sp. and *P. stutzeri* in all conditions (P-values respectively between 0.0014 and 0.0225, and between 0.0046 and 0.0339). The pH of *Bacillus* sp. and *P. stutzeri* cultures in DW varied between 5.9 and 6 in the absence of TiO$_2$ and between 4.8 and 5.6 with TiO$_2$, while that of *P. aeruginosa* cultures varied between 6.5 and 7.5, both with and without TiO$_2$. In the PCB-PBS and LB-PBS cultures the pH was between 6.5 and 7, both with and without TiO$_2$ for all strains.

Effect of photocatalytic film on P. aeruginosa planktonic cells

After 5 h photoactivation, TiO$_2$ thin film caused a significant decrease of approximately 2 orders of magnitude compared to the controls under dark condition, and no CFU were detected after 24 h (P-value 0) (figure 4). A significant reduction in viable cells was also observed after 24 h, also on uncoated illuminated cover slide (about 3 orders; P-value $1.11022 \cdot 10^{-16}$), however this decrease was intermediate between that induced by sample TiO$_2$+ UV+ and the control under dark condition. No reduction in viable cells was observed in unlit cover slides both uncoated and TiO$_2$-coated.

Effect of photocatalytic film and nanopowder on P. aeruginosa biofilms

In all the experiments with the solid-liquid system, we did not detect any decrease in the viable cell in the biofilms grown on glass cover slides, due to the presence of the

photocatalytic film, neither in 4-h old biofilm nor 24-h old biofilm (figure 5a and 5b and supporting information in Appendix 2, Figure SI 4). The oxygen amount present in the system was about 8.3 p.p.m. for all the experiments. With regard to the experiments with the solid-air system, in the 4-h old biofilm we observed, only after 24 h irradiation, a mild but significant reduction in viable cells on the cover slides with photocatalytic TiO_2 (P-value 0.0003). However the reduction was less than 1 order of magnitude compared to the control with UV-A alone. Instead, in the 24-h old biofilm there was a significant decrease in CFU/cm^2 (about 2 logs) on both the coated and the uncoated cover slides after 24 h irradiation with UV-A light (P-values respectively $1.11022 \cdot 10^{-16}$ and $6.89448 \cdot 10^{-13}$), compared to the unlit coverslides (figure 5c and 5d).

No reduction of viable cells per cm^2 in *P. aeruginosa* colony biofilms was caused by photoactivated TiO_2 nanopowders, compared to the controls with non-photoactivated TiO_2 and without photocatalyst (see supporting information in Appendix 2, Figure SI 3).

CLSM analysis of biofilm
Figure 6 shows 4-h old and 24-h biofilm observed using the CLSM. The 4-h old biofilm appeared as small agglomerates of cells attached to the surface, and exopolysaccharide production was almost absent (figure 6a). In this case, the cells are in an initial adhesion step (Van Houdt et al. 2005). The 24-h old biofilm (figure 6b) was constituted by bigger agglomerates of cells with a good production of exopolysaccharides. This is a young biofilm with early development of biofilm architecture (Van Houdt et al. 2005).
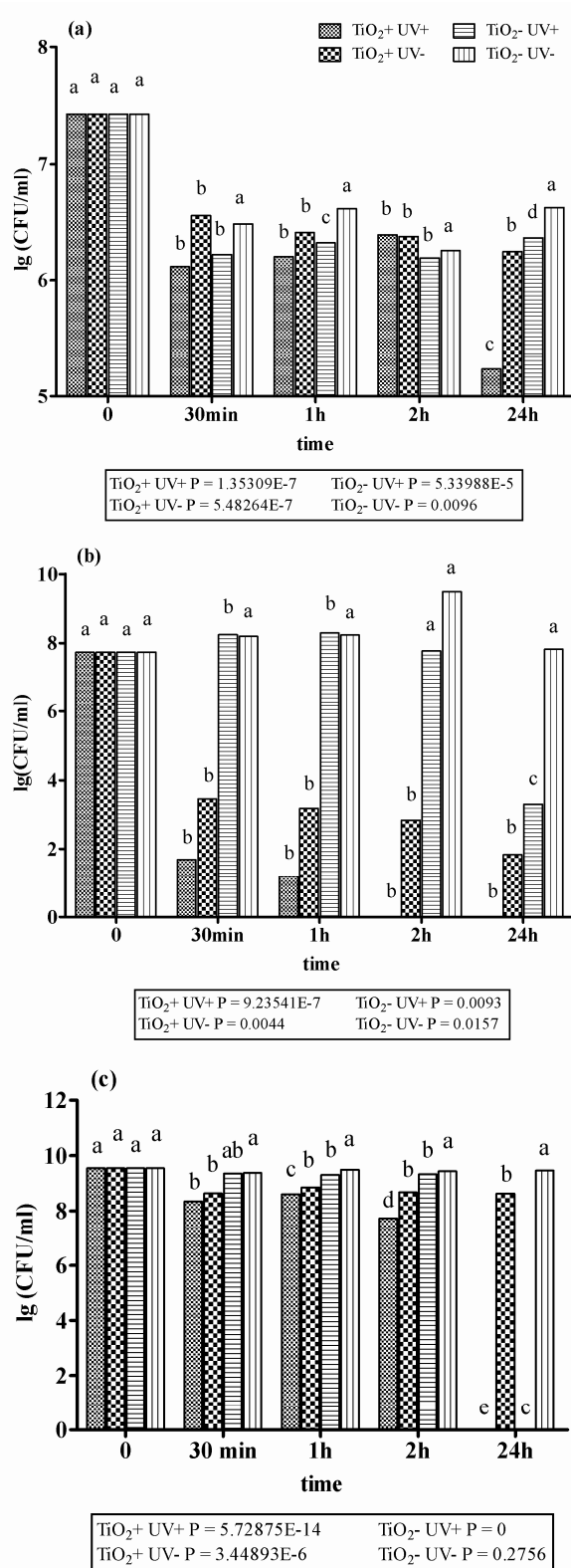
Figure 3 - *CFU/ml values obtained in the tests with photocatalytic TiO₂ nanopowder in DW and planktonic cells of (a) Bacillus sp., (b) P. stutzeri and (c) P. aeruginosa. The graphs provide the P-values obtained by ANOVA analysis. According to post-hoc analysis (Tukey-Kramer, P<0.05), means sharing the same letter are not significantly different from each other. The statistical analysis was performed separately for each experimental condition.*
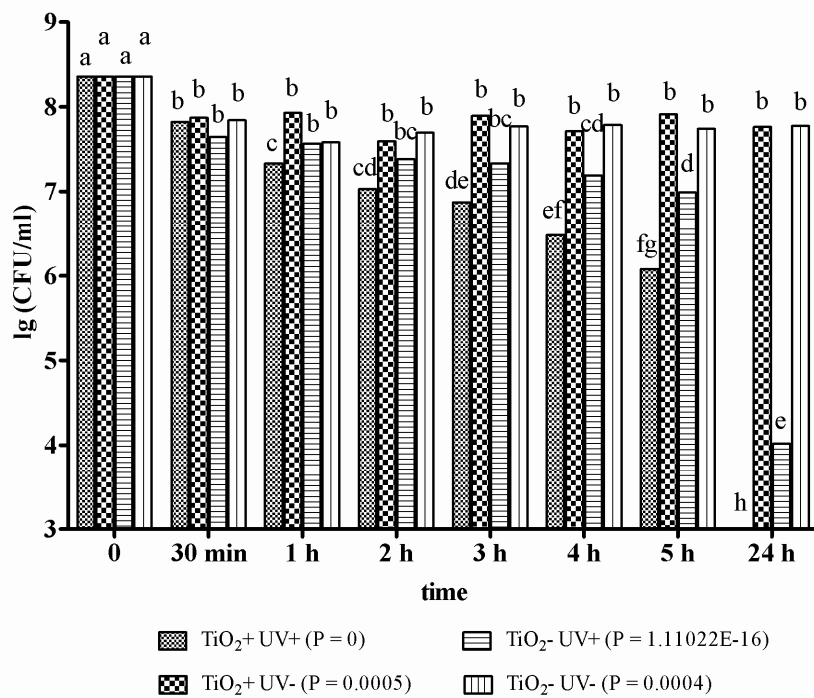
Figure 4 - *CFU/ml values of P. aeruginosa planktonic cells in DW obtained in the test with photocatalytic film. The graph provides the P-values obtained by ANOVA analysis. According to post-hoc analysis (Tukey-Kramer, P<0.05), means sharing the same letter do not differ significantly from each other. The statistical analysis was performed separately for each experimental condition.*

Figure 5 - *CFU/cm² values from the tests in solid-liquid system with SS solution with photocatalytic film and P. aeruginosa biofilm 4-h old (a) and 24-h old (b) and in solid-air system with 4-h old (c) and 24-h old (d) biofilm. The graphs provide the P-values obtained by ANOVA analysis. According to post-hoc analysis (Tukey-Kramer, P<0.05), means sharing the same letter did not differ significantly from each other. Statistical analysis was performed separately for each experimental condition.*
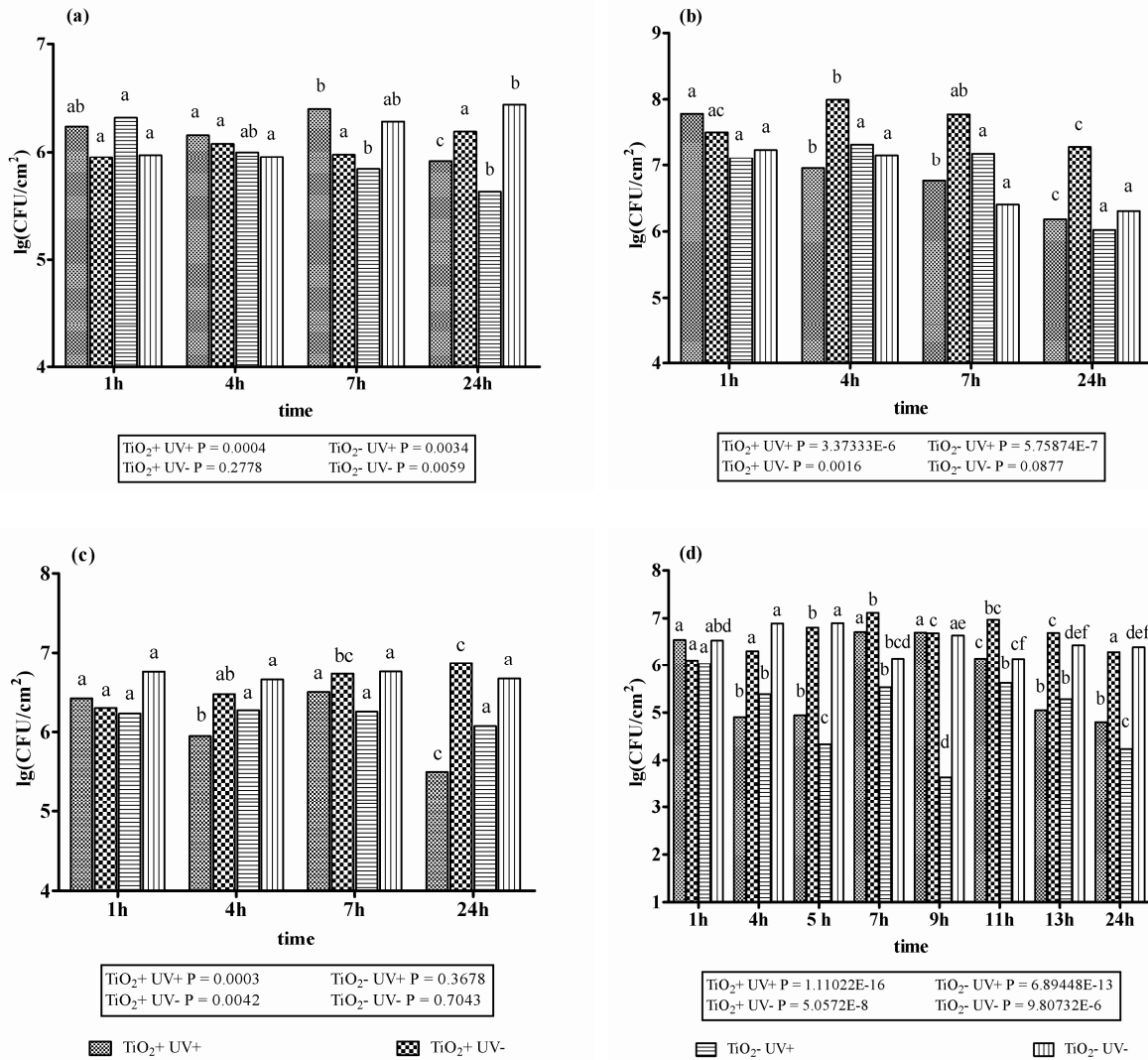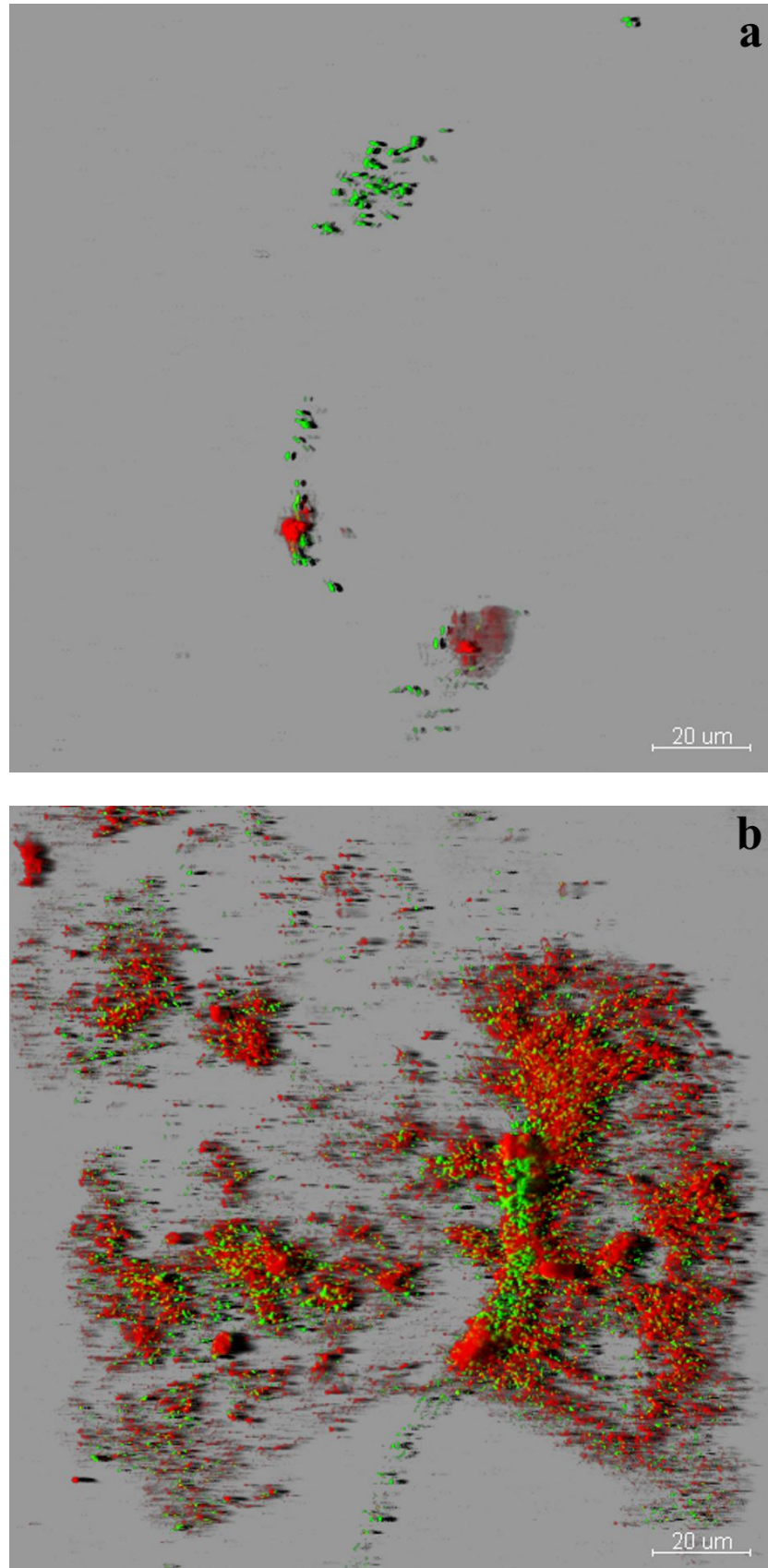
Figure 6 - *(a) 4-h old biofilm: initial cell adhesion step, (b) 24-h old biofilm. GFP-tagged P. aeruginosa shows green fluorescence and exopholysaccharides show red fluorescence.*

Discussion

In our study we employed Aeroxide P25 as the TiO$_2$ source for its widely reported excellent photocatalytic activity (Blake et al. 1999, Hurum et al. 2003, Allen et al. 2005, Verran et al. 2007).

Preliminary degradation tests were performed on rhoB, an organic dye, to set up an efficient operative protocol for use in testing on planktonic cells and on bacterial biofilms. The degradation of the rhoB chromophore structure causes the solution discoloration (Li et al. 2007), which can be observed by the naked-eye and measured by a spectrophotometer. In our experiments a UV-A light intensity of 3000 μW/cm^2 was used to simulate outdoor UV irradiation values during summer (Oka et al. 2008), in line with the similar intensities adopted to photoactivate TiO$_2$ in other works dealing with planktonic cells and biofilms (Koizumi et al. 2002, Li et al. 2005, Gage et al. 2005).

Our results proved that in the chosen experimental conditions the photoactivated TiO$_2$ successfully degraded the organic dye solutions in DW, UW, SS and PBS media: in fact, for all of these media, the rhoB was completely removed after 30 min, and complete discoloration was observed. Mild degradation of rhoB was also detected in the presence of non-photoactivated TiO$_2$ after 10 min of treatment, but no discoloration was observed by the naked eye. Furthermore, after this initial decrease, the absorbance values remained constant throughout the test, and this was probably due to a photosensitization mechanism: rhoB molecules absorb visible light, which causes the molecules photoexcitation, and the exciton transfers easily to TiO$_2$ nanoparticles onto which rhoB is adsorbed, causing the molecule degradation (Wu et al. 2004, Wu et al. 2006). As observed by the slight absorbance decrease, this mechanism has very poor degradation efficiency. This hypothesis of a photosensitization mechanism was also proposed by Li et al. (2007) who observed a slower degradation of rhoB solutions by TiO$_2$, also under visible light irradiation. Note, however, that UV-A light produced no effect. The results observed with the rhoB/DW solutions indicate a fast degradation of the organic dye, caused by the P25 TiO$_2$ dispersion exposed to UV-A light: again, this is in agreement with data reported by Li et al. (2007), and by Gage et al. (2005), who verified an analogous degradation of formic acid and glucose solutions by photocatalytic TiO$_2$ coatings. On the contrary, rhoB/PCB and rhoB/PCB-PBS solutions underwent much slower degradation than in the previously cited cases. A slight degradation non-appreciable by the naked-eye, was measured only after 24 h, and rhoB in PCB-PBS degraded slower that in PCB alone. This was ascribed to the organic component of the PCB, which could itself be a target of photocatalytic degradation activity of TiO$_2$, thus the presence of a competitive reaction slowed down the rhoB degradation. In addition, according to Blake et al. (1999) and Gage et al. (2005), phosphates, which are present in PBS, can further reduce the photocatalyst performance. However, in the experiments described here, rhoB degradation in PBS-solution happened just as fast as in DW, UW and SS-solutions. We can only assume that in these systems the measurement times were spaced out, and did not allow the degradation slowdown to be noted, as happened in the experiments with the cultural medium.

The pH decrease in rhoB/DW, rhoB/UW and rhoB/SS solutions with TiO$_2$ nanopowder was clearly caused by the photocatalyst addition. Nevertheless, the similar results obtained using the cited media and PBS demonstrated that, in the chosen conditions, the photocatalyst was just as efficient at different pHs, as reported by Neppolian et al. (2002).

DW was chosen for the tests on planktonic growth to eliminate any interference with the process by anions and organic compounds, as suggested by Blake et al. (1999), and to minimize the effects of osmotic pressure on bacterial cells compared with UW. The investigation was focused on both Gram-positive (*Bacillus* sp.) and Gram-negative (*P.*

stutzeri and *P. aeruginosa*) microorganisms due to evidence that the cell wall is a prime target of TiO_2 photoactivity (Huang et al. 2000, Amézaga-Madrid et al. 2003, Gopal et al. 2004). In addition, these strains had previously been isolated from environmental biofilms (Wagner et al. 2008, Villa et al. 2009, Myszka et al. 2009). The chosen UV-A light intensity was selected as the result of the degradation tests with rhoB. However, in experiments with *P. aeruginosa*, lower $\mu W/cm^2$ intensities were used as a consequence of the cell susceptibility to UV-A light alone. Fernández et al. (1996) reported that similar high UV-A intensities lead to consistent photodamage in *P. aeruginosa* cells, resulting in cell death, and demonstrated that such damage decreases slightly with light intensities lower than 1400 $\mu W/cm^2$. In any case, UV-A intensities always greater than 1 $\mu W/cm^2$ were used, which is sufficient to start the photocatalytic reaction reported by Oka et al. (2008).

The biocidal activity of photoactivated TiO_2 was evident in planktonic *P. stutzeri*, *P. aeruginosa* and *Bacillus* sp. after 30 min, 2 h and after 24 h respectively. These results are in agreement with studies by several authors who have reported the photocatalytic inactivation of *Escherichia coli, P. stutzeri*, *P. aeruginosa*, *Serratia marcescens*, *Staphylococcus aureus*, *Clostridium perfringens* spores, *Salmonella* ssp., *Streptococcus* spp., *Lactobacillus acidophilus*, *Actinomyces viscosus*, *Bacillus* spp., *Vibrio parahaemolyticus*, *Listeria monocytogenes* and coliform bacteria in analogous conditions (Rincon et al. 2003, Kim et al. 2003, Gage et al. 2005, Rizzo 2009). In contrast, TiO_2, both lit and unlit, had no effect on bacterial activity of *P. stutzeri*, *P. aeruginosa* and *Bacillus* sp. cultures. This proves that in our conditions TiO_2, if photoactivated, promotes only biocidal activity toward bacterial planktonic cells. In *P. stutzeri* and *P. aeruginosa* cultures with non-photoactivated TiO_2 there was also an intermediate decrease in CFU/ml. For *P. stutzeri* this reduction can be put down to the fall in pH due to the addition of the photocatalyst (Lalucat et al. 2006). However, this finding cannot be explained only by the drop in pH since, in *P. aeruginosa* cultures, the pH did not change when the photocatalyst was added. The CFU/ml decrease is also due to the weak photoactivation of the photocatalyst by the UV-A component of the white light that lit the samples during the test arrangement (Li et al. 2007). In addition, Gopal et al. (2004) and Liu et al. (2010) have suggested that Gram negative bacteria are more susceptible to photoactivated TiO_2 because it causes the breaking of the outer lipopolysaccharide membrane. Also *P. stutzeri* and *P. aeruginosa* cultures without TiO_2 but exposed to UV-A light respectively showed an intermediate decrease (4 orders of magnitude) of CFU/ml and the total inactivation of CFU/ml after 24 h. These results proved that UV-A light per se has a biocidal activity on *Pseudomonas* spp. after long exposition time, as also reported by Fernández et al. (1996) and Gage et al. (2005).

Similarly to the rhoB results, the photoactivated TiO_2 did not exhibit activity in the cultural media: no cellular activity reduction or bacterial count decrease was observed in the *Bacillus sp.*, *P. stutzeri* and *P. aeruginosa* cultures in PCB-PBS and LB-PBS. Likewise, the lack of photocatalytic activity was ascribed to the organic component of media and to phosphates. In addition, in this case, two others factors must be considered: i) in the culture media the cell growth can be faster than the photocatalytic inactivation, and ii) bacterial cells, as they grow, screen the UV-A light, minimizing the TiO_2 photoactivation.

In our study both photoactivated TiO_2 nanopowders and thin film easily killed *P. aeruginosa* planktonic cells. This efficiency on a TiO_2-coated surface exposed to UV-A is significantly higher than that due to UV-A alone. These results with photocatalytic film were in agreement with those reported by Tao et al. (2004), Gage et al. (2005) and Cheng et al. (2008) in analogous experiments with *P. aeruginosa*, *E. coli*, *Streptococcus iniae* and *Edwardsiella tarda*. In addition, unlit TiO_2 coatings did not start photocatalytic reaction as no inactivation

was produced on the TiO_2+ UV- control; conversely, the presence of TiO_2 nanopowders dispersed in solution had an effect even without UV irradiation.

Here, for the first time, *P. aeruginosa* was used to test the effect of TiO_2 nanopowders and photocatalytic thin film produced by sol-gel on biofilm. *P. aeruginosa* was chosen as it is widely considered to be a model organism for studying bacterial biofilms (Wozniak et al. 2003). In biofilm testing the system most utilized is that of a solid-liquid, so this was the system we adopted (Li et al. 2005, Raulio et al. 2006, Ciston et al. 2009). We also tested a solid-air system as it reproduces conditions similar to applications in open air. In both systems the photocatalytic treatment had neither biocidal nor antifouling effects (compared to controls), the exception being the 4-h old biofilm at the solid-air interface after 24 h of treatment (figure 5c). In this case there was a decrease, but only a slight one, in cell concentration (less than 1 order of magnitude) compared to UV-A alone. The susceptibility test of the *P. aeruginosa* biofilm in the presence of TiO_2 nanopowders confirmed the results obtained with TiO_2 immobilized film, and demonstrated the inefficiency of photocatalytic nanopowders in killing biofilm cells, in spite of the commonly recognized outstanding photoactivity of P25 (Bowering et al. 2006, Schmidt et al. 2007). Gage et al. (2005) also observed that photocatalytic treatment, compared to UV-A treatment alone, did not enhance killing in *P. aeruginosa* biofilm. Li et al. (2005) showed that TiO_2 film exposed to UV-A light produced decreased surface hydrophobicity, reducing the bacterial adhesion of *P. aerugionosa*, *E. coli*, *B. cepacia* and *B. subtilis* without killing cells, while UV light exposure had a killing effect. The results presented here differ from some cases reported by other authors in analogous studies on TiO_2 and bacterial biofilm. Rajagopal et al. (2006) observed a 4-log reduction of CFU/cm^2 in a natural biofilm, after 10 min of irradiation, due to the presence of the photocatalyst. However, this study investigated only two conditions: the co-presence of photoactivated TiO_2 and biofilm, and the evolution of only the biofilm stored under dark conditions, thus avoiding any consideration of the biocidal effect of UV light itself. Ciston et al. (2008 and 2009) observed that the photoreactive coating produced from a mix of different TiO_2 phases was effective to control *P. putida* biofilm on ceramic ultrafiltration membranes. However, in these papers, the TiO_2 coating led only to a reduction in surface hydrophobicity and cell attachment, while cell inactivation was brought about by UV-A light.

Gage et al. (2005) discussed possible explanations for the inefficiency of photocatalytic action on biofilm: 1) the presence of phosphates that could block active sites on the catalyst surface, or scavenge oxidative radicals produced at the surface; 2) insufficient presence of O_2 at the TiO_2 surface to maintain charge transfer in photocatalytic reactions; 3) biofilm or planktonic cells growing in the medium screen UV-A light, deactivating TiO_2; 4) insufficient build-up of photocatalytically generated reactive species necessary for cell inactivation; 5) genetic response of attached cells to oxidative stress.

In the experimental work described here, phosphates could have inhibited the photocatalytic reactions in the solid-liquid system experiments in ABT medium, but no phosphate was present in the SS medium or in the solid-air system, so the first explanation was discarded. In both the solid-liquid and solid-air systems the amount of oxygen was not a limiting factor, since the oxygen dissolved in the liquid media was about 8.3 p.p.m, sufficient for TiO_2 photoactivation as reported by Gage et al. (2005). In addition, observations with the confocal laser scanning microscope showed that the biofilm existed mainly as small colonies of cell (4-h old biofilm) or bigger agglomerates (24-h old biofilm) attached to the surface (figure 6). We therefore concluded that, as the surface was not fully covered, the biofilm was providing a poor screen for the oxygen and UV-A light to reach the cover slide surface. Also exopolysaccharides, which have been suggested to prevent antimicrobials access to cells

embedded in the community (Mah et al. 2001), were not responsible for the failed inhibition as they were almost absent in the 4-h old biofilm. Finally, in the solid-liquid system the cover slides were immersed in the medium ensuring a sufficiently high build-up of the reactive oxygen species (according to Kikuchi et al. 1997), and in the solid-air system there was no dilution or removal of reactive species to be taken into account.

Mah et al. (2001) reported that biofilm cells are protected from the penetration of hydrogen peroxide (one of the reactive oxygen species produced by photoactivated TiO$_2$) because of its catalase-mediated destruction, rather than by the exopolysaccharide barrier. A study by Cochran et al. (2000) demonstrated that *P. aeruginosa* cells modify gene expression when they adhere to a surface and evolve in a biofilm, and that some of the resulting gene products increase cell tolerance to antimicrobial agents, including oxidative biocides such as monochloramine and hydrogen peroxide. Some genes controlled by quorum sensing (QS) are known to be involved in the H$_2$O$_2$ resistance of biofilm-grown cells (Davies et al. 1998, Bjarnsholt et al. 2005). In fact, several authors observed that, when challenged with H$_2$O$_2$, biofilm bacteria display reduced susceptibility to disinfection (Costerton et al. 1995, Elkins et al. 1999). Elkins et al. (1999) demonstrated that this is partially explained by the enhanced catalase levels in *P. aeruginosa* biofilm cells compared to the planktonic state. However, experiments with *P. aeruginosa* biofilm by Hassett et al. (1999) revealed that there are other important H$_2$O$_2$ resistance mechanisms that may be unique to biofilm cells and controlled by QS.

On the basis of this literature survey, we came to the conclusion that the only possible explanation for the lack of cell inactivation is that sessile cells have increased resistance to the reactive oxygen species generated by photoactivated TiO$_2$. Further studies on the development of resistance to reactive oxygen species related to gene expression in bacterial biofilm may provide ways to better understand the resistance mechanisms against photocatalytic TiO$_2$, thus allowing a step forward in the search for efficient surface coating methods able to prevent the formation of biofilms or, at least, to interfere with their inconvenient high biocide resistance.

Conclusions

Biofilm often have a detrimental effect on colonized surfaces and materials generating tremendous environmental and economical problems for human society. Their eradication represents today a hard problem due to the ineffectiveness or to the low safety for human beings and the environment of traditional biocide-based strategies. Consequently, the development of new safer control strategies is a necessary goal. Photocatalytic TiO$_2$ is considered a promising alternative to traditional biocide for the biofilm control and prevention. This work shows that TiO$_2$ suspended as powder in solution, or immobilized on a surface by sol-gel method, if photoactivated, really produces significant reductions of viable cells in *P. stutzeri*, *P. aeruginosa* and *Bacillus* sp. planktonic cultures, compared to the controls with non-photoactivated TiO$_2$, with UV-A light alone and without TiO$_2$ and UV-A light. Despite that, neither the photocatalytic treatment with TiO$_2$ film nor that with TiO$_2$ nanopowder had any effect on *P. aeruginosa* cells when they life in sessile form at both solid-liquid and solid-air interfaces. Our tests suggest that the only possible explanation for the failure of photocatalytic killing is an enhanced tolerance of sessile cells to the reactive oxygen species generated by photoactivated TiO$_2$. Therefore, the findings reported here lead to revalue the potential of TiO$_2$ as solution to eradicate deleterious bacterial biofilm.

Supporting information available

Additional Figures and Graphs are provided in Appendix 2.

References

Akpan U. G., Hameed B. H. (2010). The advancements in sol-gel method of doped-TiO_2 photocatalysts. *Appl Catal* A-*Gen*, 375, 1–11.

Alhede M. Bjarnsholt T., Jensen P. Ø., Phipps R. K., Moser C., Christophersen L., Christensen L. D., van Gennip M., Parsek M., Høiby N., Rasmussen T. B., Givskov M. (2009). Pseudomonas aeruginosa recognizes and responds aggressively to the presence of polymorphonuclear leukocytes. *Microbiology*, 155, 3500–3508.

Allen N. S., Edge M., Sandoval G., Verran J., Stratton J., Maltby J. (2005). Photocatalytic coatings for environmental applications. *Photochem Photobiol*, 81, 279–290.

Amézaga-Madrid P., Silveyra-Morales R., Córdoba-Fierro L., Nevarez-Moorillón G. V., Miki-Yoshida M., Orrantia-Borunda E., Solís F. J. (2003). TEM evidence of ultrastructural alteration on Pseudomonas aeruginosa by photocatalytic TiO_2 thin films. *J Photoch Photobio* B, 70, 45–50.

Anderl J. N., Franklin M. J., Stewart P. S. (2000). Role of antibiotic penetration limitation in klebsiella pneumonia biofilm resistance to ampicillin and ciprofloxacin. *Antimicrob Agents Ch*, 44, 1818–1824.

Banerjee S., Gopal J., Muraleedharan P., Tyagi A. K., Raj B. (2006). Physics and chemistry of photocatalytic titanium dioxide: visualization of bactericidal activity using atomic force microscopy. *Curr Sci India*, 90, 1378–1383.

Bjarnsholt T., Jensen P. Ø., Burmølle M., Hentzer M., Haagensen J. A. J., Hougen H. P., Calum H., Madsen K. G., Moser C., Molin S., Høiby N., Givskov M. (2005). Pseudomonas aeruginosa tolerance to tobramycin, hydrogen peroxide and polymorphonuclear leukocytes is quorum-sensing dependent. *Microbiology*, 151, 373–383.

Bjarnsholt T., Tolker-Nielsen T., Høiby N., Givskov M. (2010). Interference of Pseudomonas aeruginosa signalling and biofilm formation for infection control. *Expet Rev Mol Med*, 12, e11, doi: 10.1017/S1462399410001420.

Blake D. M., Maness P.-C., Huang Z., Wolfrum E. J., Huang J. (1999). Application of the photocatalytic chemistry of titanium dioxide to disinfection and the killing of cancer cells. *Separ Purif Method*, 28, 1–50.

Bowering N., Walker G. S., Harrison P. G. (2006). Photocatalytic decomposition and reduction reactions of nitric oxide over Degussa P25. *Appl Catal* B-*Environ*, 62, 208–216.

Cappitelli F., Abbruscato P., Foladori P., Zanardini E., Ranalli G., Principi P., Villa F., Polo A., Sorlini C. (2009). Detection and elimination of cyanobacteria from frescoes: the case of the St. Brizio Chapel (Orvieto Cathedral, Italy). *Microb Ecol*, 57, 633–639.

Chawengkijwanich C., Hayata Y. (2008). Development of TiO_2 powder-coated food packaging film and its ability to inactivate Escherichia coli in vitro and in actual tests. *Int J Food Microbiol*, 123, 288–292.

Cheng T. C., Chang C. Y., Chang C. I., Hwang C. J., Hsu H. C., Wang D. Y., Yao K. S. (2008). Photocatalytic bactericidal effect of TiO_2 film on fish pathogens. *Surf Coat Tech*, 203, 925–927.

Chen J., Poon C.-S. (2009). Photocatalytic construction and building materials: from fundamentals to applications. *Build Environ*, 44, 1899–1906.

Ciston S., Lueptow R. M., Gray K. A. (2008). Bacterial attachment on reactive ceramic ultrafiltration membranes. *J Membrane Sci*, 320, 101–107.

Ciston S., Lueptow R. M., Gray K. A. (2009). Controlling biofilm growth using reactive ceramic ultrafiltration membranes. *J Membrane Sci*, 342, 263–268.

Cochran W. L., McFeters G. A., Stewart P. S. (2000). Reduced susceptibility of thin Pseudomonas aeruginosa biofilms to hydrogen peroxide and monochloramine. *J Appl Microbiol*, 88, 22–30.

Coleman H. M., Marquis C. P., Scott J. A., Chin S.-S., Amal R. (2005). Bactericidal effects of titanium dioxide-based photocatalysts. *Chem Eng J*, 113, 55–63.

Costerton J. W., Lewandowski Z., Caldwell D. E., Korbe D. R., Lappin-Scott H. M. (1995). Microbial biofilms. *Annu Rev Microbiol*, 49, 711–745.

Davies D. G., Parsek M. R., Pearson J. P., Iglewski B. H., Costerton J. W., Greenberg E. P. (1998). The involvement of cell-to-cell signals in the development of a bacterial biofilm. *Science*, 280, 295–298.

Dunne W. M. Jr. (2002). Bacterial adhesion: seen any good biofilms lately? *Clin Microbiol Rev*, 15, 155–166.

Elkins J. G., Hassett D. J., Stewart P. S., Schweizer H. P., McDermott T. R. (1999). Protective role of catalase in Pseudomonas aeruginosa biofilm resistance to hydrogen peroxide. *Appl Environ Microb*, 65, 4594–4600.

Fernández R. O., Pizarro R. A. (1996). Lethal effect induced in Pseudomonas aeruginosa exposed to ultraviolet-A radiation. *Photochem Photobiol*, 64, 333–339.

Flemming H.-C. (2002). Biofouling in water systems – cases, causes and countermeasures. *Appl Microbiol Biot*, 59, 629–640.

Gage J. P., Roberts T. M., Duffy E. J. (2005). Susceptibility of Pseudomonas aeroginosa biofilm to UV-A illumination over photocatalytic and non-photocatalytic surfaces. *Biofilms*, 2, 155–163.

Giraldo A. L., Peñuela G. A., Torres-Palma R. A., Pino N. J., Palominos R. A., Mansilla H. D. (2010). Degradation of the antibiotic oxolinic acid by photocatalysis with TiO_2 in suspension. *Water Res*, 44, 5158–5167.

Gopal J., George R. P., Muraleedharan P., Khatak H. S. (2004). Photocatalytic inhibition of microbial adhesion by anodized titanium. *Biofouling*, 20, 167–175.

Gupta R., Kumar A. (2008). Bioactive materials for biomedical applications using sol–gel technology. *Biomed Mater*, 3, doi: 10.1088/1748-6041/3/3/034005.

Hamal D. B., Haggstrom J. A., Marchin G. L., Ikenberry M. A., Hohn K., Klabunde K. J. (2010). A multifunctional biocide/sporocide and photocatalyst based on titanium dioxide (TiO_2) codoped with silver, carbon, and sulfur. *Langmuir*, 26, 2805–2810.

Hassett D. J., Ma J.-S., Elkins J. G., McDermott T., Ochsner U. A., West S. E. H., Huang C.-T., Fredericks J., Burnett S., Stewart P. S., McFeters G., Passador L., Iglewski B. H. (1999). Quorum sensing in Pseudomonas aeruginosa controls expression of catalase and superoxide dismutase genes and mediates biofilm susceptibility to hydrogen peroxide. *Mol Microbiol*, 34, 1082–1093.

Hazan Z., Zumeris J., Jacob H., Raskin H., Kratysh G., Vishnia M., Dror N., Barliya T., Mandel M., Lavie G. (2006). Effective prevention of microbial biofilm formation on medical devices by low-energy surface acoustic waves. *Antimicrob Agents Ch*, 50, 4144–4152.

Hoffmann M. R., Martin S. T., Choi W., Bahnemann D. W. (1995). Environmental applications of semiconductor photocatalysis. *Chem Rev*, 95, 69–96.

Huang Z., Maness P.-C., Blake D. M., Wolfrum E. J., Smolinski S. L., Jacoby W. A. (2000). Bactericidal mode of titanium dioxide photocatalysis. *J Photoch Photobio* A, 130, 163–170.

Hurum D. C., Agrios A. G., Gray K. A., Rajh T., Thurnauer M. C. (2003). Explaining the enhanced photocatalytic activity of Degussa P25 mixed-phase TiO_2 using EPR. *J Phys Chem* B, 107, 4545–4549.

Høiby N., Bjarnsholt T., Givskov M., Molin S., Ciofu O. (2010). Antibiotic resistance of bacterial biofilms. *Int J Antimicrob Ag*, 35, 322–332.

Ingle J. D. J., Crouch S. R. (1988). Spectrochemical Analysis (Englewood Cliffs/Prentice Hall), 372–381.

Kikuchi Y., Sunada K., Iyoda T., Hashimoto K., Fujishima A. (1997). Photocatalytic bactericidal effect of TiO_2 thin films: dynamic view of the active oxygen species responsible for the effect. *J Photoch Photobio* A, 106, 51–56.

Kim B., Kim D., Cho D., Cho S. (2003). Bactericidal effect of TiO_2 photocatalyst on selected food-borne pathogenic bacteria. *Chemosphere*, 52, 277–281.

Koizumi Y., Taya M. (2002). Kinetic evaluation of biocidal activity of titanium dioxide against phage MS2 considering interaction between the phage and photocatalyst particles. *Biochem Eng J*, 12, 107–116.

Lalucat J., Bennasar A., Bosch R., García-Valdés E., Palleroni N. J. (2006). Biology of Pseudomonas stutzeri. *Microbiol Mol Biol R*, 70, 510–547.

Li B., Logan B. E. (2005). The impact of ultraviolet light on bacterial adhesion to glass and metal oxide-coated surface. *Colloid Surface* B, 41, 153–161.

Li J., Ma W., Chen C., Zhao J., Zhu H., Gao X. (2007). Photodegradation of dye pollutants on one-dimensional TiO_2 nanoparticles under UV and visible irradiation. *J Mol Catal A-Chem*, 261, 131–138.

Liu P., Duan W., Wang Q., Li X. (2010). The damage of outer membrane of Escherichia coli in the presence of TiO_2 combined with UV light. *Colloid Surface* B, 78, 171–176.

Lomer M. C., Thompson R. P., Powell J. J. (2002). Fine and ultrafine particles of the diet: influence on the mucosal immune response and association with Crohn's disease. *P Nutr Soc*, 61, 123–130.

Mah T.-F. C., O'Toole G. A. (2001). Mechanisms of biofilm resistance to antimicrobial agents. *Trends Microbiol*, 9, 34–39.

Malato S., Fernández-Ibáñez P., Maldonado M. I., Blanco J., Gernjak W. (2009). Decontamination and disinfection of water by solar photocatalysis: Recent overview and trends. *Catal Today*, 147, 1–59.

Maness P. C., Smolinski S., Blake D. M., Huang Z., Wolfrum E. J., Jacoby W. A. (1999). Bactericidal activity of photocatalytic TiO_2 reaction: toward an understanding of its killing mechanism. *Appl Environ Microb*, 65, 4094–4098.

Myszka K., Czaczyk K. (2009). Characterization of adhesive exopolysaccharide (EPS) produced by Pseudomonas aeruginosa under starvation conditions. *Curr Microbiol*, 58, 541–546.

Neppolian B., Choi H. C., Sakthivel S., Arabindoo B., Murugesan V. (2002). Solar light induced and TiO_2 assisted degradation of textile dye reactive blue 4. *Chemosphere*, 46, 1173–1181.

Nonami T., Hase H., Funakoshi K. (2004). Apatite-coated titanium dioxide photocatalyst for air purification. *Catal Today*, 96, 113–118.

Oka Y., Kim W.-C., Yoshida T., Hirashima T., Mouri H., Urade H., Itoh Y., Kubo T. (2008). Efficacy of titanium dioxide photocatalyst for inhibition of bacterial colonization on percutaneous implants. *J Biomed Mater Res* B, 86B, 530–540.

Padovani L., Trevisan M., Capri E. (2004). A calculation procedure to assess potential environmental risk of pesticides at the farm level. *Ecol Indic*, 4, 111–123.

Rajagopal G., Maruthamuthu S., Mohanan S., Palaniswamy N. (2006). Biocidal effects of photocatalytic semiconductor TiO$_2$. *Colloid Surface* B, 51, 107–111.

Raulio M., Pore V., Areva S., Ritala M., Leskela M., Lindén M., Rosenholm J. B., Lounatmaa K., Salkinoja-Salonen M. (2006). Destruction of Deinococcus geothermalis biofilm by photocatalytic ALD and sol-gel TiO$_2$ surfaces. *J Ind Microbiol Biot,* 33, 261–268.

Rincon A. G., Pulgarin C. (2003). Photocatalytical inactivation of E. coli: effect of (continuous–intermittent) light intensity and of (suspended–fixed) TiO$_2$ concentration. *Appl Catal* B-*Environ*, 44, 263–284.

Rizzo L. (2009). Inactivation and injury of total coliform bacteria after primary disinfection of drinking water by TiO$_2$ photocatalysis. *J Hazard Mater*, 165, 48–51.

Schmidt C. M., Buchbinder A. M., Weitz E., Geiger F. M. (2007). Photochemistry of the indoor air pollutant acetone on Degussa P25 TiO$_2$ studied by chemical ionization mass spectrometry. *J Phys Chem* A, 111, 13023–13031.

Simões M., Simões L. C., Vieira M. J. (2010). A review of current and emergent biofilm control strategies. *Lebensm-Wiss Technol*, 43, 573–583.

Stewart P. S., Franklin M. J. (2008). Physiological heterogeneity in biofilms. *Nat Rev Microbiol*, 6, 199–210.

Tao H., Wei W., Zhang S. (2004). Photocatalytic inhibitory effect of immobilized TiO$_2$ semiconductor on the growth of Escherichia coli studied by acoustic wave impedance analysis. *J Photoch Photobio* A, 161, 193–199.

Van Houdt R., Michiels C. W. (2005). Role of bacterial cell surface structures in Escherichia coli biofilm formation. *Res Microbiol*, 156, 626–633.

Vermeire T., Rikken M., Attias L., Boccardi P., Boeije G., Brooke D., de Bruijn J., Comber M., Dolan B., Fischer S., Heinemeyer G., Koch V., Lijzen J., Müller B., Murray-Smith R., Tadeo J. (2005). European union system for the evaluation of substances: the second version. *Chemosphere*, 59, 473–485.

Verran J., Sandoval G., Allen N. S., Edge M., Stratton J. (2007). Variables affecting the antibacterial properties of nano and pigmentary titania particles in suspension. *Dyes Pigments*, 73, 298–304.

Villa F., Giacomucci L., Polo A., Principi P., Toniolo L., Levi M., Turri S., Cappitelli F. (2009). N-vanillylnonanamide tested as a non-toxic antifoulant, applied to surfaces in a polyurethane coating. *Biotechnol Lett*, 31, 1407–1413.

Wagner V. E., Iglewski B. H. (2008). P. aeruginosa biofilms in CF infection. *Clin Rev Allerg Immu*, 35, 124–134.

Walker T. S., Bais H. P., Déziel E., Schweizer H. P., Rahme L. G., Fall R., Vivanco J. M. (2004). Pseudomonas aeruginosa-plant root interactions. Pathogenicity, biofilm formation, and root exudation. *Plant Physiol,* 134, 320–331.

Walsh S. E., Maillard J.-Y., Russell A. D., Catrenich C. E., Charbonneau D. L., Bartolo R. G. (2003). Development of bacterial resistance to several biocides and effects on antibiotic susceptibility. *J Hosp Infect*, 55, 98–107.

Wang G.-J., Chou S.-W. (2010). Electrophoretic deposition of uniformly distributed TiO$_2$ nanoparticles using an anodic aluminum oxide template for efficient photolysis. *Nanotechnology*, 21, doi:10.1088/0957-4484/21/11/115206.

Wozniak D. J., Wyckoff T. J. O., Starkey M., Keyser R., Azadi P., O'Toole G. A., Parsek M. R. (2003). Alginate is not a significant component of the extracellular polysaccharide matrix of PA14 and PAO1 Pseudomonas aeruginosa biofilms. *Proc Natl Acad Sci USA PNAS*, 100, 7907–7912.

Wu J.-M., Zhang T.-W. (2004). Photodegradation of rhodamine B in water assisted by titania films prepared through a novel procedure. *J Photoch Photobio* A, 162, 171–177.

Wu J.-M., Huang B., Zeng Y.-H. (2006). Low-temperature deposition of anatase thin films on titanium substrates and their abilities to photodegrade Rhodamine B in water. *Thin Solid Films*, 497, 292–298.

Conclusion

Today, although their hazardous effect on human health and the environment, biocides remain the most used way to remove deleterious microbial biofilms from abiotic surfaces. Therefore, it is vital to achieve a more sustainable use of traditional practices.
On the base of our work we concluded that:

➢ The study and characterization of microbial communities in alterative biofilms permit to select a suitable biocidal product with a specific target from the "biocides menu" that removes efficiently most of identified deteriogen taxa.

➢ In our case-study, likely not infrequent in nature, biofilms were composed by a large taxonomical variety. Therefore, we have been forced to choose a biocide with a broad spectrum of activity, doing the opposite of the initial purpose.

Other results of our study about the feasibility of removing surface deposits on stone using biological and chemical remediation methods allowed to conclude that:

▪ The removal of sulphate-based black crusts from artistic limestone can be obtained with a fully "green" bioremediation treatment with the sulphate reducing bacterium *D. vulgaris*, preserving the original stone and the patina noble.

▪ The integrated biotechnological approach that we proposed can provide an important solution to conservators allowing the biocleaning of chemical alterations and the abatement of alterative microbial contaminations.

▪ Biotechnological methods permit also to suggest conservators guidelines to ensure longer lasting conservation of the original stone, thanks to the identification of survivors and potentially alterative microorganisms after the treatment.

As longer-term perspective the development of new and safer alternatives to traditional biocide to prevent and control deleterious biofilm becomes imperative. They must be efficient, economic and pose negligible risks for humans and the environment.
Our investigation on photocatalytic TiO_2 as promising alternative strategy led to conclude that:

➢ Photoactivated TiO_2 suspended as powder successfully degrades the organic dye RhoB in demineralised water, ultrapure water, 0.9% NaCl and PBS media. Instead, the photocatalytic action undergoes a sensible slowdown in cultural medium and in cultural medium dissolved in PBS solution. This is attributable to the presence of the organic component of medium, that can itself be a target of photocatalytic degradation, and of phosphates, that further reduce the photocatalyst performance.

➢ Photoactivated TiO_2 suspended as powder, or immobilized on a surface as a thin coating by sol-gel method successfully inhibits *P. stutzeri*, *P. aeruginosa* and *Bacillus* sp. planktonic cells in water solution.

➢ As for the RhoB degradation, photocatalyst does not produce reduction of viable planktonic cells when they are suspended in cultural media.

➢ Photoactivated TiO_2 neither suspended as powder nor immobilized by sol-gel had any effect on *P. aeruginosa* biofilm at both solid-liquid and solid-air interfaces.

➢ Our explanation for the lack of inactivation of cells in biofilm is an enhanced tolerance to the reactive oxygen species generated by photoactivated TiO_2 in cells that live in sessile form compared to those in the planktonic form.

Therefore, despite the good premises, photocatalytic TiO_2 does not constitute an efficient solution to eradicate deleterious biofilm. Further studies on the development of resistance to reactive oxygen species related to gene expression in bacterial biofilm may provide ways to better understand the resistance mechanisms against photocatalytic TiO_2.

In conclusion the research toward new efficient alternative and environmentally-friendly strategies for the control of deleterious biofilm must continue. Future work will be focused to search and test novel promising and safe compounds.

Feasibility of removing surface deposits on stone using biological and chemical remediation methods

SUPPORTING INFORMATION

Figures and Tables

Figure SI 1 - Cronos (left) and Demetra (right) sculptures from Castello del Buonconsiglio (Trento) with sampling points before and after the treatments.
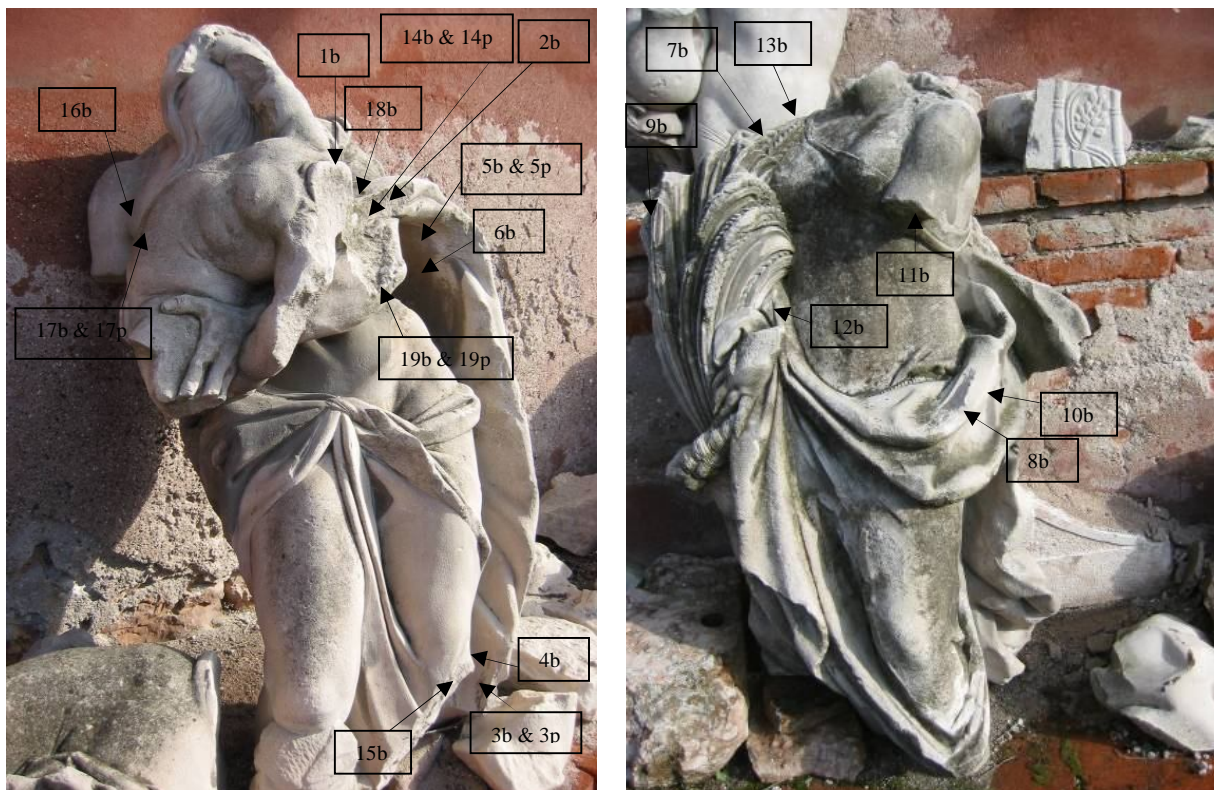
Table SI 1 - Biological alterations and black crust collected for biological analyses.

Alteration	Sample (symbol)	Alteration	Sample (symbol)
	9b (G)		15b (◯)
	10b (◯)		16b (G)
	11b (GB)		17b (G)
	12b (⬡)		18b (B)
	13b (B)		19b (B)
	14b (GB)		

Legend:

G Green microbial contamination

B Black microbial contamination

GB Green-black microbial contamination

⬡ Black crust

◯ Non altered sample

Effects of photoactivated titanium dioxide nanopowders and coating on planktonic and biofilm growth of *Pseudomonas aeruginosa*

SUPPORTING INFORMATION

Figures and Graphs

Figure SI 1 - Schematic representation of some of the main processes occurring on a semiconductor particle. (*a*), absorbtion of photon and electron–hole pair formation and migration of electron and hole: arrows marked (1) and (2) show electron–hole recombination at surface and bulk respectively, and those marked (3) reduction of acceptor and (4) oxidation of donor. (*b*), on absorbtion of photon of energy *hv*, electrons are excited from valence band (VB) to conduction band (CB). There is transfer of electron to oxygen molecule to form superoxide ion radical ($\cdot O^{-2}$) and transfer of electron from water molecule to VB hole to form hydroxyl radical ($\cdot OH$) (from Banerjee et al. 2006).
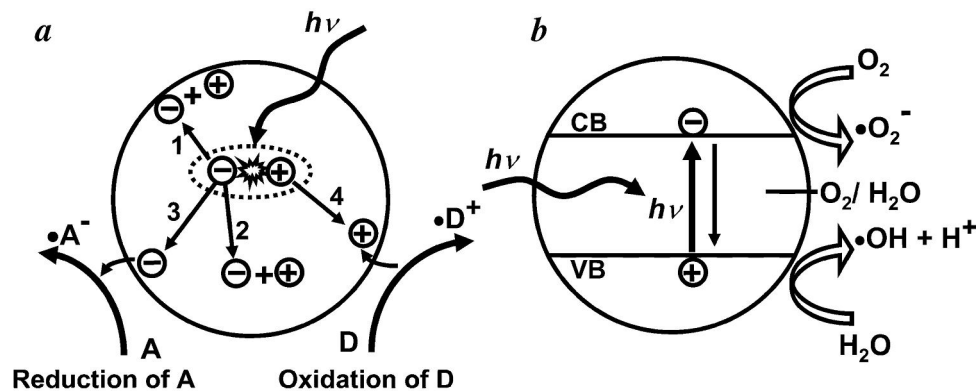

Figure SI 2 - Chain of reactions involved in the production of reactive oxygen species such as H_2O_2, $\cdot O^{-2}$, etc. and hydroxyl radical $\cdot OH$ shown illustratively (from Banerjee et al. 2006).

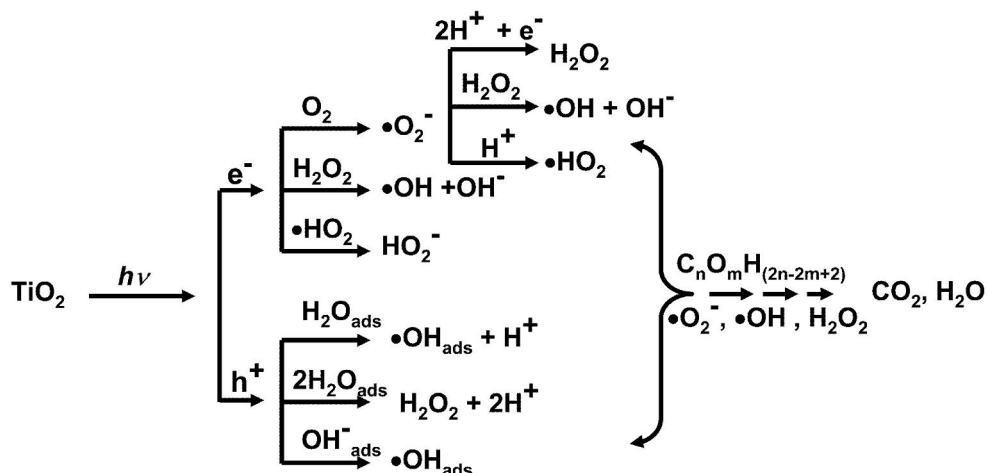**Figure SI 3 -** CFU/cm^2 values from the test with TiO$_2$ nanopowders and 48-h old *P. aeruginosa* biofilms by colony biofilm protocol. The graphs provide the P-values obtained by ANOVA analysis. According to post-hoc analysis (Tukey-Kramer, $P<0.05$), means sharing the same letter did not differ significantly from each other. Statistical analysis was performed separately for each experimental condition.

Figure SI 4 - CFU/cm^2 values from the tests in solid-liquid system with ABT minimal medium supplemented with 0.5% (w/v) glucose (a and b) and ABT minimal medium without glucose (c and d) solutions with photocatalytic film and *P. aeruginosa* biofilm 4-h old (a and c) and 24-h old (b and d). The graphs provide the P-values obtained by ANOVA analysis. According to post-hoc analysis (Tukey-Kramer, P<0.05), means sharing the same letter did not differ significantly from each other. Statistical analysis was performed separately for each experimental condition.
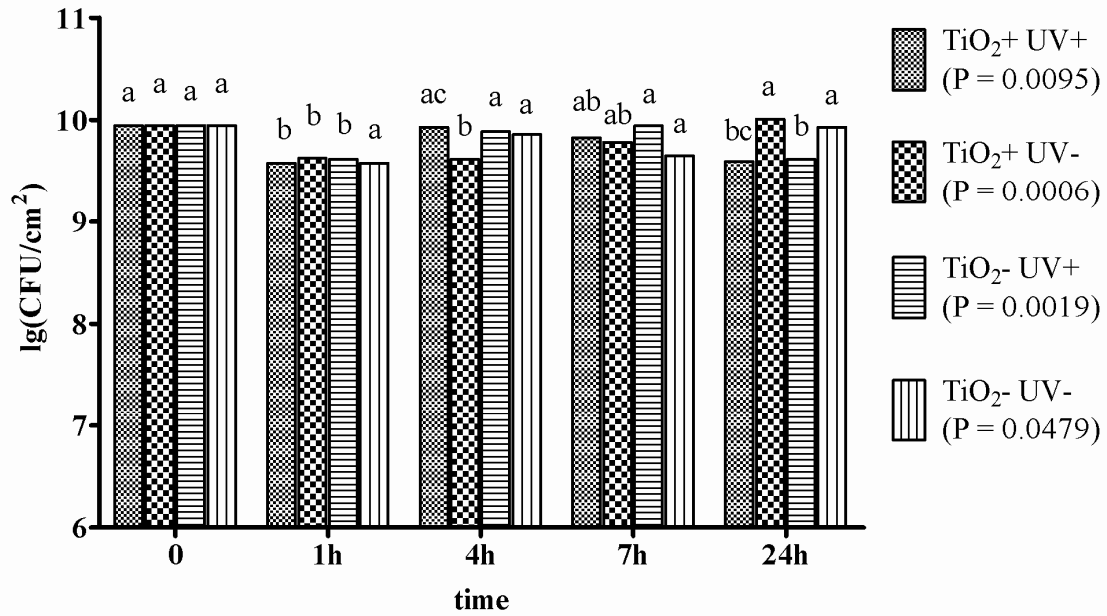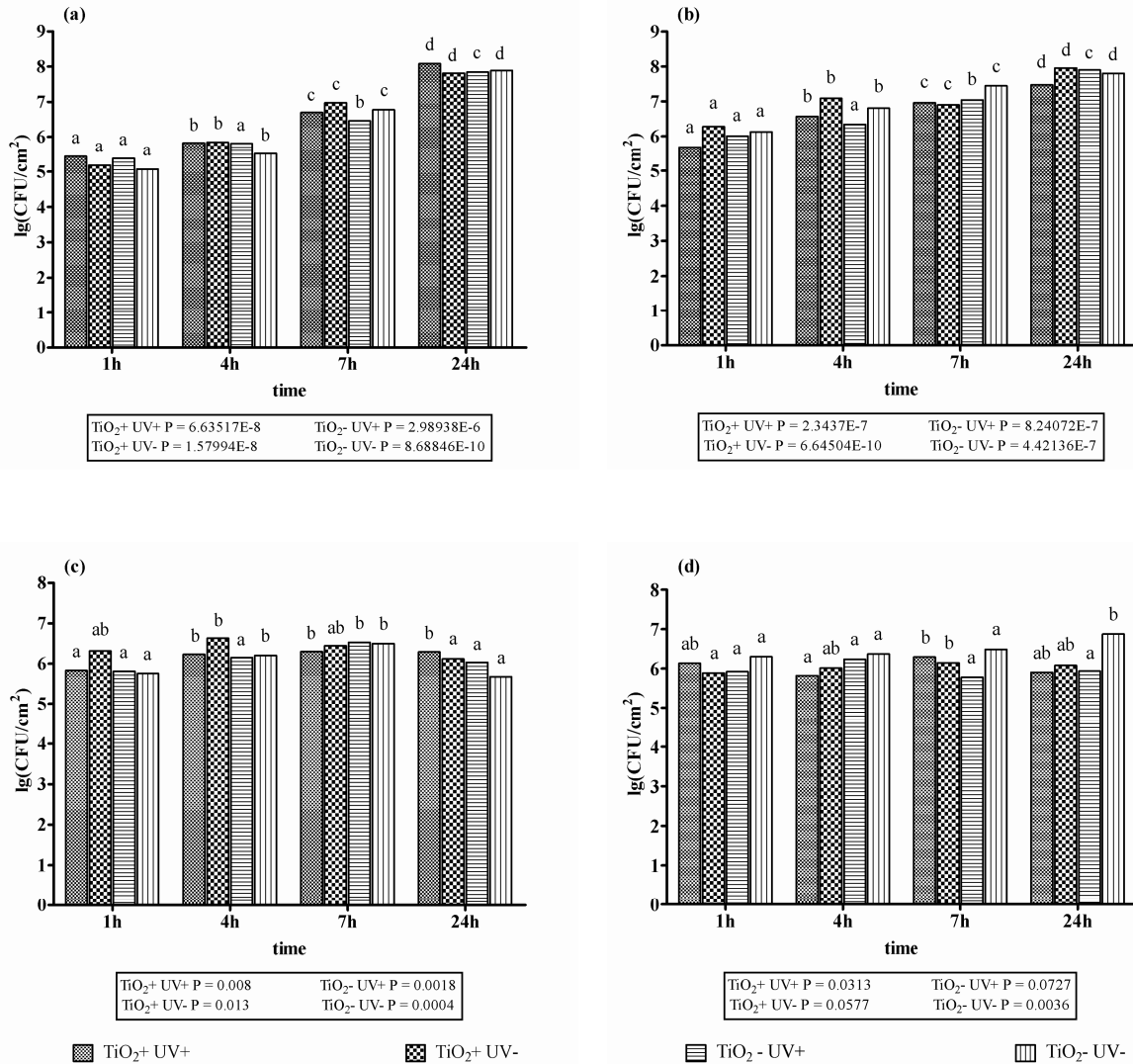
Prof. Maria Pia Pedeferri, Dr. Maria Vittoria Diamanti and Prof. Lucia Toniolo

Dipartimento di Chimica, Materiali, e Ingegneria Chimica (CMIC) "G. Natta"
Politecnico di Milano
Via Mancinelli 7, 20131 Milano, Italy.

Prof. Thomas Bjarnsholt and Prof. Niels Høiby

Department of International Health, Immunology & Microbiology
University of Copenhagen
Blegdamsvej 3, 2200 Copenhagen N, Denmark.

and

Department of Clinical Microbiology
Copenhagen University Hospital
Juliane Maries vej 22, 2100 Copenhagen Ø, Denmark

Dr. Lorenzo Brusetti

Faculty of Science and Technology
Free University of Bozen/Bolzano
Sernesistrasse 1, 39100 Bolzano, Italy

Prof. Giancarlo Ranalli

Dipartimento di Scienze e Tecnologie per l'Ambiente e il Territorio
University of Molise
C/da Fonte Lappone Pesche, 86090 Isernia, Italy

Dr. Umberto Fascio and Dr. Nadia Santo

Centro Interdipartimentale di Microscopia Avanzata (CIMA)
Università degli Studi di Milano
Via Celoria 26, 20133 Milano, Italy

Firstly, I would like to express sincerest gratitude to my supervisor, Dr. Francesca Cappitelli. During all the PhD course, she was an important guide. She offered me precious advices and opportunities, and gave me constant attention.

There are others many people that have contributed to the completion of this work. I would like to thank: Dr. Lorenzo Brusetti, Prof. Giancarlo Ranalli, Dr. Maria Vittoria Diamanti, Prof. Maria Pia Pedeferri, Prof. Lucia Toniolo, Prof. Thomas Bjarnsholt, Prof. Niels Høiby, Prof. Oana Ciofu, Prof. Tim Tolker-Nielsen, Prof. Michael Givskov, Dr. Umberto Fascio, Dr. Nadia Santo and Prof. Claudia Sorlini. It was a great pleasure and a fantastic experience to work with them.

Furthermore, a very great thanks to my dear colleagues Federica, Pamela, Lucia, Michela and Maurizio. They were the best colleagues that I could wish. A great and friendly thanks to all DD lab (and even beyond), Anna, Annalisa, Aurora, Bessem, Caterina, Daniele, Elena, Eleonora, Francesca, Giuseppe, Isabella, Lorenzo, Luigi, Massimo, Noura, Ramona, Sara and Valerio. I had three nice years in their company. Thanks to all friends from University of Copenhagen, Anne, Morten A., Morten H., Morten R., Tim, Mustafa, Helle, Anita, Tina, Stain, Martin, Maria, Louise, Wen-Chi, for their friendship and help during my 5 moths in Copenhagen. Finally, thanks to my parents and friends for their understanding, endless patience and encouragement during this adventure.

ENVIRONMENTAL MICROBIOLOGY

Feasibility of Removing Surface Deposits on Stone Using Biological and Chemical Remediation Methods

**A. Polo · F. Cappitelli · L. Brusetti · P. Principi ·
F. Villa · L. Giacomucci · G. Ranalli · C. Sorlini**

Abstract The study was conducted on alterations found on stone artwork and integrates microbial control and a biotechnological method for the removal of undesirable chemical substances. The Demetra and Cronos sculptures are two of 12 stone statues decorating the courtyard of the Buonconsiglio Castle in Trento (Italy). An initial inspection of the statues revealed putative black crusts and highlighted the microbial contamination causing discoloration. In 2006, the Cultural Heritage Superintendence of Trento commissioned us to study and remove these chemical and biological stains. Stereomicroscopy characterised the stone of the sculptures as oolitic limestone, and infrared analyses confirmed the presence of black crusts. To remove the black crusts, we applied a remediation treatment of sulphate-reducing bacteria, which removes the chemical alteration but preserves the original stone and the patina noble. Using traditional and biomolecular methods, we studied the putative microbial contamination and confirmed the presence of biodeteriogens and chose biocide Biotin N for the removal of the agents causing the discolouration. Denaturing gradient gel electrophoresis fluorescent in situ hybridisation established that Cyanobacteria and green algae genera were responsible for the green staining whereas the black microbial contamination was due to dematiaceous fungi. After the biocide Biotin N treatment, we applied molecular methods and demonstrated that the Cyanobacteria, and most of the green algae and dematiaceous fungi, had been efficiently removed. The reported case study reveals that conservators can benefit from an integrated biotechnological approach aimed at the biocleaning of chemical alterations and the abatement of biodeteriogens.

Introduction

Many historic, cultural and artistic objects and buildings are made of stone. Like all materials, stone is subject to inexorable deterioration, especially if exposed to the weather. In this regard, a particularly important role is played by pollution, which is the factor most responsible for depositing various chemical substances and biological agents on outdoor stone surfaces. This paper reports our work on two outdoor stone sculptures housed at the Buonconsiglio Castle, Trento, Italy. Before the conservation intervention, visual inspection revealed that most of the sculptures in the castle courtyard show signs of deterioration. On first inspection, the two investigated sculptures presented alterations putatively attributed to chemical agents (possible black crusts) and to microorganisms (putative microbial contamination of different colours).

In the presence of atmospheric pollution and a humid environment, calcareous stone is transformed into hydrated calcium sulphate, namely gypsum ($CaSO_4 \cdot 2H_2O$), which should be removed from surfaces as, because of hygrometric

A. Polo · F. Cappitelli (✉) · P. Principi · F. Villa ·
L. Giacomucci · C. Sorlini
Dipartimento di Scienze e Tecnologie Alimentari e
Microbiologiche, Università degli Studi di Milano,
Via Celoria 2,
20133 Milan, Italy
e-mail: francesca.cappitelli@unimi.it

L. Brusetti
Faculty of Science and Technology,
Free University of Bozen/Bolzano,
Sernesistrasse 1,
39100 Bolzano, Italy

G. Ranalli
Dipartimento di Scienze e Tecnologie per l'Ambiente e il
Territorio, University of Molise,
C/da Fonte Lappone Pesche,
86090 Isernia, Italy

fluctuations, it undergoes dissolving and crystallising processes that lead to mechanical stress. In areas sheltered from the rain, gypsum embeds mineral and smog particles, leading to the formation of the so-called black crusts that represent chemical alteration and aesthetic disfigurement.

In addition, in the same conditions, many biodeteriogens, organisms capable of causing deterioration, can be found on stone: bacteria, algae, fungi and lichens [4, 24, 35, 37, 41]. Biodeterioration can cause chemical, physical and aesthetic damage [12, 19]. The colour of the microbial contamination depends on the pigments produced by the microorganisms, and an understanding of the complex microbial ecosystem of cultural heritage surfaces is a prerequisite for controlling the growth of microbial species that cause biodeterioration [21, 41].

The importance of an efficient and careful cleaning of stone artwork for the removal of chemical and biological alterations cannot be overstressed. Indeed, before cleaning, it is fundamental to have knowledge of the type of stone and the characterisation of the chemical and biological alterations in order to choose the optimal cleaning intervention. The use of solvents and physical methods (like abrasion) for the removal of chemical alterations can affect the sound stone material and result in low selectivity [10]. In the past few years, much progress has been made using viable cells able to remove sulphates from stone ornamental surfaces [7, 42]. In removing of black crusts, Cappitelli and co-workers [6] demonstrated the advantages of using microbial technologies over traditional chemical technologies: the biological procedure resulted in a more homogeneous removal of the surface deposits without chemically compromising the substrata and preserved the patina noble under the black crust itself. In addition, biocleaning has proven to be more selective than chemicals.

With regard to biodeterioration, microbial abatement is commonly achieved using biocides. As the biocide is a toxic compound, it is very important to identify the biodeteriogens to choose a suitable product that targets only specific biodeteriogen taxa.

In our study, we successfully used, for the first time, an integrated biotechnological system that enables the cleaning of stone cultural heritage affected by chemical and biological agents. It is our belief that this system provides a useful and reliable model for conservation intervention in similar case studies.

Methods

Sculpture Description

The Buonconsiglio Castle, built in the thirteenth century for defence purposes, is the most important secular monument in Trento (Italy). In the second half of the eighteenth century, the courtyard was embellished with 12 statues probably made by Jacob Eberle in 1764. Two of these sculptures were studied in this work: Demetra and Cronos. Visual inspection revealed that the two sculptures presented the following forms of alteration: (1) putative black crusts and (2) green, green–black and black staining putatively attributed to the presence of microorganisms.

Sampling

All the samples were taken by scalpel (sterile for biological analysis) according to the Italian Cultural Heritage Ministry Recommendation [9].

Table 1 reports all the samples, indicating the sculpture from which they were taken, sampling location and description of the alteration. For the chemical analyses, six samples were taken from the Cronos sculpture (1b to 6b) and two from the Demetra (7b and 8b). Samples 4b and 8b were taken from apparently non-altered areas whereas specimens 1b and 2b were putative black microbial contaminations, and samples 3b, 5b, 6b and 7b showed a putative black crust alteration. After the biocleaning, two samples were taken. The sample 3p was collected close to the sampling area of the specimen 3b, and the sample 5p was collected close to the sampling area of the specimen 5b.

In addition, 11 samples affected by putative biological discolouration (green, black and green–black) and black crust were selected to study the microbial community. Four of them were collected from the Demetra sculpture (9b to 13b), and six specimens were taken from the Cronos sculpture (14b to 19b). Three specimens were representative of green microbial contamination (9b, 16b and 17b); three specimens were representative of black microbial contamination (13b, 18b and 19b); samples 11b and 14b were representative of green–black microbial contamination, and sample 12b most likely presented a black crust. In addition, samples 10b and 15b were taken from apparently non-altered areas. After the treatment, three samples were taken. Samples 14p, 17p and 19p were collected close to the sampling area of the specimen 14b, 17b and 19b, respectively.

Chemical Analyses

Stereomicroscope and Cross-Section Observations

Samples were observed by Wild Makroskop M420 stereomicroscope (Heerbrugg, Switzerland), equipped with an Olympus OM1 camera (Chicago, USA). The cross sections were prepared for the 5b and 6b samples and observed using the optical Leitz Ortholux microscope (Wetzlar, Germany).

Table 1 Samples collected: sculpture, location, description and chemical and microbiological analyses carried out

Samples	Sculpture	Location	Putative alteration (symbol)	Type of analysis carried out
1b	Cronos	Child collar	Black microbial contamination (B)	Chemical
2b	Cronos	Arm	Black microbial contamination (B)	
3b	Cronos	Cloak	Black crust (⬢)	
4b	Cronos	Knee	Non altered sample (◯)	
5b	Cronos	Cloak	Black crust (⬢)	
6b	Cronos	Cloak	Black crust (⬢)	
7b	Demetra	Shoulder	Black crust (⬢)	
8b	Demetra	Dress	Non altered sample (◯)	
9b	Demetra	Right-hand	Green microbial contamination (G)	Biological
10b	Demetra	Dress	Non altered sample (◯)	
11b	Demetra	Left-arm	Green-black microbial contamination (GB)	
12b	Demetra	Left-hand	Black crust (⬢)	
13b	Demetra	Right-shoulder	Black microbial contamination (B)	
14b	Cronos	Left-elbow	Green-black microbial contamination (GB)	
15b	Cronos	Left-knee	Non altered sample (◯)	
16b	Cronos	Breasts	Green microbial contamination (G)	
17b	Cronos	Child abdomen	Green microbial contamination (G)	
18b	Cronos	Left-arm	Black microbial contamination (B)	
19b	Cronos	Left-elbow	Black microbial contamination (B)	
3p	Cronos	Cloak (area of the specimen 3)	-	Chemical
5p	Cronos	Cloak (area of the specimens 5)	-	
19p	Cronos	Left-elbow (area of the specimen 19)	-	Biological
14p	Cronos	Left-elbow (area of the specimen 14)	-	
17p		Child abdomen (area of the specimen 17)	-	

Samples marked with b were collected before the treatment and specimens marked with p after the treatment

Fourier Transform Infrared Spectroscopy

Fourier transform infrared (FTIR) analyses, used to detect both inorganic minerals and organic compounds in the samples, were carried out by a Nicolet Nexus spectrophotometer (Washington, USA) coupled with a Nicolet Continuum Fourier transform infrared spectroscopy microscope equipped with a HgCdTe detector cooled with liquid N_2. Spectra were recorded by a Graseby-Specac diamond cell accessory in transmission mode between 4,000 and 700 cm^{-1}. The FTIR analyses were performed on samples collected both before and after the treatments.

Biocleaning

The remediation treatment using sulphate-reducing bacteria (SRB) was applied for the removal of the chemical alterations due mainly to gypsum. The biomass entrapped in the delivery system was prepared as described by Cappitelli and co-workers [7]: the SRB employed was *Desulfovibrio vulgaris* subsp. *vulgaris* ATCC 29579 maintained in DSMZ 63 medium, and the delivery system was Carbogel (CTS, Vicenza, Italy). Before use in the treatment, the cells were grown in DSMZ 63 medium modified by eliminating any iron source. After centrifugation and prior to mixing with the Carbogel powder, the cell pellet was suspended in deaerated phosphate buffer supplemented with 0.599 g l^{-1} sodium lactate at pH 7.0 at a concentration of 10^8 cells per millilitre. All the manipulations described above were done under anaerobic conditions in a glove box. The surfaces to be treated were moistened and covered with tissue paper before any applications began. The biologically treated areas underwent three 12-h applications for a total duration of 36 h. The biological cleaning system was covered with a polyvinylchloride film (Silplast, Italy) to reduce undesirable evaporation. After the treatment, removal of the bioformulate was accomplished by removing the tissue paper and subsequently washing the area with distilled water [6].

Biological Analyses

Culturable Community Analyses

Sample powders were inoculated in two cultural media to determine the microbial counts on the Demetra and Cronos surfaces: plate count agar medium (PCA, Merck) for aerobic heterotrophic bacteria with incubation at 30°C for 3–5 days and potato dextrose agar medium (PDA, Merck) for fungi with incubation at 30°C for 3–5 days. The samples collected after the cleaning treatment were also inoculated in PCA and PDA, under the same conditions adopted before the treatment. Quantification of microorganisms grown on PCA and PDA was expressed as colony-forming unit (CFU) per gramme.

Sample powders were also inoculated in Chu and Detmer media [5] to study the Cyanobacteria and Chlorophyta communities, respectively. The samples were incubated for 30 days under natural light at room temperature. The samples collected after the cleaning treatment were also inoculated in Chu and Detmer media under the same conditions adopted before the treatment. Presence or absence of Cyanobacteria and eukaryotic algal growths was recorded.

DNA Extraction

Total DNA was extracted directly from the stone samples as described by [2] but with the following modifications: no lysozyme was added and three cycles −80°C/70°C were performed before the addition of the proteinase K. The Cyanobacteria and eukaryotic algal DNA were also extracted from communities grown, respectively, in Chu and Detmer media, using the same protocol.

Both the microbial communities present on the sculptures before and after the treatment were studied.

Analysis of Bacteria Community

The 16S rRNA gene fragments extracted from altered stone samples were amplified with primers GC-357 F and 907 R with the following chemical conditions: 1× of polymerase chain reaction (PCR) Rxn buffer, 1.5 mM of $MgCl_2$, 0.12 mM of dNTP mix, 0.3 µM of each primer and 1 U of Taq DNA polymerase in 50-µl PCR reaction. The thermal cycling programme included an initial denaturation at 94°C for 4 min followed by ten cycles consisting of denaturation at 94°C for 30 s, annealing at 61°C for 1 min and extension at 72°C for 1 min, 20 cycles consisting of denaturation at 94°C for 30 s, annealing at 56°C for 1 min and extension at 72°C for 1 min and a final extension step at 72°C for 10 min.

Analysis of Fungal Community

The 18S rRNA gene fragments extracted from altered stone samples were amplified by two-step PCRs performed as follows: a first amplification step using the combination of primers NS1 and EF3 [30] with 1× of PCR Rxn buffer, 1.5 mM of $MgCl_2$, 0.2 mM of dNTP mix, 0.2 µM of each primer and 1 U of Taq DNA polymerase in 25-µl PCR reaction and the cycling programme as reported in Oros-Sichler and co-workers [30] except for the 56°C annealing temperature. The first PCR product was used as template for a second amplification step performed with the primers NS2 and GC-clamped NS1. The reaction mixture was identical to first-step PCR except for 0.12 mM of dNTP mix and 0.3 µM of each primer. The cycling programme consisted in an initial denaturation at 94°C for 4 min followed by 35 cycles of denaturation at 94°C for 45 s, annealing at 50°C for 45 s and extension at 72°C for 2 min and a final extension at 72°C for 10 min.

Analysis of Culturable Cyanobacterial Community

The 16S rRNA gene fragments extracted from Chu medium cultures were amplified by two-step PCRs performed as follows: a first amplification step using the primers 27 F and 1495 R with 1× of PCR Rxn buffer, 1.5 mM of $MgCl_2$, 0.2 mM of dNTP mix, 0.25 µM of each primer and 2.5 U of Taq DNA polymerase in 50-µl PCR reaction and with a touchdown thermal protocol

consisting in an initial denaturation at 95°C for 1 min and 30 s followed by five cycles of denaturation at 95°C for 30 s, annealing at 60°C for 30 s and extension at 72°C for 4 min, five cycles of denaturation at 95°C for 30 s, annealing at 55°C for 30 s and extension at 72°C for 4 min and 25 cycles of denaturation at 95°C for 30 s, annealing at 50°C for 30 s and extension at 72°C for 4 min and a final extension at 72°C for 10 min. The first PCR product was used as template for a second amplification step performed with the primers GC-357 F and 907 R and with 1× of PCR Rxn buffer, 1.5 mM of $MgCl_2$, 0.2 mM of dNTP mix, 0.3 μM of each primer and 1 U of Taq DNA polymerase in 50-μl PCR reaction. The PCR included an initial denaturation at 94°C for 4 min followed by ten cycles consisting of denaturation at 94°C for 30 s, annealing at 61°C for 1 min and extension at 72°C for 1 min, by 20 cycles consisting of denaturation at 94°C for 30 s, annealing at 56°C for 1 min and extension at 72°C for 1 min and a final extension step at 72°C for 10 min.

Analysis of Culturable Eukaryotic Algal Community

The 18S rRNA gene fragments extracted from Detmer medium cultures were amplified by PCR with the primers NS2 and GC-clamped NS1 with 1× of PCR Rxn buffer, 1.2 mM of $MgCl_2$, 0.2 mM of dNTP mix, 0.2 μM of each primer and 0.8 U of Taq DNA polymerase in 50-μl PCR reaction and the cycling programme as reported in Oros-Sichler and co-workers [30] except for the 63°C annealing temperature.

Denaturing Gradient Gel Electrophoresis and Sequencing

The amplicons obtained by amplifying bacterial and eukaryotic DNA were analysed by denaturing gradient gel electrophoresis (DGGE). The DGGE was performed as follows: 8% polyacrylamide (Sigma) gels were prepared according to the method of Muyzer and co-workers [28] using a gradient maker (Amersham Biosciences) according to the manufacturer's guidelines. The DNA fragments were separated by electrophoresis run for 15 h at 90 V performed by D-Code Universal Mutation Detection system (Bio-Rad). The gels were stained by SYBR-Green (Armersham Pharmacia Biotech) and the results observed by GelDoc (Bio-Rad) apparatus. The excised bands were eluted in 50 μl milli-Q water by incubation at 37°C for 3 h and successively overnight at 4°C. In order to compare the results, both samples, collected before and after the treatment, were loaded on the same gel.

The DGGE was performed with the following denaturant gradients: 40–60% for the Bacteria community, 25–40% for the fungal community, 30–60% for the culturable cyanobacterial community and two types of denaturing gradients, namely 35–45% and 25–35%, for the eukaryotic algal community.

All the excised bands were identified by sequencing (Primm, Milan). The sequences were analysed using the BLASTN software (www.ncbi.nlm.nih.gov/BLAST).

Fluorescent In Situ Hybridisation

The abundance of Cyanobacteria within the Bacteria community before the treatment was investigated by fluorescent in situ hybridisation (FISH). Powder samples collected before the treatment were fixed with paraformaldehyde solution (4% in phosphate-buffered solution, PBS, 0.01 M phosphate buffer, 0.0027 M potassium chloride pH 7.4 at 25°C) and incubated for 2 h on ice. After two PBS washings, the powdered samples were resuspended in an aliquot of 1/1 ethanol/PBS solution and stored at −20°C. A small amount of sample (25 μl) was pipetted onto silane-coated slides (Sigma-Aldrich), allowed to air dry and then dehydrated with an alcohol series (ethanol solutions 50%, 80% and 96% V/V). The spots with the samples were treated with 30 μl of hybridisation buffer made with 2 μl (100 ng) of the labelled probes in 28-μl hybridisation buffer. The probes chosen for the hybridisation protocol were as follows: EUB338 fluorescein-labelled, targeting Bacteria; CIV/V 1342, CYA762, CYA361 and CYA664 Texas-red-labelled, targeting Cyanobacteria [22]. Details of the probes (sequences, coverage percentage, annealing temperature and references) are reported at www.probebase.net. The slides were observed by epifluorescence microscope Leica DM 4000 B (Leica Microsystems, Milan, Italy). Images of samples were acquired by CoolSNAP CF (Photometrics Roper Scientific, Rochester, USA), and cells positive after hybridisation were counted.

Statistical Analyses

Quantitative data of FISH images were analysed by one-way factorial analysis of variance (ANOVA). The positive cells were counted from ten digital images for each sample considered, and the means were compared separately for Bacteria and Cyanobacteria by post hoc comparison according to Tukey–Kramer.

Biocidal Treatment

A chemical cleaning was applied to remove the biodeteriogens. The selected chemical was Biotin N (CTS, Italy), a broad-range biocide, soluble in water and constituted by a mixture of tributyltin naphthenate (20% w/v) and didecyl dimethyl ammonium chloride (35% w/v). It was applied as a 1.5% aqueous solution, as per manufacturer instructions.

Results

Microscopy Observations and Chemical Analyses

Using the stereomicroscope, the stone of the samples 4b and 8b was characterised as an oolitic limestone with oval or semi-circular grain structure. Despite the specimens being collected from areas that were apparently non-altered by visual inspection, FTIR spectra showed a slight degree of surface sulphatation. The samples 3b, 5b, 6b and 7b were all characterised by the presence of gypsum (3,540, 3,406, 1,685, 1,621, 1,132 and 670 cm^{-1}) and calcite (1,798, 1,429, 875 and 712 cm^{-1}) with a small amount of silicate (1,034, 1,001, 797 and 779 cm^{-1}; Fig. 1). The speculation of the presence of black crusts was therefore confirmed. The sample 3b also contained calcium nitrate (1,384 cm^{-1}). Optical and chemical analyses of the specimens 5b and 6b showed the presence of a thin yellow-ochre inner layer

composed of a mixture of calcium oxalate (1,646 and 1,324 cm^{-1}) and gypsum. In addition to calcite, silicates and a small amount of gypsum, FTIR analyses of samples 1b and 2b revealed the presence of a peptidic bond (see the peaks at 1,647 and 1,540 cm^{-1}).

Biocleaning Treatment

The biocleaning procedure was applied to three areas of the Cronos sculpture strongly altered by thick black crust. One area was where samples 5b and 6b were taken; the other areas had very similar features and corresponded to the abdomen region. Cronos' abdomen before, during and after the biocleaning is presented in Fig. 2 (a, b, c): complete removal of the black crust was observed after three applications of 12 h each. FTIR analyses performed on the samples after the treatment confirmed that the gypsum was removed almost com-
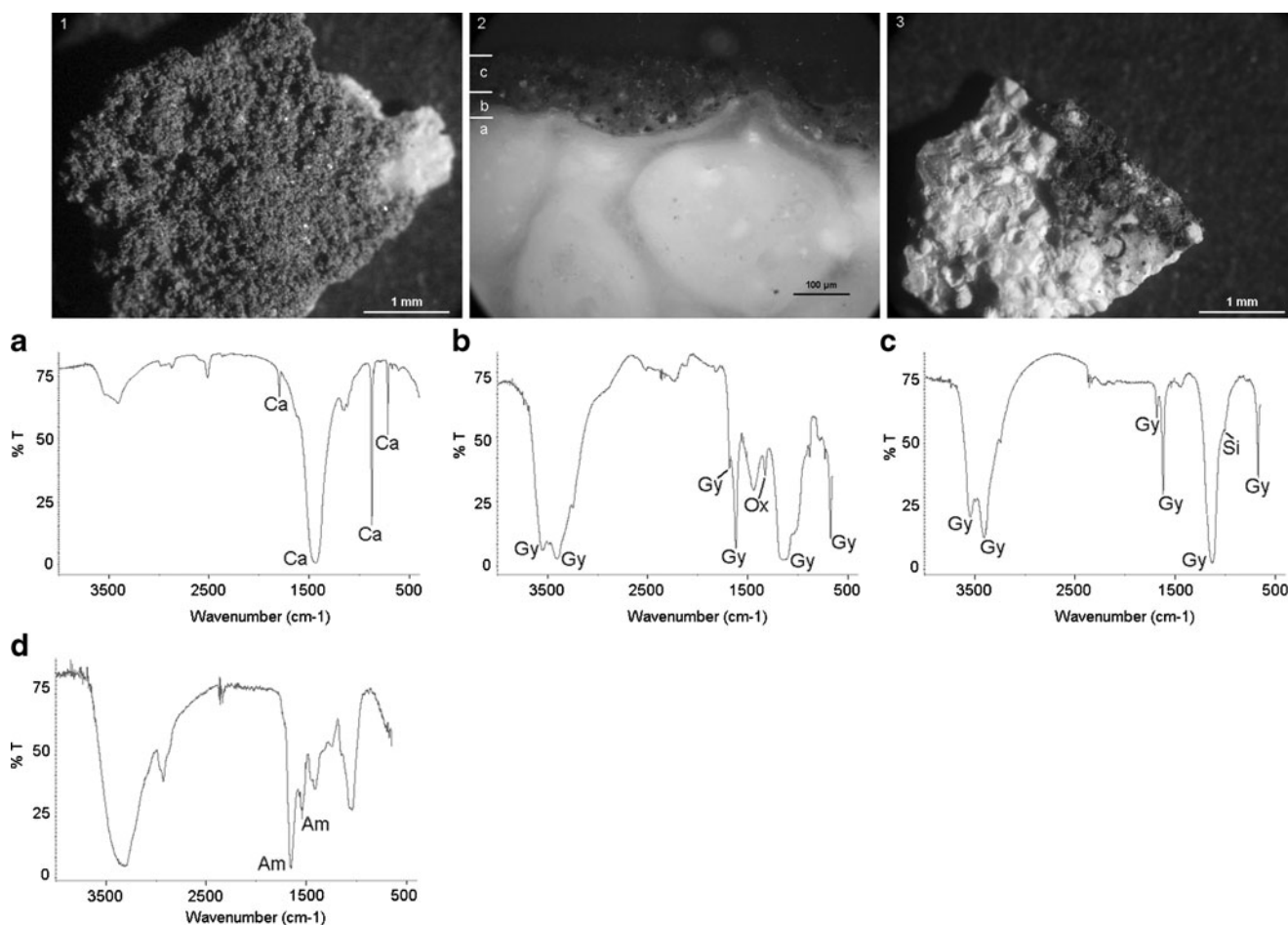

Figure 1 (*1*) Top view of sample 6b under the stereomicroscope. (*2*) Cross section of sample 6b under optical microscopy in reflected light with the presence of the three layers: oolitic limestone (*a*), noble patina (*b*) and black crust (*c*). (*3*) Top view of sample 2b under the stereomicroscope. (*a*) FTIR spectrum of the layer *a* showing the characteristic peaks of calcite (*Ca*). (*b*) FTIR spectrum of layer *b* showing the presence of calcium oxalate (*Ox*) and gypsum (*Gy*). (*c*) FTIR spectrum of layer *c*. The black crust is composed mainly of gypsum with a small amount of silicate (*Si*). (*d*) FTIR spectrum of the black patina on sample 2b. The spectrum shows mainly the presence of organic material of proteinaceous nature (amide I and amide II, *Am*)
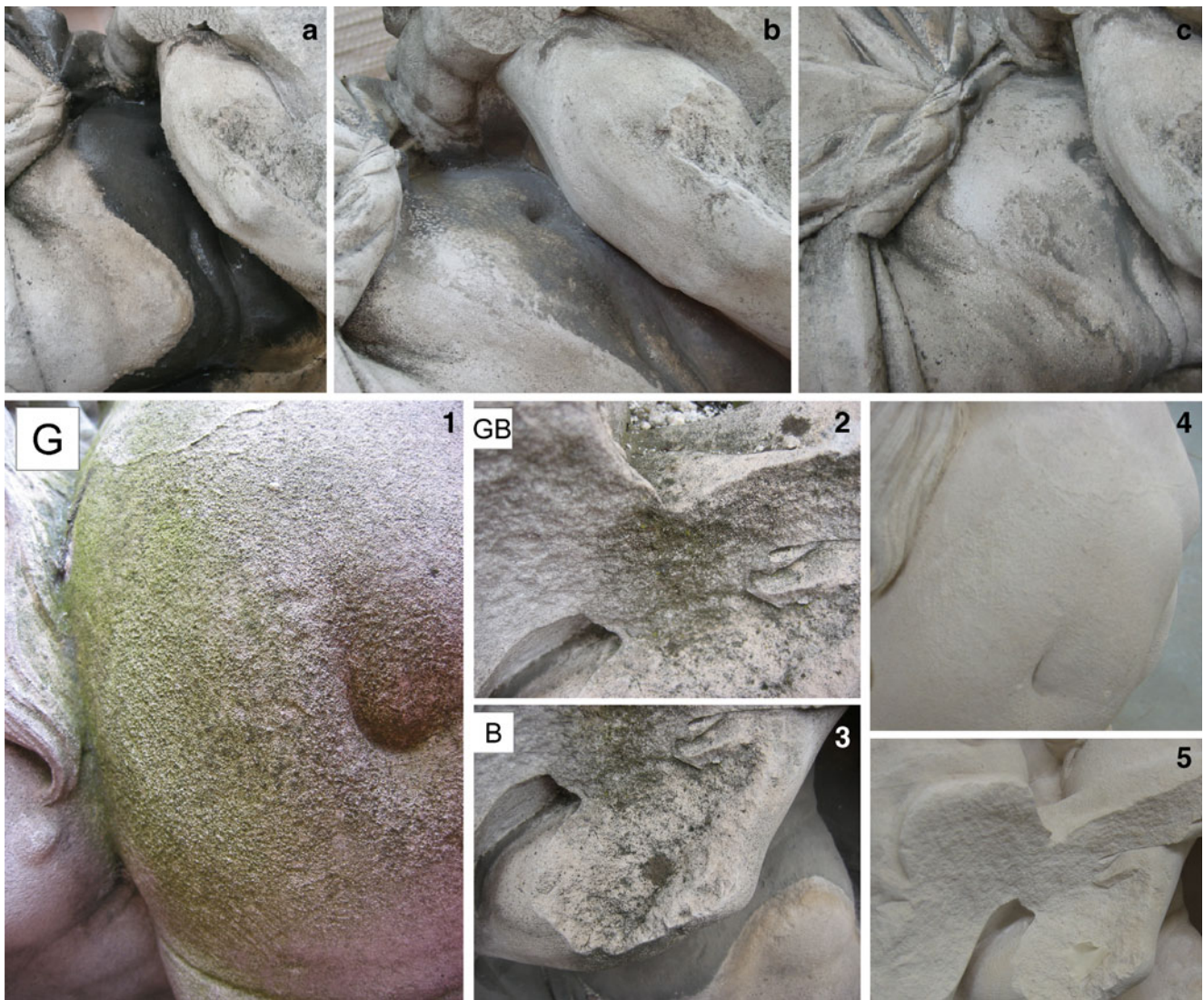
Figure 2 Bioremediation treatment of Cronos statue (*a*, *b*, *c*) and effects of the biocide on the microbial community (*1*, *2*, *3*). (*a*) Untreated surfaces showing a black crust; (*b*) result after the first 12-h application; (*c*) result after three 12-h applications, before the final washing with water and a soft brush. Green, black and green–black microbial contamination before treatment (*1*, *2* and *3*, respectively) and after treatment (*4* and *5*). Chronos child abdomen (*1*, *4*); Cronos left-elbow upper part (*2*, *5*) and lower part (*3*, *5*)

pletely. After the biocleaning process, in the area corresponding to samples 5b and 6b, the presence of a yellow-ochre layer definitively different from the limestone colour was observed, and the presence of calcium oxalate was proven by FTIR spectra.

Biological Analyses

To obtain preliminary information on the microbial community present on the samples before and after the treatments, we performed a study on the culturable community. More detailed information on the total microbial community was obtained by a molecular approach (DGGE, sequencing and FISH).

Culturable Community Analyses

The bacterial and fungal counts evaluated by cultural methods in the samples collected before any treatments were between 5 and 7 log(CFU/g) and between 4 and 6 log (CFU/g), respectively, with the only exception of sample 13b in which neither heterotrophic bacteria nor fungi were found.

In the samples collected after the biocidal treatment, no fungi were found, and the bacterial counts were two to five orders of magnitude lower than those found in the samples collected before the treatment.

Cyanobacteria and eukaryotic algae grew in all the samples except specimens 12b, 13b, 15b and 17b. The

cultural results demonstrated that the microbial communities in the samples were complex and included heterotrophic bacteria, microfungi and algae. Neither Cyanobacteria nor eukaryotic algae grew from the samples collected after treatment.

DGGE and Sequencing

To better characterise the microflora, DGGE analyses coupled with partial sequencing of 16S and 18S rRNA gene fragments were performed. Even though the amplification efficacy differed among the samples, the 16S gene amplification clearly showed a total of 28 bands separated in the DGGE gel, while for the 18S gene amplification nine bands were evidenced. The corresponding sequences were determined. Tables 2 and 3 show the band number with the identification to the closest relative strain and similarity percentage.

FISH

FISH was performed to evaluate the importance of the Cyanobacteria within the total community of Bacteria. Figure 3 shows the mean values of the Bacteria and Cyanobacteria cells positive after hybridisation in several samples. With the sole exception of samples 16b and 17b, most of the cells belonging to the domain Bacteria were also positive to the Cyanobacteria probes. Sample 13b was found to have no Bacteria cells positive to the EUB338 probe (according to cultural analysis results). The ANOVA analysis revealed statistically significant differences in the number of cells positive after hybridisation with probes specific to Bacteria and Cyanobacteria among the samples.

Biocidal Treatment

Figure 2 (1, 2, 3) shows green, green–black and black microbial contamination before the treatment and its complete removal after treatment (4, 5). To confirm the visual observations, DGGE analyses were repeated after the biocidal treatment. Figure 4 shows the taxa identified by DGGE analyses before and after the biocidal treatment, and it is to be noted how the biodiversity of the microbial community was reduced: before the biocidal treatment, 15 taxa were recovered from the DGGE bands, while after treatment only six taxa were retrieved. The biocidal treatment was effective against Cyanobacteria, Betaproteobacteria, Alphaproteobacteria, Actinobacteria, Bacteroidetes, Acidobacteria, Deinococcus-Thermus, Chlorophyta, *Cladosporium*, *Alternaria* and *Geosmithia*. In fact, these taxa were found before the treatment but were not identified after it.

Discussion

An initial visual inspection of the Demetra and Cronos sculptures allowed the detection of two putative alterations: some black crust and some biological discolouration (green, black and green–black). The chemical analyses demonstrated that the putative chemical alterations were indeed black crusts as they were composed mainly by gypsum. Calcium nitrate was also present: in addition to the transformation of calcite to calcium sulphate, it is also possible that calcium nitrate forms due to the interaction of calcite with airborne NO_x in the presence of humidity [32]. Also, the silicate particles are of atmospheric origin and are due to pollution [8]. In addition, peptidic bonds, observed in the FTIR spectra of samples 1b and 2b, were ascribed to the presence of microorganisms, as previously reported [5]. Microscopic observations and chemical analyses demonstrated that the stone is an oolitic limestone. Finally, the cross-section observations and the FTIR spectra showed that some areas affected by black crust were characterised by the presence of three different layers: the substratum (limestone), a thin yellow-ochre inner layer characterised by the presence of calcium oxalate, characteristic of a patina noble [33], and the superficial black crust. In contrast to black crusts, the patina noble is a superficial layer acquired by stone in the course of time and protects the substratum. It is associated with the best-preserved surfaces and should remain intact during cleaning [23].

In this work, the chemical alterations were removed by a biocleaning treatment before the biocidal treatment intervention on the biological contamination that had caused the discolourations; this was to avoid that the biocide acted also on the SRB cells. In the past, a biocleaning treatment by *D. vulgaris* was applied successfully to remove sulphates from marble [6]; in the present study, we applied it, for the first time, on limestone that is more porous than marble. On comparing the results of the chemical analyses performed before and after the biocleaning, it was proven that bioremediation with *D. vulgaris* successfully removes gypsum black crust from the Demetra and Cronos sculptures. After three applications, the black crusts were no longer detectable by visual inspection, and the FTIR analyses proved that the gypsum was almost completely removed. Neither nitrate nor silicate were found in the FTIR spectra after the treatment, implying that these compounds were removed together with the gypsum. In addition, as previously demonstrated for marble [6], both optical evidence and FTIR analysis showed that the noble patina was preserved on the limestone substratum of the sculptures.

The cultural analyses proved that all the four groups investigated (heterotrophic bacteria, fungi, prokaryotic and eukaryotic algae) were present and that in some samples the

Table 2 Identification of partial 16S rRNA gene sequences from DGGE profiles

Bands	Samples											BlastN reference strains				RDP taxonomic classifier	
	9b	10b	11b	12b	13b	14b	15b	16b	17b	18b	19b	Closest relative strain	Strain	Accession number	Similarity (%)	Most probable taxon	Similarity (%)
1, 4	x	x	x	x	x	x		x	x	x	x	Halospirulina tapeticola	CCC Baja-95 Cl.2	NR_026510	90	Cyanobacteria	100
2		x	x	x								Hymenobacter aerophilus	I/26Cor1; DSM 13606	NR_025398	90	Adhaeribacter	96
3	x	x	x	x	x	x		x	x	x	x	Pseudomonas geniculata	ATCC 19374	NR_024708	98	Stenotrophomonas	100
5				x		x	x					Meiothermus chliarophilus	ALT-8	NR_026244	83	Truepera	100
6		x	x			x						Loktanella salsilacus	R-8904	NR_025539	92	Rhodobacteraceae	100
7						x		x	x		x	Arthrobacter agilis	DSM 20550	NR_026198	99	Arthrobacter	100
8				x								Arthrobacter nitroguajacolicus	G2-1	NR_027199	98	Arthrobacter	100
9		x	x	x	x	x		x	x	x	x	Cryptosporangium minutisporangium	IFO 15962	NR_024746	90	Actinomycetales	99
11		x				x						Sphingomonas wittichii	RW1	NR_027525	86	Sphingomonadaceae	84
14				x	x	x	x		x		x		Methylocystis echinoides	IMET 10491	NR_025544	91	Rhizobiales	94
15				x	x	x		x	x			Mesorhizobium plurifarium	LMG 11892	NR_026426	94	Rhizobiales	94
20								x		x		Sphingomonas aquatilis	JSS-7	NR_024997	98	Sphingomonas	100
21, 22						x				x		Sporocytophaga myxococcoides	DSM 11118	NR_025463	89	Flexibacteraceae	99.5±0.5
23								x				Ralstonia mannitolilytica	LMG6866	NR_025385	92	Burkholderiales	94
24						x		x	x			Herbaspirillum frisingense	GSF30	NR_025353	93	Burkholderiales	97
25								x				Herbaspirillum chlorophenolicum	CPW301	NR_024804	93	Oxalobacteraceae	90
26						x		x		x		Herbaspirillum chlorophenolicum	CPW301	NR_024804	91	Oxalobacteraceae	98
27, 32						x						Methylobacterium extorquens	TK 0001	NR_025856	93.5±0.5	Rhizobiales	99.5±0.5
28						x		x		x		Methylobacterium fujisawaense	DSM 5686	NR_025374	96	Methylobacterium	100
29						x		x				Sphingomonas aquatilis	JSS-7	NR_024997	94	Sphingomonadaceae	99
30						x				x		Sphingomonas aquatilis	JSS-7	NR_024997	91	Alphaproteobacteria	100
31						x		x		x		Methylobacterium extorquens	TK 0001	NR_025856	95	Microvirga	89
33						x						Pseudomonas geniculata	ATCC 19374	NR_024708	88	Xanthomonadaceae	84
35, 37, 38						x		x		x		Rubritepida flocculans	H-8	NR_025221	93	Belnapia	91±5.5
36						x						Rubritepida flocculans	H-8	NR_025221	92	Acetobacteraceae	100
39											x	Bacteroides capillosus	ATCC 29799	NR_025670	82	Acidobacteriaceae	100
41						x						Ruminococcus flavefaciens	C94	NR_025931	77	Acidobacteriaceae	97
42					x							Pseudomonas umsongensis	Ps 3-10	NR_025227	97	Pseudomonadaceae	100

A cross indicates the presence of the taxon in the sample

**Table 3** Identification of partial 18S rRNA gene sequences from DGGE profiles

Bands	Samples											BlastN reference strains			
	9b	10b	11b	12b	13b	14b	15b	16b	17b	18b	19b	Closest relative	Strain	Accession number	Similarity (%)
1, 7		x	x	x	x		x	x	x	x	x	Geosmithia sp.	MKA1-b	AM947666	98
11, 13, 14		x	x	x	x		x	x	x	x	x	Isaria fumosorosea	IFO 7072	AB086629	99
2, 3, 4, 5, 6, 12, 15, 17, 19, 21		x	x	x	x		x	x	x	x	x	Verticillium leptobactrum	IAM 14729	AB214657	99±0.5
16					x					x		Verticillium leptobactrum	CBS 414.70	EF641846	99
28		x	x				x		x	x	x	Cladosporium sp.	CPC11224	DQ780937	99
30, 31			x					x	x	x	x	Alternaria sp.	CPCC 480375	EU826479	99
20, 24, 25, 26, 27		x	x	x	x	x	x		x	x	x	Klebsormidium flutans	SAG 9.96	AM490839	99.5±0.5
18			x			x				x	x	Myrmecia astigmatica	IB T76	Z47208	99
22, 32			x							x	x	Myrmecia sp.	H1VF1	AF513369	99
23									x	x	x	Friedmannia israeliensis		M62995	99

A cross indicates the presence of the taxon in the sample

counts were quite high, up to 7 log(CFU/g) for bacteria and up to 6 log(CFU/g) for fungi. However, the microbial abundance in the samples did not seem to be related to the type of alteration. The negative cultural results for samples 13b could be attributed to the small quantity (0.3 mg) of available sample; the other samples ranged from 0.4 to 15 mg. The microbial count on the black crust was comparable to the other samples. It was demonstrated that these alterations host an active microflora able to use accumulated organic pollutants as a carbon and energy source [34]. On the apparently non-altered samples, the counts were up to three orders of magnitude lower for both bacteria and fungi, partly explaining why visual inspection revealed no discolouration.

The sequences were phylogenetically most closely related to the Cyanobacteria, Actinobacteria, Bacteroidetes, Alphaproteobacteria, Betaproteobacteria and Gammaproteobacteria, Deinococcus-Thermus and Acidobacteria. One of the most common bacterial groups associated with carbonate stone biodeterioration is Actinobacteria [40]. In fact, Actinobacteria, Bacteroidetes and Alphaproteobacteria were identified on a gothic monument made of oolitic and dolomitic limestone [27], while Actinobacteria, Alphaproteobacteria, Betaproteobacteria, Gammaproteobacteria and Acidobacteria were found in limestone from a Maya archaeological site in southern Mexico [25]. Proteobacteria, Acidobacteria and Actinobacteria were the major components of microbial communities in coloured colonisations on cave walls with palaeolithic paintings [31, 38]. The bacterial group Deinococcus-Thermus is not commonly associated with limestone; however, it was identified in a cave with palaeolithic paintings by Stomeo and co-workers [36]. Despite many of these taxa being found on stone surfaces and producing discolouration [41], the FISH results demonstrated that the Cyanobacteria generally were dominant among the other prokaryotics belonging to the Bacteria domain: on average, more than 60% of the cells belonging to the Bacteria domain were also positive to the Cyanobacteria probes. Several studies conducted on monuments have proven that Cyanobacteria are among the most deteriorating biological agents dwelling on stone material [39] and are able to form colourful microbial contaminations. Cyanobacteria were identified in all the samples, which were stained by green and green–black microbial discolourations, collected before the treatment; thus, they can be thought to be among the biological agents responsible for the colour of these alterations. However, in samples 16b and 17b, characterised by green microbial contamination, most of the cells belonging to the bacterial domain were not positive to the Cyanobacteria probes. This evidence suggests that the green putative microbial contamination might also be caused by other green-pigmented microorganisms such as green algae. Indeed,

Figure 3 Mean values of cells positive after hybridisation with the Bacteria domain (*white bars*) probe and specific Cyanobacteria (*black bars*) probes in several samples. The values with different *letters* are considered significantly different according to Tukey–Kramer ($p < 0.05$)
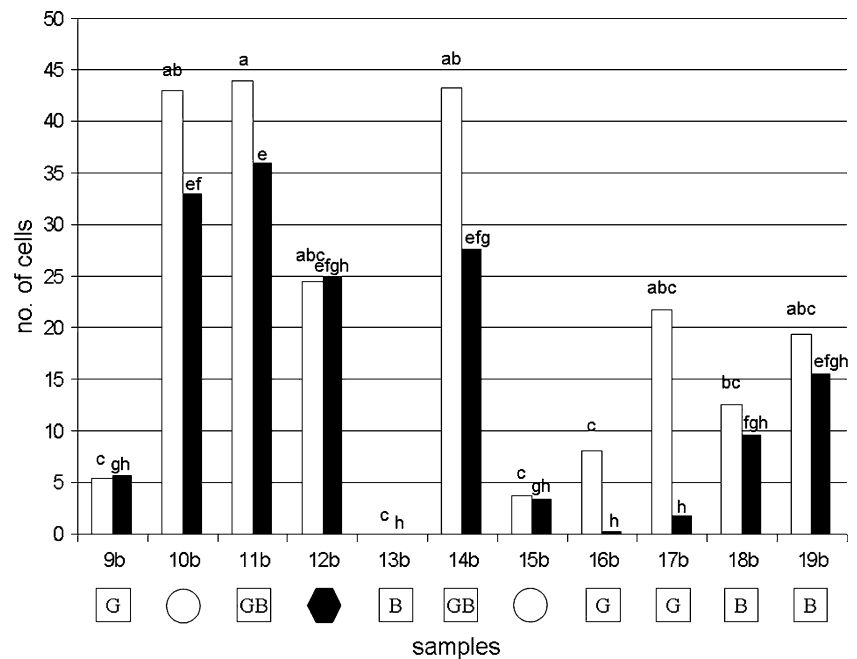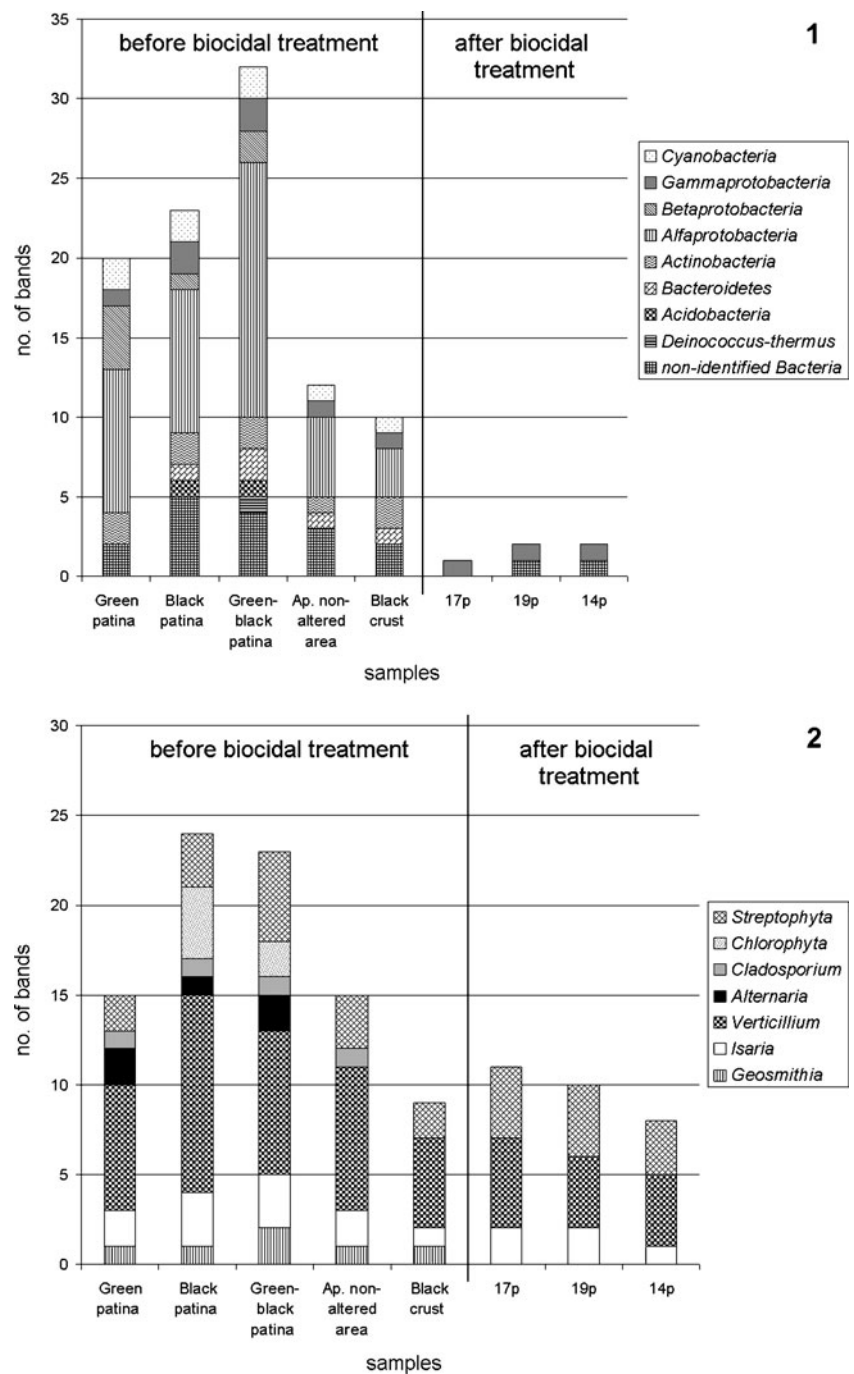

the sequencing of 18S rRNA gene fragments showed that the eukaryotic community included the algal genera *Myrmecia*, *Klebsormidium* and *Friedmannia*. Note that *Myrmecia* and *Friedmannia* are Chlorophyta green algae and *Klebsormidium* is a Streptophyta green alga characterised by an enhanced freezing tolerance [29], so it probably adapted to the rigorous climate of Trento. Tomaselli and co-workers [39] claimed that Chlorophyta algae are very frequently isolated on monuments, and Gaylarde and colleagues [11] reported that green algae are the first colonisers of outdoor buildings in Latin America. As these were the green algae genera isolated from the green microbial contamination, they, in conjunction with Cyanobacteria, can be considered responsible for the alterations on the Demetra and Cronos surfaces. Photosynthetic microorganisms can directly participate in decay processes, causing aesthetic damage and, subsequently, structural and chemical damage and, indirectly, by supporting the growth of other microorganisms [1, 16].

The sequencing of 18S rRNA gene fragments showed that the eukaryotic community included the fungal genera *Isaria*, *Geosmithia*, *Verticillium*, *Alternaria* and *Cladosporium*. The first, *Isaria*, is an entomogenous genus of fungi. In Spanish caves, the cadavers of arthropods were found covered by *Isaria*, which extended from the insect body to the adjacent soil. Arthropods are vectors of entomogenous fungi and play an important role in fungal dispersion in caves, catacombs and mural paintings [17]. *Geosmithia* spp. were recently found to be regular associates of many insect species that invade the phloem or sapwood of various plant genera [18]. Dematiaceous fungi that are characterised by the production of the black pigment melanin and manifest

meristematic growth are considered by several authors the most harmful microorganisms of outdoor stone material [20], causing mechanical damage and aesthetic alterations (black coating) [3, 26, 43]. *Alternaria* and *Cladosporium* are very well-known microcolonial black fungi [43]. Many authors have isolated them on marble and limestone in several environments, including monuments and archaeological sites [13, 36, 43]. The *Verticillium* species are common colonisers of rock substrata [3], and many of them are able to deposit melanin in the cell wall [15]. These mycetes have also been isolated from monuments [14]. For these reasons, *Alternaria*, *Cladosporium* and *Verticillium*, found in black and green–black microbial contamination, can be thought to be the biological agents responsible for black staining. From the above results, we concluded that prokaryotic and eukaryotic algae were responsible for the green microbial contamination and dematiaceous fungi for the black discolouration. Since the biodeteriogen agents were present in all the differently coloured microbial-contaminated sites, it is most likely that the colour of the contamination varied from green to black depending on the abundance of the individual biodeteriogen agent.

The variety of biodeteriogens forced us to choose a broad-range biocide to remove the discolouration. Treatment with the biocide resulted in a decrease of the bacterial load (up to five orders of magnitude), and neither culturable fungi nor culturable prokaryotic and eukaryotic algae grew on the samples collected after the treatment. Indeed, after the treatment, the DGGE results showed that the samples from surfaces that had, prior to treatment, shown green, black and green–black microbial contamination, now showed far fewer bands than before treatment. The

Figure 4 Bacterial taxa (*1*) and fungal and algal taxa (*2*), identified by DGGE before treatment, in the green microbial contamination (samples 9b, 16b and 17b), black microbial contamination (samples 13b, 18b and 19b), green–black microbial contamination (samples 11b and 14b), black crust (sample 12b) and apparently non-altered area (samples 10b and 15b) in comparison to the taxa identified in the samples collected after the treatment: samples 17p, 19p and 14p collected close to the sampling areas of specimens 17b, 19b and 14b, respectively

sequencing of these bands testified to the significant decrease, brought about by the biocide, in the biological diversity of the Bacteria, fungal and algal taxa, a result in accordance with the cultural results.

Importantly, the DGGE results proved that Cyanobacteria (among those responsible for the green microbial contamination) and most of the green algae and dematiaceous (the latter responsible for the black microbial contamination) were not identified in samples collected after the treatment. Among the taxa present on the surface

after the treatment (Gammaproteobacteria, *Verticillium*, *Isaria* and Streptophyta), only Streptophyta and *Verticillium* were potential biodeteriogen agents that remained.

Conclusions

The Demetra and Cronos statues presented two concomitant deterioration phenomena found very frequently on outdoor stone artwork: the sulphatation of limestone caused

by air pollution and surface biodeterioration. The first phenomenon caused the thick black crusts in the areas sheltered from rainfall, and the second generated colourful microbial contamination on surfaces. This work shows that an integrated biotechnological approach can provide an important solution to both these problems. In fact, the bioremediation treatment with *D. vulgaris* successfully removed black crust from limestone, and the identification of biodeteriogen agents (Cyanobacteria, green algae and black pigmented fungi) by DGGE allowed the selection of a suitable cleaning treatment for the colourful microbial contamination. However, given the presence of some green algae and melanin-containing fungi after the treatment and the constant exposure of the sculptures to atmospheric pollution, we recommended an ongoing maintenance routine to ensure longer-lasting conservation.

References

1. Ariño X, Hernandez-Marine M, Saiz-Jimenez C (1997) Colonization of Roman tombs by calcifying Cyanobacteria. Phycologia 36:366–373
2. Ausubel FM, Brent R, Kingston RE, Moore DD, Seidman JG, Smith JA, Struhk K (1994) Current protocols in molecular biology. Wiley, New York
3. Burford EP, Kierans M, GaddG M (2003) Geomycology: fungi in mineral substrata. Mycologist 17:98–107
4. Cappitelli F, Abbruscato P, Foladori P, Zanardini E, Ranalli G, Principi P, Villa F, Polo A, Sorlini C (2009) Detection and elimination of Cyanobacteria from frescoes: the case of the St. Brizio Chapel (Orvieto Cathedral, Italy). Microb Ecol 57(4):633–639
5. Cappitelli F, Principi P, Pedrazzani R, Toniolo L, Sorlini C (2007) Bacterial and fungal deterioration of the Milan Cathedral marble treated with protective synthetic resins. Sci Total Environ 385:172–181
6. Cappitelli F, Toniolo L, Sansonetti A, Gulotta D, Ranalli G, Zanardini E, Sorlini C (2007) Advantages of using microbial technology over traditional chemical technology in removal of black crusts from stone surfaces of historical monuments. Appl Environ Microbiol 73(17):5671–5675
7. Cappitelli F, Zanardini E, Ranalli G, Mello E, Daffonchio D, Sorlini C (2006) Improved methodology for bioremoval of black crusts on historical stone artworks by use of sulfate-reducing bacteria. Appl Environ Microbiol 72(5):3733–3737
8. Chapoulie R, Cazenave S, Duttine M (2008) Laser cleaning of historical limestone buildings in Bordeaux appraisal using cathodoluminescence and electron paramagnetic resonance. Environ Sci Pollut Res 15(3):237–243
9. Commissione Normal (1980) Raccomandazioni Normal B 3/80 Materiali lapidei: campionamento. Roma: C.N.R. - I.C.R.
10. Gauri KL, Bandyopadhyay JK (1999) Carbonate stone chemical behaviour, durability, and conservation. Wiley, New York
11. Gaylarde PM, Gaylarde CC (2000) Algae and Cyanobacteria on painted buildings in Latin America. Int Biodeterior Biodegrad 46(2):93–97
12. Gorbushina A, Krumbein WE (2000) Patina (physical and chemical interaction of sub-aerial biofilms with object of art). In: Ciferri O, Tiano P, Mastromei G (eds) Of microbes and art. The role of microbial communities in the degradation and protection of cultural heritage, vol 15. Kluwer Academic/Plenum, New York, pp 105–120
13. Gorbushina A, Krumbein WE, Panina L, Soukharjevski S, Wollenzien U (1993) On the role of black fungi in colour change and biodeterioration of antique marbles. Geomicrobiol J 11:205–222
14. Gorbushina AA, Lyalikova NN, Vlasov DY, Khizhnyak TV (2002) Microbial communities on the monuments of Moscow and St. Petersburg: biodiversity and trophic relations. Microbiology 71(3):350–356
15. Heale JB, Isaac I (1964) Dark pigment formation in *Verticillium albo-atru*. Nature 202:412–413
16. Hernandez-Marine M, Asencio AD, Canals A, Ariño X, Aboal M, Hoffmann L (1999) Discovery of population of the lime-incrusting genus Loriella (Stigomenatales) in Spanish caves. Arch For Hydrobiologie Algol Stud 94:121–138
17. Jurado V, Sanchez-Moral S, Saiz-Jimenez C (2008) Entomogenous fungi and the conservation of the cultural heritage: a review. Int Biodeterior Biodegrad 62:325–330
18. Kolarik M, Kubatova A, Hulcr J, Pazoutova S (2008) Geosmithia fungi are highly diverse and consistent bark beetle associates: evidence from their community structure in temperate Europe. Microb Ecol 55:65–80
19. Krumbein WE (1992) Colour change of building stone and their direct and indirect biological causes. In: Delgado Rodriguez J, Henriques F, Telmo Jeremias F (eds) Proceedings of 7th International Congress on Detection and Conservation of Stone, LNEC, Portugal, pp 443–452.
20. Krumbein WE, Diakumaku E (1996) The role of fungi in the deterioration of stone. In: Interactive physical weathering and bioreceptivity study on building stones, monitored by computerized X-ray tomography (CT) as a potential non-destructive research tool. Protection and Conservation of the European Cultural Heritage, Research Report 2, pp 140–170
21. Leznicka S, Strzelczyk A, Wandtychowska D (1988) Removing of fungal stains from stone-works. In: IV International Congress on Deterioration and Conservation of Stone, Vol. 2, Nicolaus Copernicus University, 12–14 September 1988, Torun, pp 102–110
22. Loy A, Horn M, Wagner M (2003) ProbeBase: an online resource for rRNA targeted oligonucleotide probes. Nucleic Acids Res 31:514–516
23. Maravelaki-Kalaitzaki P (2005) Black crusts and patinas on Pentelic marble from the Parthenon and Erechtheum (Acropolis, Athens): characterization and origin. Anal Chim Acta 532:187–198
24. McNamara CJ, Mitchell R (2005) Microbial deterioration of historic stone. Front Ecol Environ 3:445–451
25. McNamara C, Perry TD, Bearce KA (2006) Epilithic and endolithic bacterial communities in limestone from a Maya archaeological site. Microb Ecol 51:51–64
26. McNamara C, Perry TD, Zinn M, Breuker M, Müller R, Hernandez-Duque G, Mitchell R (2003) Microbial processes in the deterioration of Maya archaeological buildings in southern Mexico. In: Koestler RJ, Koestler VH, Charola AE, Nieto-Fernandez FE (eds) Art, biology and conservation: biodeterioration of works of art. The Metropolitan Museum of Art, New York, pp 248–265
27. Miller AZ, Laiz L, Gonzalez JM, Dionísio A, Macedo MF, Saiz-Jimenez C (2008) Reproducing stone monument photosynthetic-based colonization under laboratory conditions. Sci Total Environ 405:278–285

28. Muyzer G, De Waal EC, Uitierlinden AG (1993) Profiling of complex microbial populations by denaturing gradient gel electrophoresis analysis of polymerase chain reaction-amplified genes coding for 16S rRNA. Appl Environ Microbiol 59(3):695–700

29. Nagao M, Matsui K, Uemura M (2008) *Klebsormidium flaccidum*, a charophycean green alga, exhibits cold acclimation that is closely associated with compatible solute accumulation and ultrastructural changes. Plant Cell Environ 31:872–885

30. Oros-Sichler M, Gomes NCM, Neuber G, Smalla K (2006) A new semi-nested PCR protocol to amplify large 18S rRNA gene fragments for PCR–DGGE analysis of soil fungal communities. J Microbiol Methods 65:63–75

31. Portillo MC, Gonzalez JM, Saiz-Jimenez C (2008) Metabolically active microbial communities of yellow and grey colonizations on the walls of Altamira Cave, Spain. J Appl Microbiol 104:681–691

32. Ricci C, Miliani C, Brunetti BG, Sgamellotti A (2006) Non-invasive identification of surface materials on marble artifacts with fiber optic mid-FTIR reflectance spectroscopy. Talanta 69(5):1221–1226

33. Rossi Manaresi R (1996) Oxalate patinas and conservation treatments. In: Realini M, Toniolo L (eds) The oxalate films in the conservation of works of art. Proceedings of the 2nd International Symposium, Milan, 25 to 27 March 1996. EDI-TEAM, Bologna, pp 113–127

34. Saiz-Jimenez C (1995) Deposition of anthropogenic compounds on monuments and their effect on airborne microorganisms. Aerobiologia 11(3):161–175

35. Scott James A, Untereiner WA, Ewaze JO, Wong B, Doyle D (2007) *Baudoinia*, a new genus to accommodate *Torula compniacensis*. Mycologia 99:592–601

36. Sterflinger K (1998) Temperature and NaCl tolerance of rock-inhabiting meristematic fungi. Anton Leeuw Int J G 74:271–281

37. Stomeo F, Gonzalez JM, Saiz-Jimenez C (2007) Analysis of the bacterial communities on paintings and engravings in Doña Trinidad cave (Ardales, Malaga, Spain). Coalition 14:24–27

38. Stomeo F, Portillo MC, Gonzalez JM, Laiz L, Saiz-Jimenez C (2008) Pseudonocardia in white colonizations in two caves with Paleolithic paintings. Int Biodeterior Biodegrad 62:483–486

39. Tomaselli L, Lamenti G, Bosco M, Tiano P (2000) Biodiversity of photosynthetic micro-organisms dwelling on stone monuments. Int Biodeterior Biodegrad 46(3):251–258

40. Urzì C, Brusetti L, Salamone P, Sorlini C, Stackebrandt E, Daffonchio D (2001) Biodiversity of *Geodermatophilaceae* isolated from altered stones and monuments in the Mediterranean basin. Environ Microbiol 3(7):471–479

41. Warscheid T, Braams J (2000) Biodeterioration of stone: a review. Int Biodeterior Biodegrad 46:343–368

42. Webster A, May E (2006) Bioremediation of weathered-building stone surfaces. Trends Biotechnol 24(6):255–260

43. Wollenzien U, de Hoogb GS, Krumbeina WE, Urzi C (1995) On the isolation of microcolonial fungi occurring on and in marble and other calcareous rocks. Sci Total Environ 167:287–294

ORIGINAL RESEARCH PAPER

N-vanillylnonanamide tested as a non-toxic antifoulant, applied to surfaces in a polyurethane coating

**Federica Villa · Lucia Giacomucci · Andrea Polo ·
Pamela Principi · Lucia Toniolo · Marienella Levi ·
Stefano Turri · Francesca Cappitelli**

Abstract The potential on *N*-vanillylnonanamide (NVN) in preventing the attachment of *Pseudomonas stutzeri* and a *Bacillus cereus*-group strain was investigated. NVN up to 852 μM was not toxic, nor was it an energy source for either organism. Microbial attachment assays were carried out on glass and polylysine slides. with NVN being dispersed in or applied to the surfaces using a polyurethane coating. NVN at 205 μM inhibited *Bacillus* adhesion on glass slides by 48% and the percentage did not significantly increase at 852 μM. NVN blended into or sprayed onto the coating at 205 μmol/kg did not prevent adhesion. The compound is therefore not useful as an antifouling product under the tested coating conditions.

Keywords Antifouling · *Bacillus cereus* · Capsacinoid compound · Polyurethane-coated surface · *Pseudomonas stutzeri* · *N*-vanillylnonanamide

F. Villa · L. Giacomucci · A. Polo · P. Principi · F. Cappitelli (✉)
Dipartimento di Scienze e Tecnologie Alimentari e Microbiologiche, University of Milan, Via Celoria 2, 20133 Milan, Italy
e-mail: francesca.cappitelli@unimi.it

L. Toniolo · M. Levi · S. Turri
Dipartimento di Chimica, Materiali e Ingegneria Chimica 'Giulio Natta', Politecnico di Milano, Milan, Italy

Introduction

Biofouling is the undesirable accumulation of microorganisms, plants and animals on a surface (Whelan and Regan 2006). Bacteria are generally the first organisms to colonize surfaces exposed to different environments through adhesion and subsequent biofilm formation. As mature biofilms are invariably recalcitrant to a diversity of treatment strategies, minimizing bacterial attachment and the subsequent formation of biofilms could be advantageous in reducing the early stages of biofouling. The conventional approach to limiting biofouling is chemical abatement by the application of biocides and mechanical cleaning. However mechanical cleaning can be costly and may not be applicable due to the fouled surface's inaccessibility. On the other hand, some chemicals, such as organotin compounds, pose severe environmental and human health risks, and for this reason they have been banned (Howell and Behrends 2006). The search for suitable non-toxic, or even less-toxic, active natural compounds to incorporate into antifouling coatings could be a successful approach for the prevention of biofouling. Capsaicin (8- methyl-*N*-vanillyl-6-nonenamide), a pungent compound of hot peppers, the fruit of the *Capsicum* plant, can prevent the growth of various bacteria, including *Pseudomonas* and *Bacillus* spp. (Molina-Torres et al. 1999; Dorantes et al. 2000). Tsuchiya (2001) reported that low capsaicin concentrations fluidize membranes whereas high concentrations rigidify them. Capsaicin

was claimed to be an efficient antifoulant against *Pseudomonas putida* and other bacteria when applied in dispersion at 131 μM, a concentration below its toxic level (Turgut et al. 2004; Xu et al. 2005a, b). The synthetic analogue *N*-vanillylnonanamide, available commercially, differs from capsaicin chemically by a methyl group and a double bond.

N-vanillylnonanamide has many advantages over natural capsaicin extracts, it is cheaper (the cost of 1 g capsaicin is 5-fold higher than that of 1 g *N*-vanillylnonanamide) and has fewer impurities. In view of its potential applications, *N*-vanillylnonanamide anti-adhesion capability was tested both in dispersion and when blended into and spread onto a polyurethane coating.

Materials and methods

Materials

Dissolution of *N*-vanillylnonanamide (purity ≥ 97%, Sigma-Aldrich) was obtained following a method previously described for capsaicin (Turgut et al. 2004), expect that instead of distilled water phosphate buffer solution was used (PBS, Sigma-Aldrich). *N*-vanillylnonanamide was added to the liquid medium to give 7, 34, 68, 136, 205 and 852 μM.

Identification of bacteria, growth medium and bacterial surface hydrophobicity

The bacteria were isolated from a biofilm on a household surface; they were characterised as Gram-negaive and Gram-positive microorganisms and had previously been used in our laboratory for other biofilm studies. For identification, total DNA extraction, amplification and partial sequencing were carried out according to Brusetti et al. (2006). The two sequences were compared with the BLASTIN nucleotide sequence database.

Bacteria were grown at 30°C in Plate Count Broth (PCB, Difco) at 150 rpm and all the inocula were taken from rapidly growing cultures. Cell enumeration was calculated from OD_{540}. The wettability of the bacterial cells before and after *N*-vanillylnonanamide treatment was measured as the contact angle between the water drops and the lawns of bacteria deposited on membrane filters, with a Dataphysics

OCA-20 contact angle equipped with a CCD video camera (DataPhysics Instuments GmbH). One hundred and fifty ml of 12 h cell suspension (10^8 cell/ml) was washed three times with PBS and suspended in 30 ml. The bacterial suspension was filtered using 0.2 μm pore-size nitrile filters air-dried for 1 h to reach the "plateau contact angle".

Glass slides and coating preparation

Microscope glass slides (Menzel GmbH) and coated polylysine slides (VWR International), both of 2.5 × 7.5 cm, were used as substrata.

Polyurethane was synthesized by mixing oxydrilated polyester resin T535 (Alcea) with aliphatic biureto polyisocyanate in toluene at 10/10.66 (w/w). The coating was applied by brush onto the slide surfaces to give an average thickness of 20 μm, and then left to air dry for 48 h.

The capsaicinoid incorporation into, and its spreading onto, the polyurethane coating was achieved in two ways: (i) by dissolving the *N*-vanillylnonanamide at 205 μmol/kg; (ii) a polyurethane coating was applied to the surface, then a calculated amount of *N*-vanillylnonanamide in the same solvent was sprayed on this surface. In both cases the aim was for a final concentration of 205 μmol/kg of dried coating.

Equipment for the characterisation of the glass surfaces

Contact angle measurements (θw) were carried out at room temperature using the contact angle goniometer DataPhysics OCA 20 system (DataPhysics Instuments GmbH). The gloss of the slides and coatings was measured using a glossmeter Multi-Gloss 268 (Konica Minolta) equipped with a tungsten lamp (2.5 V/60 mA) operating at 20°, 60° and 85°. The surface morphology was evaluated with an optical microscope equipped with video camera and digital image analysis, and an Environmental Scanning Electron Microscope Evo 50EP (Zeiss). A ThermoNicolet Nexsus FT-IR spectrophotometer (Thermo Electron Corporation) equipped with ATR Silver Gate Specac and Ge crystal was used for attenuated total-reflectance measurements to indicate the changes in the main characteristics of the coating with and without the capsaicinoid.

Toxicity evaluation

Toxicity experiments were conducted at 30°C in PCB medium with both bacteria at 10^6 cells/ml, with N-vanillylnonanamide at 205 and 852 μM. The growth rates with or without N-vanillylnonanamide were determined. N-Vanillylnonanamide without cells was used as the control. The negative control was all the combinations but without the antifoulant. The toxicity of N-vanillylnonanamide was evaluated using an overnight bacterial suspension 10-fold serially diluted in PBS and 100 μl of each dilution was plated on PC A without and with 205 or 852 μM N-vanillylnonanamide. The plates were incubated overnight at 30°C and the number of colony-forming units counted.

N-Vanillylnonanamide as the sole carbon
and energy source

A mineral medium (KH_2P0_4 30 g/1, Na_2HP0_4 70 g/1, NH_4C1 10 g/1, pH 7) was used to which N-vanillylnonanamide was added up to 852 μM as the sole carbon and energy source. Bacteria were added 10^6 cells/ml and grown at 30°C. Samples were taken up to 14 days. The positive control was mineral medium supplemented with the same concentration of glucose.

DAPI staining and permeabilisation

The slides were fixed with a 4% paraformaldehyde solution in PBS, held for 2 h on ice, and then washed twice with PBS. The samples inside an in situ frame (1 cm^2 area, Eppendorf) adhered to a glass slide were stained with 25 μl DAPI (4′, 6-diamidino-2-pheny-lindole dihydrochloride, 10 μg/ml working solution), then incubated in the dark for 5 min and washed twice with PBS. Positive DAPI-stained cells were visualised by epifluorescence microscopy. Images were collected using a digital camera.

Bacterial attachment study

Glass slides held static at 90° in a 50 ml plastic flask were collected from the incubation assay after 24, 48, 72, and 144 h. Each flask contained an initial population 10^6 cells/ml in 20 ml of PCB medium added with N-vanillylnonanamide at 0, 7, 34, 68, 136,

205 and 852 μM. In addition, the bacterial media were analysed at 540 nm to evaluate if growth in liquid was inhibited by the compound. The number of adhered cells per cm^2 was esimated using ImageJ 1.34s (http://rsbweb.nih.gov/ij/). A total of 2,641 observations were considered for N-vanillylnonanamide dispersed in the liquid medium, 1,176 for N-vanillylnonanamide blended into the polyurethane coating and 1,000 for N-vanillylnonanamide spread onto the coated slides. A three- and two-way analysis of variance (ANOVA) via MATLAB software (Version 7.0, The MathWorks Inc) were applied to evaluate, for each microorganism, the effect of the substratum, N-vanillylnonanamide concentration and time on attachment. Tukey's honestly significant different test was used for pairwise comparison to determine the significance of the data (statistically significant results P values < 0.05, non-significant results $P > 0.05$).

Results

Identification of bacteria

For the Gram-positive bacterium, similarities of the closest relatives found in BLASTN searches were 99% both with *Bacillus cereus* and *Bacillus thuringiensis,* closely related bacteria of the *B. cereus* sensu-lato group. For the Gram-negative bacterium, similarities of the closest relatives found in BLASTN searches were 99% with *Pseudomanas stutzeri.*

Toxicity test and bacterial ability to use
N-vanillylnonanamide as the sole source
of C and energy

The growth test results are reported in Table 1. There was no significant difference among the growth rates with or without N-vanillylnonanamide ($P_{Bacillus}$: 0.256; $P_{Pseudomonas}$: 0.733). Furthermore, N-vanillylnonanamide did not affect the growth of the bacteria in solid medium ($P_{Bacillus}$: 0.757; $P_{Pseudomonas}$: 0.542). Hence, N-vanillylnonanamide was not toxic to either microorganism. Although the *B. cereus*-group and *P. stutzeri* strains grew in mineral media when supplemented with glucose, they did not grow on N-vanillylnonanamide as sole carbon and energy

Table 1 Summary of the results obtained from the growth tests with their corresponding standard deviations (SD)

	0^b		$205\ \mu M^b$		$852\ \mu M^b$		P
	Mean	SD	Mean	SD	Mean	SD	
Toxicity test in liquid medium (10^7 cells/h)[a]							
B. cereus	1.5	0.04	1.5	0.01	1.5	0.02	0.256
P. stutzeri	8.0	0.8	8.3	0.03	8.2	0.01	0.733
Toxicity test in solid medium (10^8 CFU/ml)							
B. cereus	9.1	0.3	8.8	0.7	9.5	0.1	0.757
P. stutzeri	4.3	0.5	5.0	0.6	4.7	0.6	0.542

N-vanillylnonanamide as the sole carbon and energy source (10^5 cells/h)[a]

	Glucose		*N*-vanillylnonanamide	
	Mean	SD	Mean	SD
B. cereus	1.2	0.07	–	–
P. stutzeri	6.9	0.29	–	–

Results were calculated considering two replicas for each combination in both the liquid and solid tests

[a] The growth rates were calculated as the regression values of the linear portion of the curve "cellular density OD_{540} versus time"

[b] Concentration of *N*-vanillylnonanamide in the toxicity test

source. The pH remained neutral and constant in all the experiments.

Superficial properties of the glass slides and bacterial cells

Without *N*-vanillylnonanamide, the water contact angles on the bacterial lawns ranged from 18.1° ± 2.0 for *P. stutzeri* to 19.5°± 5.1 for the *B. cereus*-group strain. When the cells were in a *N*-vanillylnonanamide suspension, the water contact angles on the bacterial lawns ranged from 16.7°± 1.7 for *P. stutzeri* to 21.5°± 2.9 for the *B. cereus*-group strain. Both uncoated glass substrata were very wettable. However, polylysine slightly increased the water repellence of the surface (glass slide: 18.6°± 1.0; polylysine glass slide: 29.9° ± 1.6). The polyurethane coating masked the wettability properties of the glass surfaces, making both the coated substrata hydrophobic (polyurethane-coated glass slide: 89.97° ± 1.68; polyurethane-coated polylysine glass slide: 95.6° ± 1.9, considering that water repellent surfaces show angles >90°). In addition, the selected coating did not modify surface gloss. *N*-Vanillylnonanamide in the polyurethane coating did not modify the ATR coating spectrum. Using the environmental scanning electron microscope, the surface morphology of the polyurethane-coated glass substrata without and with *N*-vanillylnonanamide appeared the same.

DAPI staining and bacterial attachment on coated and uncoated glass slides without *N*-vanillylnonanamide

Stained *Bacillus* spores are shown in the Fig. 1. Both *Bacillus* and *Pseudomonas* formed biofilms at a later time.

Table 2 shows the average of the adhered cells and the contact angle for the following substrata: the glass slide (basically slightly acid and wettable), the polylysine glass slide (probably conferring a positive
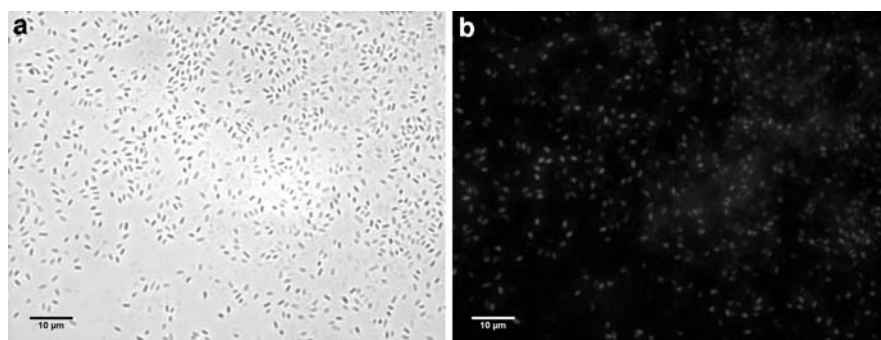

Fig. 1 DAPI-staining of *B. cereus-group* spores. Cells were dehydrated in an ethanol series (50, 80, and 100% v/v ethanol) for 1 min. Adhesion of spores to the surface: first step of biofilm formation. The same area is shown in the bright-field view (**a**) and epifluorescence microscope field with DAPI filter cube (**b**). Magnification of 1,000X under oil immersion. Bars represent 10 μm

Table 2 Average of the adhered cells and their contact angles to the different substrata with their corresponding standard deviations (SD)

Microrganism	Surface	No. cells/cm^2		Contact Angle		% Decreasing in adhesion
		Mean	SD	Mean	SD	
B. cereus	Glass slide	6.4×10^4	4.8×10^3	18.6	1	
	Polylysine glass slide	1.4×10^4	8.7×10^3	29.9	1.6	
	Coated glass or polylysine glass slide	1.5×10^4	7.2×10^3	90.3	1.6	**76.3**
P. stutzeri	Glass slide	1×10^4	1.3×10^3	18.6	1	
	Polylysine glass slide	1.2×10^4	1.9×10^3	29.9	1.6	
	Coated glass or polylysine glass slide	5.4×10^3	1.8×10^3	90.3	1.6	**57.1**

The percentage of adhesion decrease was determined by comparing the cellular density onto uncoated surfaces with that onto polyurethane-coated slides. Two replicates for each combination were utilised

charge to the surface) and the inorganic glass slide and polylysine glass slide coated with polyurethane (probably conferring water repellence properties to the surfaces). Coated glass slide and polylysine glass slide showed no significant difference in attachment whatever the microorganism considered (P$_{Bacillus}$: 0.616; P$_{Pseudomonas}$: 0.677). Thus, we refer to coated polylysine glass slide and coated glass slide as polyurethane-coated glass slides. *B. cereus*-group strain adhesion was more abundant on glass slide rather than polylysine glass slide, but it did not changed when *P. stutzeri* adhesion was considered. The lowest microbial adhesion was obtained for hydrophobic polyurethane-coated slides.

In summary our studies determined that the microbial adherence to materials occurred in the following order: (i) for *P. stutzeri*, polylysine glass slide = glass slide > polyurethane coated slides, (ii) for the *B. cereus*-group strain, glass slide > polylysine glass slide = polyurethane coated slides.

Bacterial attachment on slides immersed in liquid medium containing *N*-vanillylnonanamide

Cell growth (i.e. the OD$_{540}$) was not inhibited by the compound. *N*-Vanillylnonanamide led to a significant reduction in the *Bacillus* coverage: 48% on glass slide when 205 µM of *N*-vanillylnonanamide was
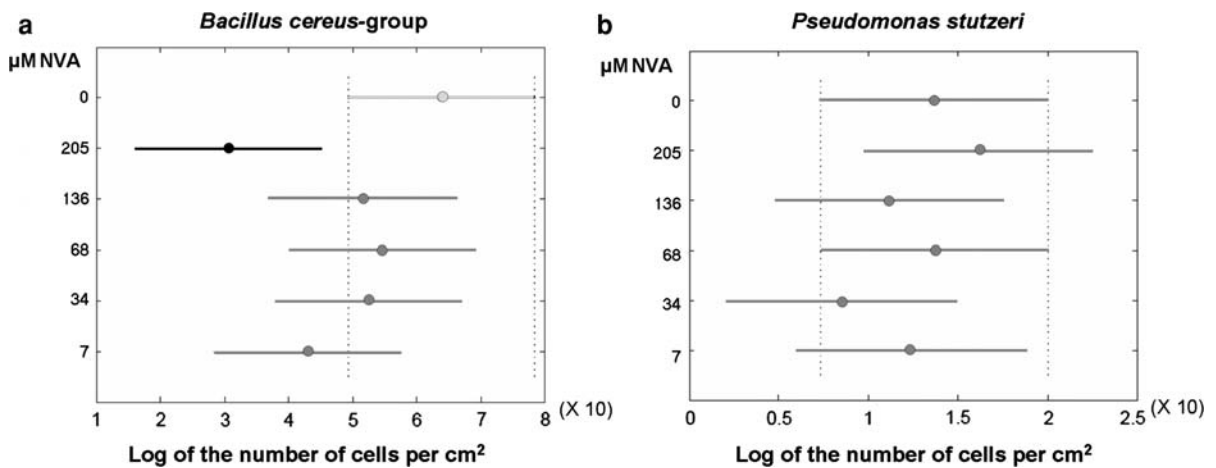

Fig. 2 Adhesion assay on glass slide: significative reduction in the *B. cereus*-group coverage at 205 µM *N*-vanillylnonanamide concentration (**a**). No significative differences were observed for *P. stutzeri* whatever the concentration of *N*-vanillylnonanamide (**b**). Graphs were obtained by multicomparison analysis at 95% confidence interval. NVA = *N*-vanillylnonanamide

dispersed in buffer (P: 0.03) (Fig. 2a). The maximum concentration of 852 μM *N*-vanillylnonanamide did not significantly improve the above performance. Dispersed *N*-vanillylnonanamide did not hinder cell adhesion on polylysine glass slide (Fig. 2b). *P. stutzeri* adhesion on both glass slide and polylysine glass slide was not affected by the presence of *N*-vanillylnonanamide up to 205 μM ($P_{glass\ slide}$: 0.55;$P_{polylysine}$: 0.95). The maximum concentration of 852 μM *N*-vanillylnonanamide exhibited no adhesion inhibition activity.

Bacterial attachment on slides coated with polyurethane containing *N*-vanillylnonanamide

N-Vanillylnonanamide when entrapped in the coating was at 205 μmol per kg dried polymer, corresponding to the effective liquid concentration used in the tests. The ANOVA results clearly showed that the *N*-vanillylnonanamide-incorporated coating was not able to reduce bacterial adhesion across all surfaces, neither for *P. stutzeri* nor for the *B. cereus*-group ($P_{Pseudomonas}$: 0.870; $P_{Bacillus}$: 0.06). Also when we sprayed the *N*-vanillylnonanamide the results were not indicative of decreased microbial adhesion ($P_{Pseudomonas}$: 0.107; $P_{Bacillus}$: 0.159).

Discussion

The anti-adhesion capability of *N*-vanillylnonanamide has been said to be the same as the natural analogue capsaicin (Dombkowski et al. 2006). Although *N*-vanillylnonanamide at 30 μM strongly inhibited zebra mussel macrofouling (Angarano et al. 2007), no detailed investigation at the biofilm level has ever been carried out.

Before evaluating *N*-vanillylnonanamide as a potential antifoulant we studied its potential impact on the growth of two bacteria. The selected bacteria seemed good candidates for anti-biofilm studies as they were previously isolated from a biofilm. They were chosen for this study as *Bacillus* and *Pseudomonas* had already been target genera for antifouling research using capsaicin (Molina-Torres et al. 1999; Dorantes et al. 2000). Dorantes et al. (2000) observed that about 0.044 μmol of natural capsaicin showed inhibitory activity towards the growth of the *Listeria monocytogenes, Salmonella typhimurium* and *Bacillus*

cereus. In our study the synthetic analogue of capsaicin, *N*-vanillylnonanamide, did not affect, in terms of toxicity, bacterial growth at concentrations of up to 852 μM.

It was recently claimed that capsaicin and vanillylamine were utilised as a sole source of carbon and energy by, respectively, *Capsicum*-associated strains of *Variovorax* and *Ralstonia,* and *Pseudomonas* and *Variovorax* (Flagan and Leadbetter 2006). Both the *B. cereus*-group and *P. stutzeri* strains grew well in a mineral salt medium supplemented with the same concentration of glucose, but they were not able to utilise *N*-vanillylnonanamide as a growth nutrient. When the attachment of hydrophilic *P. stutzeri* and *B. cereus*-group strains to the uncoated and polyurethane-coated surfaces in the absence of *N*-vanillylnonanamide was investigated, bacterial adhesion was found more efficient on uncoated slide surfaces compared to polyurethane-coated ones, suggesting that just coating with polyurethane is already an antifouling option. This could be easily explained by the fact that the contact angle measurements showed a more hydrophobic behaviour for the polyurethane-coated surfaces.

With 205 μM of *N*-vanillylnonanamide in dispersion, the adhesion of the *B. cereus*-group on glass slide (but not on polylysine glass slide) was reduced by 48% compared to the control. Increasing the *N*-vanillylnonanamide concentration did not significantly improve this percentage. No bacterial adhesion reduction was observed for *P. stutzeri* whatever the surfaces and concentrations considered. As there were no obvious differences in the wettability of the *B. cereus*-group and the *P. stutzeri* cells, with or without antifoulant, we must search for other explanations of the mechanism of action of *N*-vanillylnonanamide rather than look at the changes of hydrophobicity.

We proved that after the addition of the *N*-vanillylnonanamide to the polymeric coating, there were neither surface modifications nor significant differences in bacterial adhesion. This result suggests that the capsaicinoid, once blended into a polyurethane coating, is no longer able to affect bacterial attachment. A possible reason could be the low leaching of the substance from the polyurethane coating, so we sprayed the antifoulant on the polyurethane coating surface. However, also *N*-vanillylnonanamide on the polyurethane coating was ineffective against biofouling, therefore the possible explanation of leaching was

excluded. The fact that the compound did not work when immobilized on the substratum might also be explained by the fact that it does not act to change membrane fluidity (Tsuchiya 2001).

This study suggests that *N*-vanillylnonanamide, tested at the same concentrations successfully adopted in other studies (Xu et al. 2005b), is not an effective antifoulant compound when embedded in a polymer matrix.

References

Angarano M-B, McMahon RF, Hawkins DL, Schetz JA (2007) Exploration of structure-antifouling relationships of capsaicin-like compounds that inhibit zebra mussel *(Dreissena polymorpha)* macrofouling. Biofouling 23:295–305

Brusetti L, Borin S, Mora D, Rizzi A, Raddadi N, Sorlini C, Daffonchio D (2006) Usefulness of length heterogeneity-PCR for monitoring lactic acid bacteria succession during maize ensiling. FEMS Microbiol Ecol 56:154–164

Dombkowski RA, Doellman MM, Head SK, Olson KR (2006) Hydrogen sulfide mediates hypoxia-induced relaxation of trout urinary bladder smooth muscle. J Exp Biol 209: 3234–3240

Dorantes L, Colmenero R, Hernandez H, Mota L, Jaramillo ME, Fernandez E, Solano C (2000) Inhibition of growth of some foodborne pathogenic bacteria by *Capsicum annum* extracts. Int J Food Microbiol 57:125–128

Flagan SF, Leadbetter JR (2006) Utilization of capsaicin and vanillylamine as growth substrates by *Capsicum* (hot pepper)-associated bacteria. Environ Microbiol 8:560–565

Howell D, Behrends B (2006) A methodology for evaluating biocide release rate, surface roughness and leach layer formation in a TBT-free, self-polishing antifouling coating. Biofouling 22:303–315

Molina-Torres J, Garcia-Chavez A, Ramirez-Chavez E (1999) Antimicrobial properties of alkamides present in flavouring plants traditionally used in Mesoamerica: affinin and capsaicin. J. Ethnopharmacol 64:241–248

Tsuchiya H (2001) Biphasic membrane effects of capsaicin, an active component in *Capsicum* species. J Ethnopharmacol 75:295–299

Turgut C, Newby BmZ, Cutright T (2004) Determination of optimal water solubility of capsaicin for its usage as a non-toxic antifoulant. Environ Sci Pollut Res 11:7–10

Whelan A, Regan F (2006) Antifouling strategies for marine and riverine sensors. J Environ Monitor 8:880–886

Xu Q, Barrios CA, Cutright T, Newby BZ (2005a) Evaluation of toxicity of capsaicin and zosteric acid and their potential application as antifoulants. Environ Toxicol 20:467–474

Xu Q, Barrios CA, Cutright T, Newby BZ (2005b) Assessment of antifouling effectiveness of two natural product antifoulants by attachment study with freshwater bacteria. Environ Sci Pollut Res 12:278–284

ENVIRONMENTAL MICROBIOLOGY

Detection and Elimination of Cyanobacteria from Frescoes: The Case of the St. Brizio Chapel (Orvieto Cathedral, Italy)

F. Cappitelli · P. Abbruscato · P. Foladori ·
E. Zanardini · G. Ranalli · P. Principi · F. Villa ·
A. Polo · C. Sorlini

Abstract A rosy discoloration partly masking the Luca Signorelli frescoes in St. Brizio Chapel (Orvieto Cathedral, Italy) for many years proved to be a biological alteration, so the present research focused on investigating biodeteriogens and selecting an appropriate biocide to treat them. Optical epifluorescence and electronic microscopic observations of the rosy powder revealed a prevalent autofluorescent coccoid form with a diameter bigger than 5 μm. Chlorophylls a and b were extracted, suggesting the presence of cyanobacteria, a thesis subsequently confirmed by flow cytometry. Cultural media were inoculated with the rosy powder, and microorganisms grew as a green patina in phototrophic conditions and as a rosy patina when organic compounds were added to the mineral medium. The rosy discoloration was most likely caused by the presence of phycoerythrin. The sequencing of the cyanobacteria-specific polymerase chain reaction (PCR)–DGGE bands matched, with a similarity percentage >94, uncultured cyanobacteria, and the sequences were deposited in the GenBank under EU874241, EU874242, EU874243, EU874244, EU874245, EU874246, and EU874247. Finally, the efficiency of the two biocides Neo Desogen and Metatin 5810-101, both based on benzalkonium chloride, was evaluated using adenosine triphosphate measurements and PCR-based detection of cyanobacteria. Metatin, used in situ at 2% of the trade product, proved to be the better biocide, no cyanobacteria being detected after the Metatin treatment.

F. Cappitelli (✉) · P. Abbruscato · P. Principi · F. Villa · A. Polo ·
C. Sorlini
Dipartimento di Scienze e Tecnologie
Alimentari e Microbiologiche,
University of Milan,
via Celoria 2,
20133 Milan, Italy
e-mail: francesca.cappitelli@unimi.it

P. Foladori
Dipartimento di Ingegneria Civile e Ambientale,
University of Trento,
via Mesiano 77,
38100 Trento, Italy

E. Zanardini
Dipartimento di Scienze Chimiche e Ambientali,
Facoltà di Scienze MM.FF.NN., University of Insubria,
Via Valleggio 11,
Como, Italy

G. Ranalli
Dipartimento di Scienze e Tecnologie
per l'Ambiente e il Territorio,
University of Molise,
C/da Fonte Lappone Pesche,
86090 Isernia, Italy

Introduction

It is well known that microorganisms can cause physical–chemical damage to cultural heritage [13, 26, 34], often leading to discoloration [30, 31]. Prior to the last conservation treatment, the Orvieto Cathedral (Italy) was showing many forms of deterioration, including chromatic alterations on both the stonework and the frescoes. Red spots on its stone façade [36] were considered to be of the same nature as the red stains found on the marble statues of the fountain of Villa Litta [27] and on the marble façade of the Certosa of Pavia [35]. These chromatic alterations were not connected with any physical–chemical decay of the substratum. However, inside the Orvieto Cathedral another kind of chromatic alteration, a rosy discoloration was observed, particularly on the Signorelli frescoes in the St. Brizio Chapel. Indeed, the formation of rosy powders on

frescoes is a well-known form of alteration. As long ago as 1917, it was observed that chromatic and structural alterations, rosy in color and extremely fragile, had occurred on the internal wall surfaces and plasters [20]. In 1971, this rosy powder alteration was definitely associated with microorganisms [8], and in 1979, the alteration was tentatively connected to phototrophs, both chlorophyta and cyanobacteria [17]. Phototrophic microorganisms have been reported to cause the deterioration of cultural heritage in environments where there is low light intensity and high humidity [1, 2], the very same conditions occurring in the St. Brizio Chapel. The patinas formed by phototrophs vary in color according to the characteristics of the taxa from greenish-yellow to dark green and black and from rosy to grey and brown. The morphology and color of these patinas can change, depending on the physiological cell state and the environmental conditions. Thus, Giacobini et al. [17] hypothesized that the rosy color of the powder alteration observed on the Signorelli frescoes was due to the aging of algal cells under particular ecological conditions. Also Bassi [7] described a microbiological attack in the form of pink powder on frescoes in the house of Aurighi (Rome, Italy) which had been restored many times. The pink powder patches on the frescoes were characterized by constantly present capsulated coccoid forms. The aim of this paper has been to confirm the presence of the coccoid forms, to relate them with the environmental conditions and rosy discoloration, and to abate the causative alteration agent.

Materials and Methods

Sampling

Samples were taken from rosy powdered areas on the frescoes in the St. Brizio Chapel (Orvieto Cathedral). Few grams of surface material were scraped off using a sterile scalpel, and this powder was transferred in sterile conditions to the laboratory.

The sampling taken from areas on the right wainscot included plaster reconstruction, the grotesque painting, and original plaster and from the left wainscot original plaster. Also, the "Resurrection of the Body" fresco was sampled: the legs of the resurrected people, the skull, the areas close to the skull, and the venters of male and female figures.

Pretreatment

A pretreatment step to dislodge cells from the mineral matrix was done by sonicating the samples for 20 min at 4°C in sterile phosphate-buffered saline solution (Sigma, Italy), using an ultrasonicator (Sonicator HD 2700 plus, Bandelin) equipped with a 2 mm tapered microtip and amplitude set at 35 W.

Cultural Media

The cultural media employed for the detection of cyanobacteria and chlorophyta were, respectively, Chu and Detmer mineral media, and Chu and Detmer media added with glucose (10 g/L) and casein (5 g/L) and incubated under light and dark conditions at room temperature and at 4°C. The cultural media had organic matter added to it as, in the past, compounds such as casein had been used on the studied frescoes for conservation purposes.

Contrast Phase Microscope and Epifluorescence Microscope Observations

Observations were carried out with a Leica DM4000B, digital epifluorescence microscope equipped with Cool-Snap CF camera (Photometrics, Roper Scientific) controlled by the software WinSpec Ver. 1.9.2 (Roper Scientific). Autofluorescence was detected.

Scanning Electron Microscopic Observations

Scanning electron microscopic observations of the rosy powder were carried out in order to estimate the presence of microorganisms on the decayed surface. Samples were fixed overnight in 2% glutaraldehyde in 0.01 M phosphate buffer, dehydrated in serial higher concentrations of ethanol (50%, 60%, 70%, 80%, 90%, and absolute), dried at critical point, and gold coated. The observations were made using a Jeol JSM 35 C microscope.

Chlorophyll Extraction

Chlorophyll extraction and determination was carried out according to the US Environmental Protection Agency method 446.0 [6] with the following modifications: 0.1 g of rosy powder was suspended in 10 ml of ddH$_2$O and sonicated as described above. The pigment was extracted in 90% acetone, allowed to steep for 2 h, and centrifuged at 1,000×g for 5 min. An aliquot of the surnatant was transferred to a glass cell and absorbance was measured at two wavelengths, 665 nm for chlorophyll a and 650 nm for chlorophyll b, using a spectrofluorimeter Perkin Elmer mod. LS-3B Fluorescence Spectrometer.

The chlorophyll a and b ratio was quantified using the formula: $Chl\,a = (16.5 \times A_{665}) - (8.3 \times A_{650})$ and $Chl\,b = (33.8 \times A_{650}) - (12.5 \times A_{665})$ [12].

Flow Cytometry

The flow cytometric approach was applied to two samples taken from the "Resurrection of the Body," the samples being obtained from two agar cultures with Chu (sample A) and Detmer (sample B) media added with organic matter.

For debris microorganism (with or without photosynthetic pigments) discrimination, the samples were stained with the DNA-specific dye SYBR-Green I (λ_{ex}=495 nm, λ_{em}=525 nm; Molecular Probes Inc.). An amount of 10 μL of dye after dilution in dimethyl sulfoxide (1:30 v/v) of commercial stock was dosed in 1-mL samples and incubated in the dark for 15 min. Samples were analyzed using a Bryte-HS flow cytometer (Bio-Rad, Hercules, CA, USA) with an excitation of 470–490 nm. For each microbial cell, the following signals were recorded: (1) green fluorescence, produced by staining with SYBR-Green I, collected with a 525±30 nm band-pass filter; (2) orange and red fluorescence, produced by photosynthetic pigments, collected between 550–600 and over 600 nm, respectively. Green fluorescence triggers the data acquisition, and distinguishes the fluorescent microorganisms from the noise produced by nonfluorescent particles or debris. For each sample, about 20,000 cells were analyzed. Cytograms were drawn with WinMDI freeware (http://facs.scripps.edu/software.html).

Biocides

The two biocides Metatin (Metatin 5810–101 now Rocima 110, Acima Chemical, tributyl tin naphthenate with lauryl dimethyl benzyl ammonium bromide) and Neo Desogen (Ciba-Geigy 10% alkyl-dimethyl benzyl-ammonium solution) were tested on the rosy powder of the right wainscot, plaster reconstruction.

The biocides were sprayed on the surface, and the adenosine triphosphate (ATP) bioluminescence assay was applied to both treated and untreated areas. Under laboratory conditions we assessed the minimal inhibiting concentration as described in Andrews [5]. In subsequent experiments, we tested the biocides by spraying them over 10×10 cm in situ areas, at two, three, and four times the MIC concentrations.

Then, for future operations, we took note of the lowest biocide concentration that inhibited cell viability on the frescoes. The final concentration of the two biocide solutions used for the conservation treatments was 2% of the trade products.

Biocide application to the altered areas was done by conservators spraying the more effective biocide at the selected concentration.

ATP Assay

For the evaluation of total ATP content, the Microbial Biomass Test Kit, including NRM™ reagent and standard ATP assay (Celsis-Lumac, Lumac B.V., Landgraaf, The Netherlands) were used. Bioluminescence values were measured in Tris-HCl buffer solution (0.001 M, pH 7.75) by placing an appropriate solution of ATP standard (10 μg). RLUs recorded by the Bioiocounter P 1500 (Lumac B.V., Landgraaf) luminometer were converted into pg ATP 100 μl^{-1} by a standard ATP curve. Further information can be found in previous works [18].

Extraction of Total Genomic DNA

From 20 mg of sonicated rosy powder, total genomic DNA was extracted as described by Schabereiter-Gurtner et al. [25] for artwork samples and plaster. Genomic DNA was purified through silica gel membranes (QIAamp Viral RNA Mini Kit Qiagen) following the manufacturer's protocol.

Polymerase Chain Reaction Specific for Cyanobacteria

To detect the presence of cyanobacteria in the samples before and after treatment with biocides, 16S rDNA fragments specific for cyanobacteria taxa were amplified in both treated and untreated samples. As positive control, a nonaxenic culture was included. A nested PCR approach was applied. The first amplification was carried out with 27f and 1522r primer set [28]. Then, a nested amplification step with primers CYA359f and CYA781r targeting cyanobacterial 16S rRNA gene was performed as described by Nubel et al. [21]. We used 50 pmol of each primer, 25 nmol of each deoxynucleoside triphosphate, 200 μg of bovine serum albumin, and 2 μl of the first PCR amplicon as template. After a hot start step consisting of 95°C for 15 min, the following thermal protocol was applied: denaturation temperature was 94°C for 2 min, followed by 35 cycles consisting of 1 min at 94°C, 1 min at 60°C, and 1 min at 72°C. All PCR reactions were carried out in 100 μL volumes in a PCR-Express thermocycler (Hybaid), using 0.5 U of Taq (Fast Start Taq, Roche) and including a negative control (sterile water). PCR products were separated in standard 2% agarose gels in 0.5× Trisborate-EDTA buffer [24].

DGGE Specific for Cyanobacteria and Sequencing of Bands

DGGE was performed using the DCode universal mutation detection system (Bio-Rad, Italy) with a 6% acrylamide gel and a denaturing gradient from 35% to 55% (100%

denaturation was defined as 7 M urea and 40% formamide), with the same cyanobacterial specific primers used in the PCR protocol described above, and adding a GC-clamp to the Cya359f primer.

Electrophoresis was run at 90 V and a constant temperature of 60°C, for 15 h. The gel was stained in a SYBER green solution (Molecular Probes, Leiden, The Netherlands) for 30 min and its image photographed using the GelDoc UV Transilluminator (Bio-Rad, Italy). The dominant bands of the DGGE gel were excised with a sterile surgical scalpel, and the DNA was extracted by incubating the gel fragments in 50 μl sterile distilled water at 37°C under agitation for 12 h. Subsequently, a 5-μl volume of the solution was used as a template for reamplification with the same DGGE primers and PCR conditions described above but without the GC clamp. The PCR products were purified using a QIAquick PCR purification kit (QIAGEN, Milan, Italy) according to manufacturer instructions. Purified DNA was sent to Primm (Primm srl San Raffaele Biomedical Science Park, Milano Italy) for sequencing. Sequencing was performed using the same forward primer as in DGGE but without the GC clamp as sequencing primer.

The sequences were deposited in the GenBank [9] database. Possible chimeric sequences were screened using the online Ribosomal Database Project (RDP release 8.1) Chimera Check program (http://rdp8.cme.msu.edu/html/analyses.html) [11]. Similarity comparisons to known 16S rDNA sequences in the database were performed using the online Basic Local Alignment Search Tool program (BLAST; http://www.ncbi.nlm.nih.gov/BLAST) [4].

Results

Microscopic Observations of the Rosy Powder

The optical microscope revealed the microbial cells forming a biofilm, often including the mineral matrix. Among the detected cell morphologies we observed mainly coccoid cells, with a diameter bigger than 5 μm. The samples were also tested for autofluorescence signals and the results were positive. Scanning Electronic Microscopy of the samples showed the dominance of capsulated coccoid cells in the biofilm (Fig. 1).

Characterization of Microbial Groups Present in the Rosy Powder

To separate the microorganisms from the matrix, the samples were subjected to sonication.

To characterize the phototrophic microorganisms, the samples were cultivated in liquid media (Chu and Detmer)
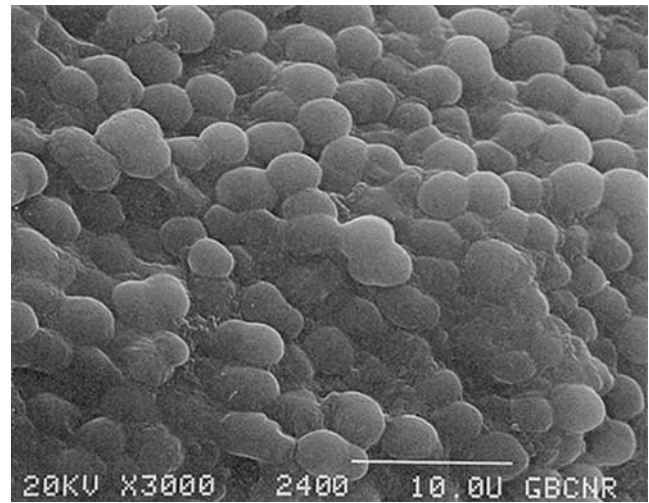

Figure 1 Scanning electron microscopy of biofilm sample with dominance of capsulated coccoid cells

and growth was observed after 2 months. At this point, as the microscopic observations indicated the presence of large coccoid autofluorescent cells, we suspected them to be cyanobacteria and/or eukaryotic algae. To test this hypothesis we plated the inoculated Chu and Detmer media under different incubation conditions: under illumination and in the dark, at 4°C and 28°C, with and without organic matter.

Under the different conditions, no difference due to temperature was noted. Without organic matter no growth was observed in the dark, and a green color was observed under illumination. Miming the conditions of the frescoes, agarised Chu and Detmer added with organic compounds were incubated under conditions of illumination and darkness, growth was evident after 3–5 days. In addition, there were rosy colonies like the alteration on the frescoes. Also worthy of note was the green patina streaked on a medium with organic compounds: this developed a rosy-red coloration.

Pigment Analysis (Chlorophyll a and b Ratio and Flow Cytometry)

In order to prove the presence of cyanobacteria and eukaryotic algae and to understand the cause of the rosy-red color development, we focused our investigations on the microorganisms forming the rosy-red patina and proceeded with pigment analyses.

After chlorophyll extraction, the Chlorophyll a and b ratios were assessed for the rosy powder samples, and were found to be 8:1.

Flow cytometry was applied to study the nature of the pigments on the rosy-red patina present on agarised media added with organic matter. Discrimination between cells

with and without pigments was carried out on the basis of the presence of autofluorescence caused by phototrophs. Briefly, microorganisms without pigments appear only SYBER-green stained, while pigmented cells are both green and red/orange fluorescent. Red fluorescence is induced by the presence of chlorophyll (660–700 nm), while orange fluorescence is due to phycoerythrin (560–590 nm). Thus two cell subgroups with different combinations of green fluorescence and orange–red fluorescence can be observed in the 2D cytograms. The nonphotosynthetic cells are easily differentiated from the photosynthetic ones and fall in Region 1 (R1). The cells in Region 2 (R2) exhibit both green and orange fluorescence due to the simultaneous presence of nucleic acids stained by SYBR-Green I and natural pigments emitting orange fluorescence, therefore the cells in R2 with high orange fluorescence can be associated with cyanobacterial cells. This confirms that the rosy discoloration was caused by cyanobacteria. In sample A, the nonphotosynthetic prokaryotes represented 5% of the total cells counted, while the other 95% was made up of cyanobacteria (Fig. 2). In sample B, nonphotosynthetic bacteria were 20% of the total cell concentration, while cyanobacteria were 80%.

DGGE Specific for Cyanobacteria and Sequencing of Bands

To better characterize the cyanobacterial microflora, a DGGE analysis coupled with partial sequencing of 16S rRNA gene fragments was performed. Seven bands were
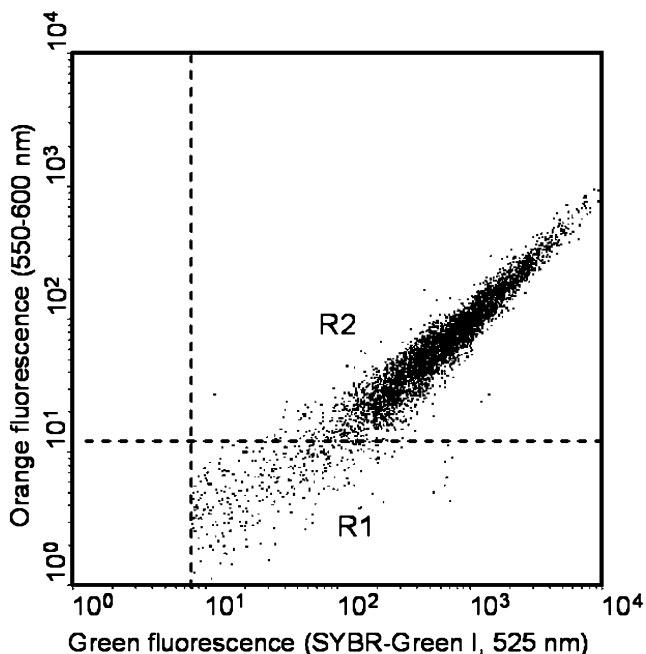

Figure 2 Cytogram of sample A: green fluorescence (515–560 nm) vs. orange fluorescence (550–600 nm)

clearly visible and the corresponding sequences were uploaded in the GenBank database under the following accession numbers: EU874241, EU874242, EU874243, EU874244, EU874245, EU874246, and EU874247. A BLAST similarity search in the GenBank database of the retrieved sequences indicated that all seven sequences showed 94–98% similarity to uncultured cyanobacteria from soil and rock samples.

Analysis of Biocide Efficiency by ATP Assay

The most effective biocide concentration in the in situ application was four times the MIC and was obtained with 2% of the trade product. The experiment was carried out 1 week after the treatment and the results were the following: sample treated with Neo Desogen 90,000 pg ATP/g, sample treated with Metatin 15,000 pg ATP/g versus 68,000 pg ATP/g for the untreated surface.

Detection of Cyanobacteria after Biocide Treatment by PCR

The expected band size of 424 bp, corresponding to the CYA359f and CYA781r amplified fragment, was found in the lanes corresponding to the untreated and Neodesogen-treated samples, while there was no band in the lane corresponding to the sample treated with Metatin. No band was observed in the negative control.

Discussion

In recent research, Imperi et al. [18] related the rosy discoloration of ancient wall paintings to the presence of coccoid cells of 1–1.5 μm diameter, proved to be actinobacteria. Also, in a survey of common biological alterations on frescoes, Bassi et al. [7] related the rosy discoloration particularly the pink powder-like patches, to the presence of capsulated small, and even large, coccoid forms.

In the present research, we observed rosy powder samples by optical, epifluorescent, and scanning electronic microscope, and have been able to prove that the dominant species is a capsulated coccoid form bigger than 5 μm in diameter and characterized by autofluorescence. Due to the dimension and autofluorescence, we hypothesized that the cells were phototrophic, in agreement with previous studies on frescoes in the Orvieto Cathedral [29] where the rosy discoloration was associated with cyanobacteria and chlorophyta.

To prove the role of algae in the rosy discoloration, chlorophyll was searched for in the rosy powder and then subjected to pigment analysis. The investigations on the chlorophylls extracted from the powder showed the Chloro-

phyll a presence to be approximately eight times that of Chlorophyll b. Then, as the Chlorophyll a to Chlorophyll b ratio in eukaryotic algae is generally 2:1 or 3:1 [19], and cyanobacteria possess Chlorophyll a but not Chlorophyll b, we presumed cyanobacteria predominance. Further proof of algal presence can be seen in the massive growth with the same large coccoid form that occurred when the rosy powder was inoculated onto the Chu and Detmer liquid media.

In order to provide evidence of a cause relationship between the rosy discoloration and phototrophic microorganism presence, we made a simulation of the fresco conditions and the environment of the St. Brizio Chapel: we added organic matter and tested different light and temperature conditions in this simulation. We found that the key factor in the development of the rosy discoloration was the presence of organic matter. Under conditions of light, a green patina on solid Chu and Detmer media was observed, while under both light and dark conditions a rosy patina developed on the agarized mineral media added with organic matter.

Among the pigments in cyanobacteria that could play a dominant role in this biological alteration, one responsible for the rosy color development, could be phycoerithrin. In fact, not all cyanobacteria are blue-green, some common forms are red or pink due to the presence of phycoerythrin such as *Oscillatoria* sp. [14].

The final proof that the rosy discoloration was caused by phycoerythrin was the strong orange fluorescence in the cytometry analysis.

The results presented in this paper lead us to believe that cyanobacteria can grow under dark conditions because they are able to use the organic compounds present on the fresco surface. Previous research on photosynthetic bacteria in rosy powders claims that the color change of the algae is due to cell age [17]. However our research has demonstrated that just the presence or absence of organic matter determines the color of the alteration despite the intensity of the light. Indeed, the environmental conditions described by Van Baalen et al. [32], for the heterotrophic growth of the unicellular cyanobacterium *Agmenellum quadruplicatum*, are very close to those observed for the Signorelli frescoes, indicating cyanobacteria that are able to utilize organic compounds.

However, the sequence homologies of the cyanobacterial biofilm failed to identify the genera, which is not surprising as DNA databanks comprise mainly aquatic cyanobacteria; therefore, xerophytic cyanobacteria are not well represented [15, 16]. It was interesting to note that two of the analyzed sequences (EU874242 and EU874246) showed 94% and 96% similarity with an uncultured cyanobacterium found in a sample from the Altamira Cave (Spain), where the wall paintings are affected by discoloration. Furthermore, other researchers [33] found that the cyanobacteria community in this Cave was composed by coccoid-shaped taxa.

In the conservation field, benzalkonium chloride and benzalkonium chloride-based products are often used, e.g., benzalkonium chloride is particularly efficient as an algaecide against algal microflora, as demonstrated on the fountain of "99 Cannelle" in L'Aquila Italy [22] and on the wall paintings of the St. Christopher Church in Milan [3]. Indeed, quite a few disinfectants contain this quaternary ammonium compound, for instance both Neo Desogen and Metatin 5810–101 are based on benzalkonium chloride. With regard to the efficiency of such biocide products, there are many different ways of assessing this, e.g., cell counts and ATP measurements [23].

In this research, two biocides based on benzalkonium chloride, Neo Desogen and Metatin, were used. We decided to adopt the bioluminescence ATP assay to measure the different ATP content of the control and treated samples. The results strongly suggest that the Metatin 5810–101 was the more effective. The increase in ATP content after the application of Neo Desogen was most likely due to its function as a nutrient source, as previously noted for other organic biocides [34]; in fact, such nutrition depends on the presence of other compounds in the formulation rather than on the active substance of the trade products Caneva et al. [10].

Biocide efficiency in reducing cyanobacterial populations was further assessed by amplifying the 424 bp cyanobacterial specific fragment. The presence of a band in the Neo Desogen-treated samples confirmed the presence of cyanobacteria cells even after treatment with Neo Desogen, while the efficiency of Metatin was also confirmed by the absence of the cyanobacterial specific DNA fragment.

In conclusion, our evidence shows cyanobacteria to be the main agent responsible for the rosy discoloration on the Signorelli frescoes in the St. Brizio Chapel and, needless to say, on many other wall paintings. In addition, the efficiency of the biocide Metatin 5810–101 in reducing such discoloration has been verified by the results of our research.

References

1. Albertano P, Barsanti L, Passarelli V, Gualtieri P (2000) A complex photoreceptive structure in the cyanobacterium Leptolyngbya sp. Micron 31:27–34

2. Albertano P, Urzì C (1999) Structural Interactions among Epilithic Cyanobacteria and Heterotrophic Microorganisms in Roman Hypogea. Microb Ecol 38:244–252

3. Alessandrini G, Dassu G, Zanolini P, Bassi M, Barbieri N, Bonecchi R (1984) St. Christopher church in Milan; 1) chemical and physical analyses and restoration; 2) biological investigations. Arte Lombarda no. 68–69, 1–12

4. Altschul SF, Gish W, Miller W, Myers EW, Lipman DJ (1990) Basic local alignment search tool. J Mol Biol 215:403–410

5. Andrews JM (2001) Determination of minimum inhibitory concentrations. J Antimicrob Chemother 48(Suppl. 1):5–16

6. Arar EJ (1997) Method 446. in vitro determination of chlorophylls a, b, c1 + c2 and pheopigments in marine and freshwater algae by visible spectrophotometry/http://purl.access.gpo.gov/GPO/LPS68148 United States Environmental Protection Agency, Office of Research and Development, National Exposure Research Laboratory US

7. Bassi M, Giacobini C (2001) Scanning electron microscopy: a new technique in the study of the microbiology of works of art. Int Biodeter Biodegr 48:55–66

8. Bassi M, Giacobini C (1971) Nuove tecniche di indagine nello studio della microbiologia delle opere d'arte. Proceeding of the XXVI A.T.I. National Congress (Rome, Italy) 8–11

9. Benson DA, Karsch-Mizrachi I, Lipman DJ, Ostell J, Wheeler DL (2008) GenBank. Nucleic Acids Res 36:D25–D30

10. Caneva G, Nugari MP, Pinna D, Salvadori O (1996) Il controllo del degrado biologico. In: Nardini (ed) I biocidi nel restauro dei materiali lapidei. Nardini, Fiesole, p 51

11. Cole JR, Chai B, Marsh TL, Farris RJ, Wang Q, Kulam SA, Chandra S, McGarrell DM, Schmidt TM, Garrity GM, Tiedje JM (2003) The Ribosomal Database Project (RDP-II): previewing a new autoaligner that allows regular updates and the new prokaryotic taxonomy. Nucleic Acids Res 31(1):442–443

12. Commissione Normal (1990) Commissione Normal, Raccomandazioni Normal: 9/88 Microflora autotrofa ed eterotrofa: tecniche di isolamento in coltura. C.N.R.-I.C.R, Rome

13. Drewello R, Weissmann R (1997) Microbially influenced corrosion of glass. Appl Microbiol Biotechnol 47:337–346

14. Dworkin M, Falkow S, Rosenberg E, Schleifer K-H, Stackebrandt E (2007) In: The Prokaryotes. vol. 1–7. 3rd edn. Springer, New York

15. Gaylarde PM, Crispim CA, Neilan BA, Gaylarde CC (2005) Cyanobacteria from Brazilian building walls are distant relatives of aquatic genera. Omics 9(1):30–42

16. Gaylarde CC, Gaylarde PM, Copp J, Neilan B (2004) Polyphasic Detection of Cyanobacteria in Terrestrial Biofilms. Biofouling 20(2):71–79

17. Giacobini C, Andreoli C, Casadoro G, Fumanti B, Lanzara P, Rascio N. (1979) Una caratteristica alterazione delle murature. In proceedings of Third International Congress Deterioramento e Conservazione della Pietra. Venezia, Italy, pp 289–299

18. Imperi F, Caneva G, Cancellieri L, Ricci MA, Sodo A, Visca P (2007) The bacterial aetiology of rosy discoloration of ancient wall paintings. Environ Microbiol 9(11):2894–2902

19. Margalith PZ (1992) Pigment microbiology. Chapman & Hall, London, pp 82–85

20. Mattirolo O (1917) Sulla natura della colorazione rosea della calce dei muri vetusti e sui vegetali inferiori che danneggiano i monumenti e le opere d'arte. Riv Archeologica della Provincia e Antica Diocesi di Como 73/75:1–19

21. Nubel U, Garcia-Pichel F, Muyzer G (1997) PCR primers to amplify 16S RNA genes from cyanobacteria. Appl Environ Microbiol 63(8):3327–3332

22. Quaresima R, Di Giuseppe E, Volpe R (1995) Impiego di biocidi per la rimozione della microflora algale. In: Biscontin G, Driussi G (ed) La pulitura delle superfici dell'architettura; proceedings of Convegno di studi, Bressanone, 3–6 luglio 1995, Scienza e beni culturali, 11. Libreria Progetto editore, pp 267–275

23. Ranalli G, Zanardini E, Pasini P, Roda A (2003) Rapid biodeteriogen and biocide diagnosis on artwork: a bioluminescent low-light imaging technique. Ann Microbiol 53:1–13

24. Sambrook J, Fritsch EF, Maniatis T (1989) Molecular cloning: a laboratory manual, 2nd ed. Cold Spring Harbor Laboratory Press, Cold Spring Harbor

25. Schabereiter-Gurtner C, Piñar G, Lubitz W, Rolleke S (2001) An advanced molecular strategy to identify bacterial communities on art objects. J Microbiol Methods 45:77–87

26. Sorlini C, Sacchi M, Ferrari A (1987) Microbiological deterioration of Gambara's frescoes exposed to open air in Brescia, Italy. Int Biodet 23:167–179

27. Sorlini C, Zanardini E, Albo S, Praderio G, Cariati F, Bruni S (1994) Research on chromatic alterations of marbles from the fountain of Villa Litta (Lainate, Milan). Int Biodeter Biodegr 33:153–164

28. Suzuki MT, Giovannoni SJ (1996) Bias caused by template annealing in the amplification of mixtures of 16S rRNA genes by PCR. Appl Environ Microbio 62(2):625–630

29. Tomaselli M, Margheri MC, Florenzano G (1979) Indagine sperimentale sul ruolo dei cianobatteri e delle microalghe nel deterioramento di monumenti ed affreschi. Deterioramento e Conservazione della Pietra. Third International Congress (Venezia, Italy) 314–325

30. Urzì C, Realini M (1998) Color changes of Noto's Calcareous sandstone as related with its colonization by microorganisms. Int Biodeter Biodegr 42:45–54

31. Valls del Barrio S, Garcia-Vallès M, Pradell T, Vendrell-Saz M (2002) The red–orange patina developed on a monumental dolostone. Eng Geol 63:31–38

32. Van Baalen C, Hoare DS, Brandt E (1971) Heterotrophic growth of blue-green algae in dim light. J Bacteriol 105:685–689

33. Warren-Rhodes K, Rhodes KL, Pointing SB, Ewing SA, Lacap DC, Gómez-Silva B, Amundson R, Friedmann EI, McKay CP (2006) Hypolithic Cyanobacteria, Dry Limit of Photosynthesis, and Microbial Ecology in the Hyperarid Atacama Desert. Microbial Ecology 52:389–398

34. Warscheid T, Braams J (2000) Biodeterioration of stone: a review. Int Biodeter Biodegr 46:343–36

35. Zanardini E, Andreoni V, Borin S, Cappitelli F, Daffonchio D, Talotta P, Ranalli G, Sorlini C, Bruni S, Cariati F (1997) Lead-resistant microorganisms from red stains of marble of the Certosa of Pavia (Italy) and use of nucleic acids based techniques for their distinction. Int Biodeter Biodegr 40:171–182

36. Zanardini E, Bruni S, Cariati F, Ranalli G, Sorlini C (1994) Investigations on the red spots present on the Carrara marble façade of Orvieto Cathedral. In: Fassina V, Ott H, Zezza F (eds) The conservation of Monuments in the Mediterranean Basin. IGCMM, Venezia, pp 349–352

ORIGINAL ARTICLE

Permeabilization method for *in-situ* investigation of fungal conidia on surfaces

F. Villa, F. Cappitelli, P. Principi, A. Polo and C. Sorlini

Dipartimento di Scienze e Tecnologie Alimentari e Microbiologiche, Università degli Studi di Milano, Milano, Italy

Abstract

Aims: 4′,6-diamidino-2-phenylindole (DAPI) staining and fluorescent *in-situ* hybridization (FISH) show great potential for the detection of fungal conidia, also conserving the spatial architecture of their colonization. These investigations are often greatly hampered by the complicated wall structure of many fungal taxa. The aim of the present study was to develop an efficient permeabilization strategy for both DAPI staining and the FISH technique, applicable to various fungal species and maintaining their relationships with surfaces.

Methods and Results: We compared different DAPI staining permeabilization strategies based on alcohol dehydration, surfactants and osmotic shock, tested with *Aspergillus niger* conidia. Among four permeabilization methods leading to a strong DAPI signal, only one, based on Triton X-100, EDTA and β-mercaptoethanol followed by hyperosmotic stress, appeared suitable for FISH investigation and was successfully applied to an additional 10 fungal taxa and three environmental samples.

Conclusions: The effective permeabilization method, which employed a combination of surfactant and osmotic strategies, was successfully applied as preliminary step in both DAPI staining and the FISH protocol.

Significance and Impact of the Study: The method described is reproducible, simple and inexpensive and might be attractive for other direct visualization techniques.

Introduction

The adhesion of fungal conidia to surfaces is a widespread phenomenon. Fungal agents on surfaces can cause detrimental effects such as biodeterioration and infection (Douglas 2003; Cappitelli *et al.* 2007) and be involved in practices using biocontrol and biocatalysis (Wolken *et al.* 2003; Ramachandran *et al.* 2007). As a consequence, there is a considerable interest in the development of specific strategies to visualize the relative local arrangements of fungal conidia on surfaces.

Traditional culture-based techniques for mycological investigations are time-consuming and sometimes biased by the lack of morphological distinction between some species that limits their taxonomic identification (Valinsky *et al.* 2002; Wu *et al.* 2003; Prigione *et al.* 2004). Although DNA-based methods, such as polymerase chain reaction coupled with denaturing gradient gel electrophoresis, real-time PCR and automated ribosomal intergenic spacer analysis, are very efficient for their detection, they not give any information about the relationships between micro-organism and the surface itself (Barlocher 2007). In this contest, direct visualization techniques, such as fluorescent *in-situ* hybridization (FISH), appear interesting approaches for investigating the spatial arrangement of micro-organisms at the single-cell level (Amman and Ludwing 2000; Aoi 2002; Bottari *et al.* 2006). The success of most of these techniques depends on the accessibility of the intracellular target site. The complicated cell wall structure of many taxa, e.g. *Aspergillus niger*, which are very common damaging agents of biotic and abiotic surfaces, as well as having important industrial applications (Schuster *et al.* 2002; Xie and West 2006; Gorbushina 2007), can hinder the entry of the detection reagents and the emission of the fluorescent signal (Prigione and Marchisio 2004; Pawlowska 2005; Barlocher 2007). Until

now, a few permeabilization protocols have been proposed in attempts to overcome this difficulty. For example, before staining fungal propagules with the nucleic acid-based stain 4′,6-diamidino-2-phenylindole (DAPI), Prigione *et al.* (2004) developed an efficient microwave irradiation permeabilization method. Unfortunately, this permeabilization protocol cannot be applied to the detection of fungal structures which have adhered to surfaces, because some substrata are incompatible with microwave irradiation. Alternatively, the microwave irradiation practice requires the fungal dislodgment from the surface using different strategies such as sonication and strong washing, totally losing any information on conidial spatial distribution (Oulahal-Lagsir *et al.* 2000; Guillemot *et al.* 2006). The use of FISH in mycological studies has been generally restricted to the detection of those taxa of clinical relevance or implied in food processes (Teertstra *et al.* 2004; Kempf *et al.* 2005; Xufre *et al.* 2006). In these cases, the access to the intracellular target was made possible after sectioning the hyphae or removing the cell wall with lysing enzymes, often heavily interfering with the fungal morphology (de Vos and Nelis 2003; Teertstra *et al.* 2004). Finally, although treatment with lysing enzymes or with slow freezing and embedding steps is convincing and repeatable using specific peptide nucleic acid (PNA) 18S rRNA and PNA SC3 mRNA probes after only a mild chemical fixation, it produces a low and not reproducible signal with the traditional probes for 18S rRNA (Rigby *et al.* 2002; Teertstra *et al.* 2004).

The aim of the present study was to develop an efficient permeabilization strategy for both DAPI staining and FISH technique, applicable to various fungal species and maintaining their relationships to surfaces. Firstly, the effectiveness of the permeabilization strategies was demonstrated with the DAPI staining procedure. The successful permeabilization methods leading to a strong DAPI signal were then tested for FISH. To this end, we used *A. niger* as its melanized conidia, allowing an easy counting by means of light microscope observation. Finally, the best permeabilization method was successfully applied to an additional 10 fungal taxa adhered to glass slides and three environmental surfaces collected with a nondestructive adhesive tape strip technique that offers the possibility of gaining information on the microbial colonization without being destructive for surfaces.

Materials and methods

Fungal strains and culture conditions

Aspergillus niger ATCC 9642 and *Chaetomium globosum* ATCC 6205 and the following taxa from the DiSTAM, University of Milan, microbial collections were used: *Aspergillus versicolor*, *Aspergillus flavus*, *Emericella nidulans*, *Alternaria* sp., *Penicillium* sp., *Trichoderma virens*, *Acremonium* sp., *Fusarium oxysporum* and *Cladosporium* sp. Cultures were grown at 25°C for 10 days on Potato Dextrose Agar (PDA, Merck, Milan, Italy). The experiment with *A. niger* conidia was repeated three times.

Conidia collection and fixation

Mature conidia were collected from 10-day cultures by washing the colony surface with phosphate-buffered saline (PBS, 0·01 mol l^{-1} phosphate buffer, 0·0027 mol l^{-1} potassium chloride pH 7·4 at 25 °C, Sigma-Aldrich) supplemented with 0·05% w/v Tween-20 (Sigma-Aldrich) and gently scraping it with a sterile handle. Conidia were fixed with a 6% paraformaldehyde solution (Sigma-Aldrich) in PBS and incubated for 1 h on ice. After two PBS washing steps, the fungal conidia were resuspended in 500 µl of 1/1 ethanol/PBS solution and stored at –20 °C. A small amount of sample (25 µl) was dropped on a poly-L-lysine coated slides (VWR International srl, Milan, Italy) and air-dried.

Environmental samples

The following three mouldy surfaces were tested to assess the permeabilization performance: (i) an inner wall recently painted; (ii) a plastic suction cup and (iii) a carrot.

Adhesive tape strips (Fungi Tape™, DID Milan, Italy) were gently applied to mouldy areas and then placed on glass slides to facilitate the microscope observations. Before the FISH investigations, all samples were examined with light microscopy to provide visual evidence of fungal colonization. *In-situ* frames (1·0 cm^2 area; Eppendorf Italia, Milan, Italy) were used to confine the hybridized areas. Chitin stain Fluorescent Brightener 28 (Sigma-Aldrich) was adopted as the standard for comparison.

Permeabilization strategies

The conidial population was permeabilized with four different protocols:
1. *Alcohol strategy*. Samples were dehydrated by successive passages in 50%, 80% and 100% ethanol series (3 min each).
2. *Surfactant strategies*. The fungal conidia were treated with: (i) the nonionic surfactant Tween-80 (Merck, Milan, Italy; 0·1% or 0·5% w/w in H$_2$O, overnight at 50°C); (ii) the nonionic surfactant Triton X-100 (Merck, 0·1% w/w in H$_2$O, 90 min at 25°C and 1% w/w in a solution of 0·05 mol l^{-1} Tris–HCl, Sigma-Aldrich, 0·04 mol l^{-1} ethylene diamine tetra-acetic acid, EDTA,

Sigma-Aldrich and 0.1 mol l^{-1} β-mercaptoethanol; Appli-Chem GmbH, Darmstadt, Germany); (iii) the anionic surfactant sodium dodecyl sulfate (SDS; Sigma-Aldrich srl, Milan, Italy, 1% and 10% w/w in H$_2$O, with incubation of 30 min at 25°C and overnight at 50°C respectively). The surfactants were used alone or in combination with an ethanol or an isopropanol series (50, 80, 100%) at 25°C for 4 min.

3. *Osmotic strategies.* The conidia were covered with 100 μl of glycerol/water solution at different concentrations. The necessary mass of glycerol (Sigma-Aldrich) was determined using the Norrish equation (Norrish 1966). Glycerol was added to 1 g of water with the following weights: 0.4, 1.0, 1.4 and 4.7 g. Fungal conidia were maintained at these osmotic pressures for 30 min on ice before rehydratation.

4. Combination of surfactant and osmotic strategies (a combination of the strategies 2 and 3).

DAPI staining

The concentration of DAPI (Sigma-Aldrich) in the working solution was 10 μg ml^{-1} in distilled water. Samples were incubated with DAPI for 30 min in the dark at room temperature.

FISH protocol

To test the best permeabilization methods to be coupled to a FISH protocol, the oligonucleotide DNA probe directed against the 18S rRNA sequence of Eukaryotes EUK 516 (5′-ACCAGACTTGCCCTCC-3′) (Amann *et al.* 1990) was used. In addition, the probe Non EUB 338 (5′-ACT-CCTACGGGAGGCAGC-3′) (Wallner *et al.* 1993) was used as a negative control to check for the nonspecific binding of probe EUK 516 (Inàcio *et al.* 2003). Furthermore, the specificity of the rRNA hybridization was checked by treating permeabilized conidia with an RNase cocktail as reported by Teertstra *et al.* (2004) and by a probe with specificity for one of the fungal genus examined. We tested the specificity of the *Aspergillus*-probe cocktail (Asp1: 5′-TCCACACCCTATGGTCGTATGT-3′ and Asp2: 5′-GTACGGCTGAGCGGACGGGAA-3′) (Hayden *et al.* 2003) to a mixed conidial population of *A. flavus* and *F. oxysporum*. The autofluorescence of unstained conidia was also examined. The probes were 5′-labelled with the fluorophore Texas Red because we observed a weak green and blue autofluorescence of the conidia. FISH of conidia on glass slides was performed as previously described by Manz *et al.* (1992) with the following modifications. Briefly, permeabilized conidia were rapidly covered by a prewarmed hybridization buffer (0.9 mol l^{-1} NaCl, 0.02 mol l^{-1} Tris–HCl pH 7.2, 0.01% w/v SDS,

20% v/v deionized formamide). A probe concentration of 50 ng μl^{-1} was used and incubation was carried out at 47°C for 4 h for the probe EUK516 and at 58°C for 4 h for the *Aspergillus*-probe cocktail on an *in-situ* PCR block (VWR International srl, Milan, Italy). Following incubation, a washing buffer (0.2 mol l^{-1} NaCl, 0.02 mol l^{-1} Tris-HCl pH 7.2, 0.01% w/v SDS) was applied for 20 min at 47°C to remove the unbound probe and finally samples were rinsed with distilled water.

Epifluorescence microscopy

DAPI-stained and hybridized fungal conidia were observed both with bright-field microscopy and under epifluorescence microscopy using the Leica DM 4000 B microscope at a magnification of 400× and 1000× under oil immersion. Digital images from about 10 fields per sample were acquired using a CoolSNAP CF digital camera (Photometrics Roper Scientific, Ottobrunn, Germany) and elaborated using the IMAGEJ ver. 1.34s software (Rasband, 1997–2007, downloaded from http://rsbweb.nih.gov/ij/).

Statistical data screening

The number of stained and hybridized conidia cm^{-2} from each of the triplicate cultures were statistically processed with ANOVA. The analysis of variance was carried out using MATLAB software (ver. 7.0; The MathWorks Inc, Natick, MA, USA) to assess the significance ($P \leq 0.05$) of differences among means of the same conidial population observed in bright-field microscopy and after DAPI staining and *in-situ* hybridization in epifluorescence mode. The percentage of fluorescent conidia was also determined.

Results

The strategy that included osmotic shocks did not produce any positive and reproducible results for DAPI staining and therefore was not further considered. As a weak-moderate and nonhomogenous signal was observed with the surfactants SDS and Tween-80 alone or in combination with ethanol, also these permeabilization methods were not included in the FISH experiments.

The permeabilization strategies that gave the strongest and most homogenous fluorescent DAPI signals and that were tested as the first step of the FISH protocol are reported in Table 1.

Firstly, the standard ethanol treatment strategy was applied to *A. niger* conidia (Table 1, method 1). The treatment was successful with the DAPI staining, but failed to produce any satisfying results as the preliminary step in the FISH protocol. Hybridization combined with methods 2 and 3 failed to give any red fluorescent signals.

Table 1 Details of the permeabilization strategies tested on *Aspergillus niger* conidia that produced the most intense 4′,6-diamidino-2-phenylindole signal

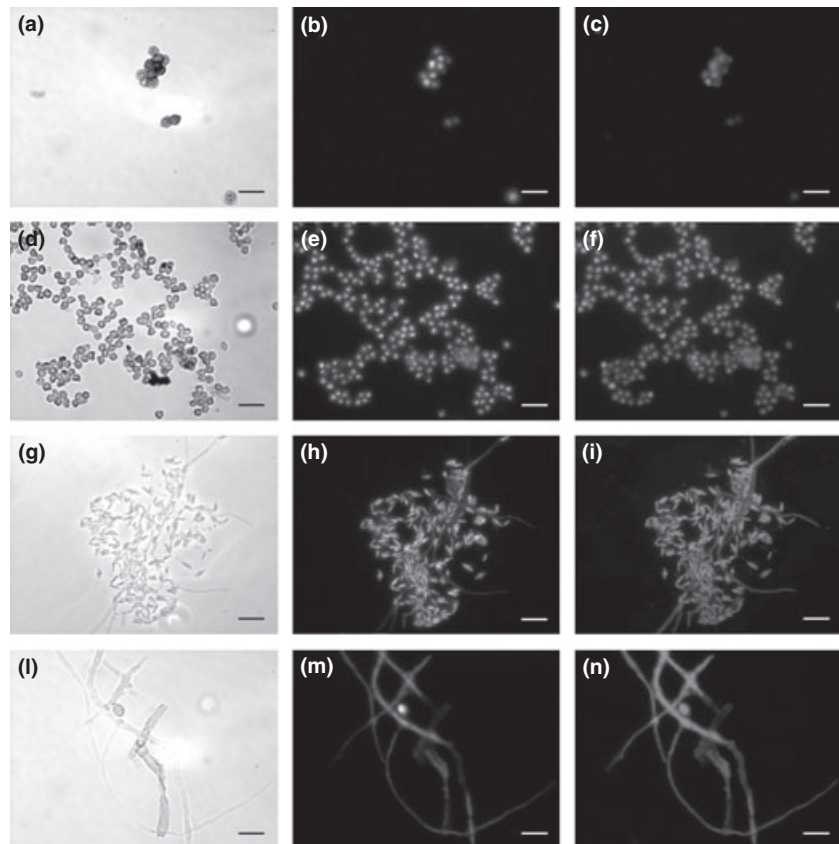| Method	Permeabilization details	Incubation time (min)	Temperature, °C
1	Ethanol series (50%, 80%, 100%)	3	25
2	Isopropanol series (50%, 80%, 100%)	2	25
	Triton X-100 (0·5% in H$_2$O)	90	25
	Isopropanol series (50%, 80%, 100%)	1	25
3	Triton X-100 (1% in buffer containing	30	30
	0·05 mol l^{-1} Tris–HCl, 0·04 mol l^{-1}	15	40
	EDTA and 0·1 mol l^{-1} β-mercaptoethanol)		
4	Method 3	30	On ice
	Glycerol (0·4 g in 1 g of H$_2$O)		

Figure 1 Microscopic images of conidia of *Aspergillus niger* (a–c), *Aspergillus versicolor* (d–f), *Acremonium* sp. (g–i) and *Cladosporium* sp. (l–n) after the effective permeabilization method 4. The same area is shown in the bright-field view (a, d, g, l) and epifluorescence microscope field respectively with DAPI filter cube (b, e, h, m) and Texas Red filter cube (c, f, i, n). Bars represent 10 μm.

In contrast, method 4 was the only permeabilization treatment that allowed a detectable and homogeneous fluorescent signal (Fig. 1a–c).

Using the Non EUB 338 probe, we proved that no signal was caused by unspecific binding of the EUK 516 probe. The negative control with an RNase treatment gave no signal showing that the probe binds exclusively with the target rRNA. No false positive was noted when *Aspergillus*-specific probes were tested against *F. oxysporum* conidia (Fig. 2).

The results of method 4 were processed statistically revealing that there were no significant differences among the number of conidia observed in bright-field microscopy and after the DAPI staining and probe hybridization ($P = 0.998$). This method allowed us to obtain a high percentage of DAPI-stained and hybridized conidia, corresponding to 96·4% and 97·2% of the conidial population respectively.

The most effective FISH permeabilization protocol screened on *A. niger* conidia was then used to detect attached conidia of different fungal species by means of DAPI staining and FISH. In all the experiments a perfect match between the conidia observed in bright-field microscopy, the DAPI-stained conidia and the hybridized
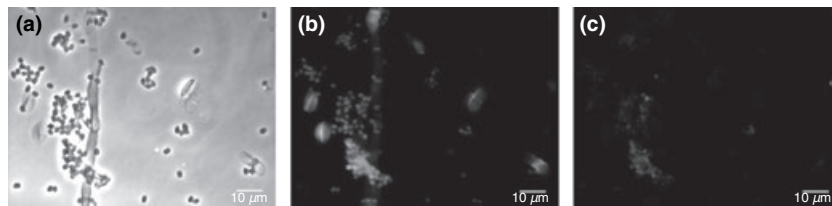
Figure 2 The *Aspergillus*-specific probe cocktail was used with mixed conidial population of *Aspergillus flavus* and *Fusarium oxysporum*: in the phase contrast view (a), and under epifluorescence view with the filter cube for the Fluorescent Brightener 28 staining (b) and under epifluorescence view with the filter cube for the *Aspergillus*-specific probe fluorochrome (c). Bars represent 10 μm.

conidia was noted. We observed that the intensity of the fluorescent signal varied from strain-to-strain. Darkly pigmented conidia like those of *Cladosporium* sp., *Alternaria* sp. and *C. globosum* presented slightly lower signal intensities than hyaline or brightly coloured fungal conidia. Fig. 1d–n shows the DAPI and FISH staining of fungal conidia of *A. versicolor*, *Acremonium* sp. and *Cladosporium* sp. Using the optical microscope, all of the environmental samples exhibited evidence of fungal colonization as indicated by the presence of hyphae.

For all the environmental samples, FISH results with the EUK 516 probe showed an agreement with results obtained from the chitin-staining assay (Fig. 3). However, a slightly signal intensity was observed in comparison with the fluorescence obtained with conidia on glass slides.

Discussion

It is claimed that one of the limiting steps for a successful FISH is the wall permeabilization (Teertstra *et al.* 2004;
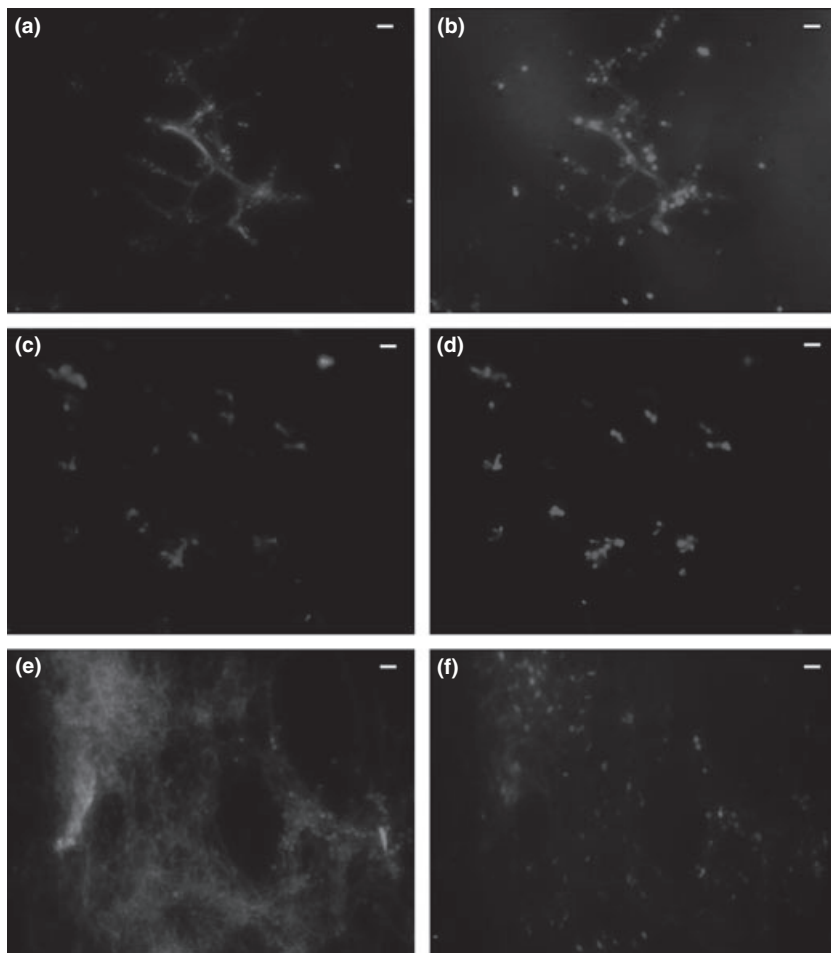

Figure 3 Epifluorescent images of fungal structures on adhesive tape strips sampled from different environmental surfaces: inner wall (a, b); plastic suction cup (c, d) and carrot (e, f). The same images are shown after Fluorescent Brightener 28 staining (a, c, e) and hybridization of the probe EUK 516 (b, d, f). Bars represent 10 μm.

Bottari *et al.* 2006). In our work, several permeabilization methods were first screened with DAPI staining and the successful ones were subsequently applied to a complete FISH protocol. The first screening with DAPI was performed as it is cheaper and less time-consuming than the hybridization protocol. Only the Triton X-100-based strategy alone or in combination with the osmotic shock passed the first screening (Table 1). The success of the surfactant permeabilization strategy was previously reported as Triton X-100 increased the fungal wall permeability enhancing, for example, the enzymes secretion (Singh *et al.* 2007). In addition, Triton X-100 is a non-toxic, easy to handle and cheap product (van der Werf *et al.* 1995). The same signal intensity was obtained using Triton X-100 in combination with either an isopropanol series or EDTA and β-mercaptoethanol. It is likely that isopropanol showed a better affinity for the proteinaceous layer than ethanol because of its higher hydrophobicity. The use of EDTA as a permeabilizer is also widespread (Chen 2007). The chemical β-mercaptoethanol is usually employed in proteomic investigation for its ability to convert cystine in its reduced form cysteine (Cheatko and Bald 2000). The reducing agent β-mercaptoethanol most likely acts on disulfide bridges, affecting the structure of the rodlet coating (Paris *et al.* 2003; Linder *et al.* 2005).

Among the four effective permeabilization methods emerging from the DAPI staining studies (Table 1), only method 4 gave a good performance in the FISH investigations. The surfactant strategies alone were not able to promote entry of the fluorescent oligonucleotide probe.

We chose glycerol as the water activity depressor because it both allows reaching very low water activities and for its low interaction with other molecules (Mille *et al.* 2005). The experiments showed that a solution of 0·4 g glycerol in 1 g of water kept at 0°C for 30 min was sufficient to make the fungal conidia ready for the FISH investigation. The same osmolyte concentration was found to successfully permeabilize yeast cells and germinated spores for enzyme assays (Stestak and Ferkas 2001). The strength and the homogeneous distribution of the fluorescent signal in the subsequent repetitions suggested the success and repeatability of the method. In addition, we observed that the morphology of the conidia was not affected by the permeabilization treatment. This protocol ensured a high intensity and homogeneity of the fluorescence signal without damaging the conidia.

The most effective permeabilization protocol screened on *A. niger* conidia was tested on other fungal species. All the fungal species were hybridized, but the fluorescence intensity varied from strain to strain. We observed no different localizations of the ribosomal signal between different species and the fungal hyphae appeared homogenously fluorescent. In particular, under our experimental conditions we did not observe any weak fluorescent intensity in the apical hyphae compartment, as reported by Teertstra *et al.* (2004).

Finally, the effective permeabilization method was successfully applied to the FISH investigation of mouldy surfaces. The samples were collected using adhesive tape strips (Sarkany and Gaylarde 1968) that reproduce the mirror image of the biofilm present in the selected area. All of the samples examined showed a massive fungal colonization, and the fungal structures were successfully hybridized. In this respect, an efficient permeabilization protocol for DAPI staining and *in-situ* hybridization of conidial population was found. This permeabilization method is reproducible, simple and inexpensive and might therefore be attractive as a first step in other direct visualization techniques such as *in-situ* PCR and *in-situ* reverse transcriptase–PCR.

References

Amann, R.I., Binder, R.J., Olson, S.W., Chisholm, R., Devereux, R. and Stahl, D.A. (1990) Combination of 16S rRNA-targeted oligonucleotide probes with flow cytometry for analyzing mixed microbial population. *Appl Environ Microbiol* **56**, 1919–1925.

Amman, R and Ludwig, W. (2000) Ribosomal RNA-targeted nucleic acid probes for studies in microbial ecology. *FEMS Microbiol Rev* **24**, 555–565.

Aoi, Y. (2002) In situ identification of microorganisms in biofilm communities. *J Biosci Bioeng* **6**, 552–556.

Barlocher, F. (2007) Molecular approaches applied to aquatic hyphomycetes. *Fungal Biol Rev* **21**, 19–24.

Bottari, B., Ercolini, D., Gatti, M. and Neviani, E. (2006) Application of FISH technology for microbiological analyisis: current state and prospects. *Appl Microbiol Biotechnol* **73**, 485–494.

Cappitelli, F., Nosanchuk, J.D., Casadevall, A., Toniolo, L., Brusetti, L., Florio, S., Principi, P., Borin, S. *et al.* (2007) Synthetic consolidants attacked by melanin-producing fungi: case study of the biodeterioration on Milan (Italy) cathedral marble treated with acrylics. *Appl Environ Microbiol* **73**, 271–277.

Cheatko, G. and Bald, E. (2000) Determination of cysteine in human plasma by high-performance liquid chromatography and ultraviolet detection after pre-column derivatization with 2-chloro-1-methylpyridinium iodide. *Talanta* **5**, 509–515.

Chen, R.R. (2007) Permeability issue in whole-cell bioprocesses and cellular membrane engineering. *Appl Microbiol Biotechnol* **74**, 730–738.

Douglas, L.J. (2003) *Candida* biofilms and their role in infection. *Trends Microbiol* **11**, 30–36.

Gorbushina, A.A. (2007) Life on the rocks. *Environ Microbiol* **9**, 1613–1631.

Guillemot, G., Vaca-Medina, G., Martin-Yken, H., Vernhet, A., Schmitz, P. and Mercier-Bonin, M. (2006) Shear-flow induced detachment of *Saccharomyces cerevisiae* from stainless steel: influence of yeast and solid surface properties. *Colloid Surf B* **49**, 126–135.

Hayden, R.T., Isotalo, P.A., Parret, T., Wolk, D.M., Qian, X., Roberts, G.D. and Lloyd, R.V. (2003) In situ hybridization of the differentiation of *Aspergillus*, *Fusarium*, and *Pseudallescheria* species in tissue section. *Diagn Mol Pathol* **12**, 21–26.

Inàcio, J., Behrens, S., Fuchs, B.M., Fonseca, A., Spencer-Martins, I. and Amann, R. (2003) In situ accessibility of *Saccharomyces cerevisiae* 26S rRNA to Cy3-labeled oligonucleotide probes comprising the D1 and D2 domains. *Appl Environ Microbiol* **69**, 2899–2905.

Kempf, V., Mandle, T., Schumacher, U., Schafer, A. and Autenrieth, I.B. (2005) Rapid detection and identification of pathogens in blood cultures by fluorescence in situ hybridization and flow cytometry. *Int J Med Microbiol* **295**, 47–55.

Linder, M.B., Szilvay, G.R., Nakari-Setala, T. and Penttila, M.E. (2005) Hydrophobins: the protein-amphiphiles of filamentous fungi. *FEMS Microbiol Rev* **29**, 877–896.

Manz, W., Amann, R., Ludwig, W., Wagner, M. and Schleifer, K.H. (1992) Phylogenetic oligonucleotide probes for the major subclasses of proteobacteria: problems and solutions. *Syst Appl Microbiol* **15**, 593–600.

Mille, Y., Beney, L. and Gervais, P. (2005) Compared tolerance to osmotic stress in various microorganisms: towards a survival prediction test. *Biotechnol Bioeng* **92**, 479–484.

Norrish, R.S. (1966) An equation for the activity coefficients and equilibrium relative humidities of water in confectionery syrups. *J Food Technol* **1**, 25–39.

Oulahal-Lagsir, N., Martial-Gros, A., Boistier, E., Blum, L.J. and Bonneau, M. (2000) The development of an ultrasonic apparatus for the non-invasive and repeatable removal of fouling food processing equipment. *Lett Appl Microbiol* **30**, 47–52.

Paris, S., Debeaupuis, J.P., Crameri, R., Carey, M., Charles, F., Prévost, M.C., Schmitt, C., Philippe, B. *et al.* (2003) Conidial hydrophobins of *Aspergillus fumigatus*. *Appl Environ Microbiol* **69**, 1581–1588.

Pawlowska, T.E. (2005) Genetic processes in arbuscolar mycorrhizal fungi. *FEMS Microbiol Lett* **251**, 185–191.

Prigione, V. and Marchisio, V.F. (2004) Methods to maximise the staining of fungal propagules with fluorescent dyes. *J Microbiol Meth* **59**, 371–379.

Prigione, V., Lingua, G. and Filipello Marchisio, V. (2004) Development and use of flow cytometry for detection of airborne fungi. *Appl Environ Microbiol* **70**, 1360–1365.

Ramachandran, S., Fontanille, P., Pandey, A. and Larroche, C. (2007) Spores of *Aspergillus niger* as reservoir of glucose oxidase synthesized during solid-state fermentation and their use as catalyst in gluconic acid production. *Lett Appl Microbiol* **44**, 155–160.

Rigby, S., Procop, G.W., Haase, G., Wilson, D., Hall, G., Kurtzman, C., Oliveira, K., Von Oy, S. *et al.* (2002) Fluorescence in situ hybridization with peptide nucleic acid probes for rapid identification of *Candida albicans* directly from blood culture bottles. *J Clin Microbiol* **40**, 2182–2186.

Sarkany, I. and Gaylarde, C.C. (1968) Bacterial colonisation of the skin flora of the newborn. *J Pathol Bacteriol* **95**, 115–122.

Schuster, E., Dunn-Coleman, N., Frisvad, J.C. and van Dijck, P.W.M. (2002) On the safety of *Aspergillus niger* – a review. *Appl Microbiol Biotechnol* **59**, 426–435.

Singh, A., Van Hamme, J.D. and Ward, O.P. (2007) Surfactants in microbiology and biotechnology: Part 2. Application aspects. *Biotechnol Adv* **25**, 99–121.

Stestak, S. and Ferkas, V. (2001) In situ assays of fungal enzymes in cells permeabilized by osmotic shock. *Anal Biochem* **292**, 34–39.

Teertstra, W.R., Lugones, L.G. and Wosten, H.A.B. (2004) In situ hybridization in filamentous fungi using peptide nucleic acid probes. *Fungal Genet Biol* **41**, 1099–1103.

Valinsky, L., Della Vedova, G., Jiang, T. and Borneman, J. (2002) Oligonucleotide fingerprinting of rRNA genes for analysis of fungal community composition. *Appl Environ Microbiol* **68**, 5999–6004.

de Vos, M.M. and Nelis, H.J. (2003) Detection of *Aspergillus fumigatus* hyphae by solid phase cytometry. *J Microbiol Meth* **55**, 557–564.

Wallner, G., Amann, R. and Beisker, W. (1993) Optimizing fluorescent in situ hybridization with rRNA-targeted oligonucleotide probes for flow cytometric identification of microorganisms. *Cytom Part A* **14**, 136–143.

van der Werf, M.J., Hartmans, S. and van den Tweel, W.J.J. (1995) Permeabilization and lysis of *Pseudomonas pseudoalcaligenes* cells by Triton X-100 for efficient production of D-malate. *Appl Microbiol Biotechnol* **43**, 590–594.

Wolken, W.A.M., Tramper, J. and van der Werf, M.J. (2003) What can spores do for us? *TRENDS in Biotechnol* **21**, 338–345.

Wu, Z., Tsumura, Y., Blomquist, G. and Wang, X-R. (2003) 18S rRNA gene variation among common airborne fungi, and development of specific oligonucleotide probes for the detection of fungal isolates. *Appl Environ Microbiol* **69**, 5389–5397.

Xie, G. and West, T.P. (2006) Citric acid production by *Aspergillus niger* on wet corn distillers grains. *Lett Appl Microbiol* **43**, 269–273.

Xufre, A., Albergaria, H., Inacio, J., Spencer-Martins, I. and Girio, F. (2006) Application of fluorescence in situ hybridization (FISH) to the analysis of yeast population dynamic in winery and laboratory grape must fermentations. *Int J Food Microbiol* **108**, 376–384.